Understanding 6th-Century Barbarian Social Organization and Migration through Paleogenomics

Supplementary Information

Carlos Eduardo G. Amorim, Stefania Vai, Cosimo Posth, Alessandra Modi, István Koncz, Susanne Hakenbeck, Maria Cristina La Rocca, Balazs Mende, Dean Bobo, Walter Pohl, Luisella Pejrani Baricco, Elena Bedini, Paolo Francalacci, Caterina Giostra, Tivadar Vida, Daniel Winger, Uta von Freeden, Silvia Ghirotto, Martina Lari, Guido Barbujani, Johannes Krause, David Caramelli, Patrick J. Geary, Krishna R. Veeramah

Contents (click on links to move directly to section of interest)

S1. BRIEF HISTORY OF THE LOMBARDS AND THE MIGRATION PERIOD

Walter Pohl, Patrick J. Geary, Cristina La Rocca

The Longobardi first appear in Roman texts early in the first century of the Common Era (CE), when the Roman historian Velleius Paterculus, writing about the military expedition of Tiberius around 10 CE in which he himself participated, listed among the peoples defeated by the Romans the "Longobardi, a people surpassing even the Germans in savagery." The geographer Strabo, writing around the same time, considered the Longobards a part of the Suebi and stated that they were at present living on the eastern banks of the Elbe. He described their lifestyle as essentially nomadic, saying that they lived for the most part from their flocks dwelling in temporary huts and packing all of their goods into wagons when moving. At the end of the first century, the Roman historian Cornelius Tacitus, in his *Annales*, briefly describes the Longobardi along with the Semnones as among those who revolted against the Romanized Suebian king Maroboduus around 17 CE. In his *Germania*, written around 98, his only mention of the Longobards is the terse comment that they are distinguished by their small numbers and find safety only in battle. After this the Longobards disappear from Roman texts; only Cassius Dio, writing in the early third century, states that during the reign of Marcus Aurelius (161 to 180), six thousand Longobardi and Obii crossed the Danube but were soundly defeated, sued for peace, and then returned home[1].

The name of the Longobardi reappears ca. 490 again beyond the Danube, but these Longobardi are, according to the Byzantine historian Procopius, a Christian people under the domination of the Heruli, a barbarian people that in the course of the later fifth

century occupied territory in what is now northern Austria and the southern Czech Republic. Procopius further wrote that ca. 508 the Longobards defeated the Heruli, killing their king Rodulf and driving out the Heruli. These territories south of the Danube were in the former Roman province of Pannonia, from which Roman administrative and military infrastructure had been removed in the course of the fifth century. Pannonia had fallen first under Hunnic, then under Ostrogothic control, when the Ostrogoths moved into the Balkans in 473. Soon after, in 476, Odoacer, a Roman commander of barbarian origin in Italy who led a mixed army of Heruli, Rugii and others, overthrew the last West Roman emperor and ruled Italy as king and patricius by arrangement with the East Roman emperor in Constantinople. He exerted loose control over the former Roman provinces to the north and east including Pannonia. The population of the region thus presumably comprised descendants of Roman provincials as well as members of the various barbarian populations that had entered the region over the previous two centuries[2–4].

In 493 the Ostrogothic king Theoderic the Great, acting on the orders of the Roman Emperor Zeno, who had made him patrician and master of the military in the West, killed Odoacer and took over the Kingdom of Italy which he ruled nominally as a representative of the Emperor until his death in 526. Taking advantage of a troubled succession within the Ostrogothic kingdom, in 535 the Byzantine (East Roman Empire) invaded Italy and began a reconquest under Emperor Justinian I. From around this time, Byzantine diplomacy began to develop treaties with the Longobards in order to isolate the Ostrogoths and to counter the Gepids, another barbarian people along the Danube and

Tisa Rivers, and granted them the "city of Noricum and the fortifications in Pannonia as well as other towns and a great amount of money". This probably took place around 547/48, and legitimized the entry of the Longobards into the former Roman provinces south of the Danube. Thereafter the fortunes of the Longobards were progressively intertwined with those of the Romans: Romans sided with the Longobards in their increasingly serious conflicts with the Gepids, and the Longobards provided troops to aid the Romans against the Ostrogoths. After the death of Justinian in 565 and the succession of Justin II, however, Roman policy shifted to support for the Gepids and in 566 the latter defeated the Longobards with Roman support. This drove the Longobards into an alliance with the central Asian Avars who had newly arrived in the vicinity of the Carpathian basis east of the Gepids, an alliance that made possible the Longobard's final defeat of the Gepid kingdom in 567[2].

King Alboin did not use his victory to build a hegemonial kingdom along the Middle Danube (as the Avars would soon do), but to assemble a large army to invade Italy. Later Longobard texts date the beginning of this march to April 1, 568. Even though some historians have argued that it may also have happened in 569, we can be rather precise about the date, and also about the route taken along the ancient Roman Via Postumia to Aquileia and Verona, even though no archaeological evidence survives for these events. Seventh-century sources attribute the Longobard invasion of Italy in 568 to an invitation issued to the Longobard King Alboin by the Roman commander Narses, although this is not mentioned in sixth-century sources and is greeted with skepticism by modern scholars[2], p. 98-100). It was clear that the battered infrastructure in Pannonia

could not meet the ambitions of a growing Longobard army, which now had also incorporated part of the defeated Gepids. Later sources claimed that Alboin had left his former kingdom to his Avar allies. The invasion met with surprisingly little organized Roman resistance, but still the Longobard conquest of parts of Italy was a poorly organized and long-drawn out affair. The main army moved westward and took Pavia, which would later become the Longobard capital, after a siege, but did not move on to attack Ravenna or Rome. Instead, Alboin's army began to fall apart into separate bands led by individual dukes who went their own ways, some into southern Italy and others into Burgundy, and some straight into Roman service. Alboin and his immediate successor were both assassinated, and unity, at least in the north, was only reestablished after a decade by Authari and his Bavarian wife Theodelinda, a descendant of an earlier Longobard king. Upon Authari's death in 590, Theodelinda then married his successor, Agilulf (591-616), duke of Turin but described by sources as a Thuringian. In spite of its consolidation, the Longobard kingdom only controlled the North of Italy with the exception of the modern Romagna around Ravenna, and Tuscany; the Longobard duchies of Spoleto and Benevento ruled much of the inland areas of the peninsula, while the coastal strips and the land around Ravenna and Rome remained under Roman control[3,5].

Under the patronage of Theodelinda, Secundus of Non/Trent, wrote a short history of the Longobards that has subsequently disappeared. During dynastic disputes in the second half of the seventh century, the Origo Gentis Langobardorum, a brief account of the mythic origins of the Lombards written within the context of rival dynastic interests, presented their origins in "Scandanan," where they carried the name of the

Winnili. Attacked by the Vandals, they obtained favor from Wodan through the intervention of his wife Frea, and acquired the name Longobardi or long-beards. The text then tells of their migration through various regions before establishing themselves in the former land of the Rugii, where they fought with and defeated the Heruls and then came into conflict with the Gepids. The text details the various royal marriage alliances with Gepids, Thuringians, Franks, and Herules prior to the movement of the Longobards into Pannonia. It tells of the final defeat of the Gepids in which King Alboin killed the Gepid king Cunimund, the king's marriage with the daughter of Cunimund, Rosemund, and the invasion of Italy. This text makes no mention of alliances with the Byzantines nor does it credit the invasion of Italy to an invitation from Narses[5,6].

At the end of the eighth century, after the Longobard kingdom had been conquered by the Frankish king Charles the Great (Charlemagne) in 774, the Longobard cleric Paul the Deacon wrote a much fuller history of the Longobards[7], drawing on the *Origo Gentis Langobardorum*, the now-lost history of Secundus, and other seventh-century sources. His account, although written over two centuries or more after the events it recounts, has nevertheless been taken, often uncritically, as a reliable account of Longobard history, a position increasingly disputed[8,9]. Concerning the invasion of Italy, he states that Alboin's invading army included not only Longobards but Gepids, Bulgars, Sarmatians, Pannonians, Suevi, Noricans, and others[6,10].

The social structure of pre-Migration Longobard society is extremely difficult to reconstruct. Much depends on whether one sees the seventh-century legal compilations, and in particular, the Edict of King Rothari promulgated in 643 as containing some

indication of pre-migration social and cultural organization. Judging from the compensation tariffs attached individuals, the society was divided into three strata: free-born (termed *exercitales* or soldiers in later laws); *aldii* or clients, and *servi*, slaves [11]. An important but poorly understood social institution was the *fara*. Marius of Avenches describes the invasion of Italy as having taken place *in fara*, and the Edict of Rothari includes a provision for a free man to move about "with his *fara*." A number of place names, both in Italy and in other regions such as Burgundy occupied by barbarian armies include the term *fara*, as do some personal names from Burgundy, although the interpretation of this evidence is uncertain. By the late eighth century, Paul the Deacon defined *fara* as a kin group. However recent scholarship has argued on etymological grounds that the term originally designated not a kindred but a small, mobile military unit, which only acquired the meaning of a kindred following the establishment of the Longobard Kingdom in Italy[4,12–16].

S2. ARCHAEOLOGICAL CONTEXT OF SZÓLÁD

Tivadar Vida, Uta von Freeden, Daniel Winger

This Longobard-associated/period cemetery is located above the modern village of Szólád in the Somogy County in present day Hungary, about 5 km south of Lake Balaton (latitude 46º17 ', Longitude 17º51') in a 30 km long and at this point about 400-600 m wide valley of the Transdanubian hills. It is situated on a Löss-slope inclined to the south, which is covered with about 40-50 cm thick calcareous Chernozem (black earth). The valley today consists of a marshy lowland that reaches to Lake Balaton. It is a now silted-up branch of the lake[17] which means that in Lombard time the actual shore of Lake Balaton was near the cemetery and the associated settlement which was situated most probably on a terrace beside the bay. Already before and during the highway excavations in 2003, some further Longobard sites were discovered in the region around Lake Balaton (Figure S2.1). Most of the Longobard-period burial grounds in Pannonia are located near former Roman villas, forts and camps, and the Szólád cemetery seems not to be an exception, since there are hints of a Roman villa nearby.

The first grave was discovered in 2003 during the development of an access road from Szólád to the M7 motorway (Grave 1[18]). Preceding the excavation of the burial ground, extensive geomagnetic prospecting took place (in 2005 and 2007 conducted by the Thuringian State Office for the Preservation of Monuments and Archeology, Weimar, and in 2009 and 2011 undertaken by the Römisch-Germanische Kommission, D. Winger), which also included the surrounding area north and south of the cemetery and in the probable settlement area.

In 2005, an international research team began the archeological investigation of the sixth century cemetery. It consisted of the Institute of Archaeology of the Hungarian Academy of Sciences (lead by Tivadar Vida) in cooperation with the Römisch-Germanische Komission des Deutschen Archäologischen Instituts in Frankfurt (lead by Uta von Freeden and from 2010 by Daniel Winger). The project was also joined by the Anthropological Institute of the Johannes Gutenberg-Universität Mainz (from 2008 Kurt W. Alt) to conduct the physical anthropological, mitochondrial and isotopic analyses.

The burial ground can be considered as completely excavated: borders are recorded on three sides, only in the southwest there are small inaccessible plots, on which perhaps very few burials could still lie. Even around grave 44, which is located separately in the south, there was no indication of further burials in a review of the environment in the last year of excavation. The excavation also revealed numerous Neolithic, Iron Age and Avar period structures.

The bone preservation in the calcareous soil was excellent and allowed scientific analyses, which to some extent were performed for the first time on early medieval populations. The cemetery contained forty-five graves from the sixth century. Sixteen were the burials of adult men. Grave goods suggested that boys and male juveniles had been interred in seven graves, and the anthropological analyses revealed that four graves without any grave goods had been male burials too. Males were buried in a well-defined cluster in the middle/western part of the cemetery, while the female burials (ten adult women and two young girls) are situated around the male graves in a semi-circle in the

south-eastern part (Figure S2.2). The number of child and infant burials was surprisingly high – possibly also due to the careful excavation technique.

The burials were up to 4.5 meters deep in the loess, and partly designed elaborately with wood. Graves of women and children are generally less deep, but correspond in their dimensions and structures to those of men[19]. Different findings and grave forms – partly observed for the first time in Hungary – are identical for both sexes: graves with ledges and straight walls, wood interiors, grave borders in the form of trenches, as well as plank and tree coffins are documented. The equipment with grave goods can be regarded as very high quality and extensive – despite the also documented grave disorders and the reopening of interments, that took place already in ancient times in approximately 40% of the graves.

Our knowledge regarding the period's archaeological material and especially regarding the funerary practices and grave constructions was substantially enriched by the Szólád excavations. After the removal of the humus, the soil stains outlined 45 graves, including six graves ringed by a circular ditch (e. g. grave 30, Figure S2.3) and two graves enclosed by a rectangular ditch (e. g. grave 5, Figure S2.4). Grave ditches of this kind were previously unknown in Pannonia. Comparable round grave ditches are known from Merovingian cemeteries in central Europe[20] and may be interpreted as an indication of a burial mound raised over the grave of high-status individuals. Interestingly enough, comparable rectangular grave ditches have only been reported from Gaul in Saint-Vit[21], St. Pölten-Unterradlberg in Austria[22] and Britain in Burton Farm[23], both former provinces of the Roman Empire and newly from Hiddestorf in Northern

Germany[24]. Such rectangular grave structures possibly imitate Late Antique burial customs.

A not entirely new phenomenon in the Longobard period grave constructions in Pannonia are graves with ledges on the long sides of the grave pits. 32 of the 45 burials in Szólád had such ledges, to be seen for example in grave 31 (Figure S2.5). Their average depth turns out to be gender-dependent: around 3 m for men; just under 2.5 m for women; round about 2 m in the cases of child burials. The width of the pit narrows to the bottom: the average value of the 32 has an upper width of 128 cm and a lower width of 60 cm.

Excavation pictures illustrate what these ledges on the long sides could have served for. In the case of grave 4 (Figure S2.6) with a square enclosure, a completely intact beamed ceiling was uncovered. The beams rested on the heels on the long sides. On this wooden structure grave goods were deposited, for example, food gifts.

As shown by the intact timbers of this undisturbed grave and the broken planks of a the robbed burial 24 (Figure S2.7), the chamber was covered and furthermore protected by such wooden constructions. Comparable constructions are known from Merovingian Europe as well as contemporary Pannonia (e.g. Szentendre). This burial type also survived in Italy, where in some cases the wooden steps were replaced by stone and the 'chamber' was covered with stone slabs (as at Castel Trosino[25]). Most graves contained tree coffins e g. grave 13 (Figure S2.8), a few burials yielded the remains of rectangular plank coffins e. g. grave 38 (Figure S2.9), reflecting only slightly different funerary customs.

The smaller number of twelve graves with straight walls are only deepened from 1.60 to 0.65 m. They are found clustered in the southeast of the cemetery – except for burial 19. With such a shallow depth, it probably does not make sense to subdivide the long sides with ledges. The distribution of tombs with ledges and those with straight walls marked a clear subdivision of the burial ground. This is reflected in the archaeological material as well: graves with straight walls contained hardly any grave goods. Exceptions are the atypical adult female grave 19 with a bracelet (Figure S2.10) and the girl grave 38 – which contained a bracelet as well (Figure S2.9).

Female burials generally contained up to four brooches (Figure S2.11), which is typical for this period's female costume in Merovingian Europe. Bigger bow brooches hung from the belt. Parallels to the small S-shaped brooches worn on the torso are known from both Pannonia and from today South Germany, as well as from Italy and Slovenia. The technological and decorative traits of the S-shaped brooches and the bow brooches with rectangular head plate suggest that these jewelry items represent the emerging phase of the so-called Pannonian-Italian style, an independent phase of local Pannonian metalwork[26]. Beads and pins are also part of the female dress, whereas pottery and combs were deposited in both male and female burials. Weapons on the other hand are parts of purely male equipment. The number of weapons deposited in the Szólád graves is unusually high compared to other burial grounds in Pannonia. Nearly every male burial contained at least one weapon, and the joint occurrence of spatha, spear/lance and shield was quite common. Spathas were especially frequent, deposited in about 60 percent of

the male burials, reflecting a strongly military organization (and, indirectly, the military nature of the sixth century society).

In addition to vessels of northern origin, the grave pottery from Szólád includes local Pannonian wares such as stamped vessels, and spouted vessels with smoothed-in decoration[27]. The community's contacts with faraway regions are reflected by finds of an ivory ring from Grave 38, the fragments of a Mediterranean glass chalice from Grave 30, or the weights and scales of the male buried with his horse in grave 13.

Grave 19, a grave with straight walls, contained the burial of a woman in a wooden plank coffin, whose single grave good was a bronze bracelet on her left arm (Figure S2.10). This custom has been observed among the Romanized populations of Pannonia, the Eastern Alpine region and the Mediterranean. The woman came perhaps from one of the surviving Late Roman communities, and the strontium isotope analyses of this individual indeed showed a completely different background compared with the other individuals. Traditionally, most tombs would be considered as "Longobard" due to the furniture with weapons and brooches, the food offerings, the pottery, the grave robbery, and the dating in to the mid-sixth century (i.e. fitting to the historical knowledge of this region). But the case of grave 19 (or grave 38) (Figure S2.9-10) as well as different grave constructions (straight walls, rectangular grave enclosures) illustrates the difficulties of the interpretation of early medieval societies solely by archaeological means. It is obvious that there is something new, foreign or at least different in general, but the different aspects within the cemetery show also the variety of the interpretation of

any individual identity. For this reason in previous publications on Szólád, the term “Longobard period” instead of the pure ethnic "Longobard" was used.

As noted by Alt et al.[28] the burial ground was used only for a single generation in the middle of the sixth century – based on archaeology as well as selected radiocarbon dating (see below)– without any antecedent or successor.

The findings in Szólád show a relatively rich, well-nourished population of the mid-sixth century with long distance contacts to modern South-, West- and Central-Germany, to Moravia and Austria, to Slovenia and northern Italy. There are no older traditions known in Pannonia regarding the grave constructions or grave goods: something new or foreign occurs in this cemetery. But at the same time different further, perhaps late Roman, perhaps local, influences are integrated in this burial society.

Since it was a research excavation, anthropological and scientific methods were integrated into the archaeological project as early as possible in order to obtain all imaginable information in an exemplary way – only few can be mentioned here. Physical anthropological, ancient DNA (aDNA) and isotope analyses offered many new possibilities for a better understanding of this community[29]. This includes classical analysis like age, sex, and state of health as well as isotopic analyses for the reconstruction of dietary habits and possible origin of individuals[28].

In summary, the small Longobard period cemetery from Szólád is the necropolis of a small, wealthy, highly mobile and population from the middle of the sixth century. In grave construction and grave goods at least two groups can be distinguished, which suggest the integration of different traditions. The small population settled for only one

generation in Pannonia at the shore of Lake Balaton and therefore appears to have been very mobile - especially the women indicate isotopically and genetically heterogeneous backgrounds[28].

For new radiocarbon (^{14}C) dating performed in this study, collagen was extracted from bone material for 8 samples (including 2 lacking grave goods, SZ37 and SZ43) at the Curt-Engelhorn-Center for Archaeometry, purified by ultrafiltration (fraction >30kD) and freeze-dried. Collagen was then combusted to CO_2 in an Elemental Analyzer (EA). CO_2 was then converted catalytically to graphite. Dating was performed using the MIni CArbon DAting System (MICADAS-AMS) of the Klaus-Tschira-Archäometrie-Zentrum.

^{14}C ages were normalized to δ13C=-25%[30]. The ^{14}C ages were given in BP (before present) meaning years before 1050. In order to provide absolute calendar ages the ^{14}C ages were calibrated using the dataset INTCAL13 dataset[31] via the software `SwissCal 1.0`. Results of the calibration are shown in columns "Cal 1-sigma" and "Cal 2-sigma" using the 1-sigma and 2-sigma uncertainty of the ^{14}C ages, respectively in Table S3.1. C:N ratios and C concentrations were within the range of normal values, except for samples SZ43, SZ21, SZ27B and AV2, which has elevated C:N ratios that could indicate degraded collagen and negatively affected ^{14}C ages. Collagen content of the sample material was considered good. All samples dated to the early Medieval (range of 412-604 CE across all samples and both sigma estimates for our Lombard-era samples and 541-641 for the two Avar period samples)

Figure S2.1. Map of the Longobard period Balaton lake region. Color coding: Yellow = late antique; blue = cemeteries, red = settlement. (1) Castle of Keszthely-Fenékpuszta; (2) Vörs, (3) Balatonkeresztúr, (4) Balatonlelle, (5) Szólád, (6) Zamárdi, (7) Várpalota, and (8) Tamási.

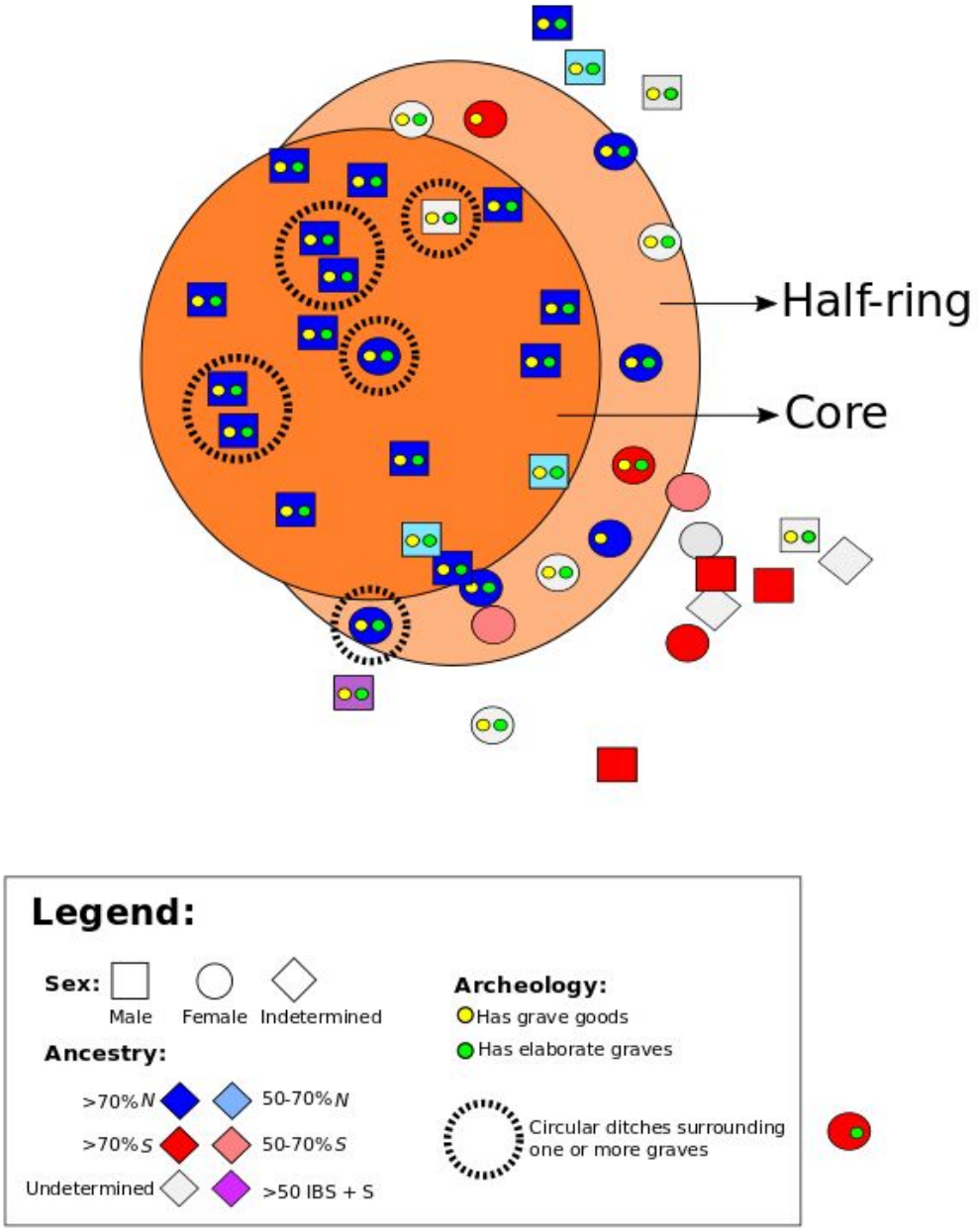

Figure S2.2. Core/half-ring structure of graves in Szólád. Symbols follow the same specification as defined for Fig 1 in the main text.

Figure S2.3. Szólád grave 30 during the excavation ringed by a circular ditch.

Figure S2.4. Szólád grave SZ5 during the excavation surrounded by a rectangular ditch.

Figure S2.5. Szólád grave SZ31 profile of the ledges.

Figure S2.6. Szólád grave SZ4 during the excavation with an intact wooden layer lying on the ledges above the grave.

Figure S2.7. Szólád grave SZ25 during the excavation with wooden broken layer due to antique grave robbery.

Figure S2.8. The rounded corners are the result of tree coffins, as seen here in the main grave of Szólád (SZ13).

Figure S2.9. Opposite tree coffins there are rectangular wooden coffins used, for example, in the case of the rich equipped girl in grave SZ38

Figure S2.10. Grave SZ19 (female) with straight walls and a bracelet. Grave construction and goods in this case are different from the typical Longboard period graves.

Figure S2.11. Four brooch costume in grave SZ21.

Table S2.1. 14C results for 8 samples from Szólád

Sample Name	14C age (yr BP) +-	Cal 1-sigma (CE)	Cal 2-sigma (CE)	C:N	C (%)	Collagen (%)
SZ13	1579±25	433-533	422-541	3.2	16.3	1.9
SZ19	1567±24	435-537	426-549	3.6	33.0	3.8
SZ21	1524±24	470-591	434-602	4.1	45.2	4.0
SZ27B	1595±27	423-532	412-538	4.3	35.4	5.2
SZ37	1544±26	437-560	430-577	3.2	19.4	2.1
SZ43	1521±25	475-595	435-604	4.2	52.7	1.6
AV1	1487±26	556-605	541-637	3.2	18.9	2.8
AV2	1472±27	566-619	548-641	4.4	57.6	1.8

S3. ARCHAEOLOGICAL CONTEXT OF COLLEGNO

Caterina Giostra, Luisella Pejrani Baricco, Elena Bedini

Collegno is located 7 km west of the city of Turin, in Piedmont, near a crossing of the river Dora. It is located along the road leading to Val di Susa and the Alpine passes to Gaul which in the later sixth and early seventh centuries were controlled by the Frankish kingdom.

Between 2002 and 2006, the then Superintendence for Archaeological Heritage of Piedmont investigated an extensive area during the works for the construction of the Torino subway. A long-standing village and two funerary areas were found at the archaeological site (Figure S3.1) containing a group of eight tombs that chronologically and culturally suggested Gothic presence, including two cases of artificial modification of the skull (Figure S3.2) and a large cemetery from the Longobard period. The village related to the funerary contexts was also in use in both the Gothic and the Longobard periods as evidenced by the presence of sunken-feature buildings (Figure S3.3) and stamped pottery of northern European tradition[32–34].

The necropolis was completely excavated; it contained 157 graves (Figure S3.4), although the loss of some superficial burials cannot be excluded because of modern agricultural activities. Some small sectors and some burials were damaged before the start of the archaeological excavation. The graves have a broad chronology, which stretches from the late sixth to eighth centuries. We can recognize a progressive expansion from the center to the outside, toward both the east and the west; only in the last phase (8th century) burials are again located among the central graves.

The use of the cemetery can be divided into three phases based on grave typologies, objects found in the tombs and location plausibility:

- Phase 1: 570/590 – 630/640 (orange on the plan, Figure S3.4). It is not easy to establish precisely when burials began. It is possible that they started a few years after the arrival of the Longobards in Italy. Regardless, the first phase has a broad range and we can identify two sub-phases within the first phase: 1A: end of the sixth century - first years of the seventh century, 1B: early decades of the seventh century.

- Phase 2: 640 - 700 ca. (green on the plan). During this time, the eastern and western most sectors of the cemetery were used.

- Phase 3: eighth century (grey on the plan). During this period, new graves without grave goods are placed once again in the central areas of the cemetery, among the existing oldest graves. The chronology has been confirmed by radiocarbon analysis of individuals from this phase , which was performed at Beta Analytic Radiocarbon Dating Laboratory in Miami, Florida (see Pejrani Baricco[32]). Estimates from calibration curves ranged from 675 to 880 CE with 95% probability, and from 700 to 795 CE with 68% probability.

In the early stages of cemetery use (1A and 1B), the determination of sex and age on an anthropological and archaeological basis according to Ferembach et al.[35] shows that the number of male individuals is clearly higher than the number of female individuals; children and adolescents consist of only 20% of the graves[36]. The graves of men, women, and children are integrated, and this likely reflects the organization and use of space based on parental ties.

The graves are oriented along an west-east axis, with the head of the deceased to the west. They are often aligned along short lines with a north-south development. The graves of the first phase (Figure S3.5) are pits in the earth not deeper than 1m from the present ground elevation. Among the oldest graves (Phase 1A; up to 600-610 ca.) several contained wooden chambers, but these disappear after the first decades, in line with what generally occurred in Italy. Thus graves dating from 600 to 630/640 (Phase 1B) lack these wooden chambers. Various male graves have weapons sets (Figure S3.6). Progressively belts for the suspension of weapons acquire more numerous seals which are decorated with the "animal style" (Figure S3.7)[37,38]. The female tombs often appear to have few grave goods, perhaps because of the age of little girls or older women, and also in line with the evolution of Italian funeral rituals in the 7th century. Among the offerings one finds pottery of the stamped type already produced in Pannonia. Even a horse was also found, which was buried headless.

The necropolis at least in part has been associated with the Longobards because of these practices and because of the material culture encountered (typologies, production features and decorative style), along with the typology of the sunken-feature buildings in the settlement. These elements present the following traits: a clear discontinuity with respect to the previous Italian context in which these distinctive features are absent; continuity with respect to areas inhabited by barbarian groups, especially the Longobards in Pannonia; internal consistency with respect to these factors from the same site and absence in other coeval sites in the same area; coexistence with the arrival of migrant groups described by written sources (end of sixth century)[39].

There appear to be two older nuclei, one in the center (1A), which expands to the west (1B; 2), and a more eastern one (1, A) that expands to the east (1, B; 2) (Figure S3.8). This second nucleus is centered on a row of tombs with gold foil crosses (Figure S3.4). The horse was found within this group. Some female tombs (CL48, CL47, CL147 and perhaps others) contained non-Italian but transalpine objects (Figure S3.9) which suggested the presence of some individuals of a different origin that differs from both Italy and Pannonia, especially women who may have moved from neighboring regions (possibly from the Frankish-Burgundian area in south-eastern Gaul, starting from the nearby Val di Susa) due to exogamy, perhaps accompanied by some subordinate individuals[37]. Strontium isotope data suggest a non-local origin different from the other individuals for women CL48 and CL147. Unfortunately it was not possible to obtain DNA from CL48, but they may be linked with neighboring grave CL47. Anthropological analysis has shown that the skulls of women CL48 and CL47 both had probably hereditary scaphocephaly, making kinship more credible (Figure S3.10).

The two men from graves 49 (also a non-local individual, based on strontium isotope data) and 70 (with grave goods very similar to the tomb 53) both had an inherited pathology, DISH (Diffuse Idiopathic Skeletal Hyperostosis), allowing us to potentially enlarge the network of parental relationships in this group of graves. In the necropolis, even the possible symbolic transmission of some objects, especially parts of belts, has allowed us to speculate on possible relations of kinship between some individuals[36].

Some graves, however, are distinct as they lack wooden chambers, weapons, or objects that are barbarian by type and decoration; these are found in both marginal sectors

and between the two different kin groups with these elements (Figure S3.8).

Skeletal remains have different degrees of preservation, with individuals from the first phase tending to be worse. Metric and morphometric analysis on six individuals has found the presence of elongated skulls, in a marked or intermediate measure[40]. Male individuals are especially tall, with almost all individuals reaching or exceeding 170-175cm. Skeletal analysis published in 2004 suggested aspects of lifestyle which appear to have changed significantly in the second period and even more in the third[36]. In the first phase, men with weapons show a marked muscular development and skeletal alterations that indicate an intense physical activity, including evidence of horseback riding. At least 4 individuals of the first phase have cranial lesions produced from cutting of the weapons (Figure S3.11). The data suggest an intense military training and even fighting.

In the second phase (640-700 ca.) the physical effort extended was still stressful, but less risky than in the previous phase: none of the few traumas found appear to have been produced by aggression. In the third period of use of the necropolis (eighth century) both the degree of muscular development and the traumatic pathologies, while still indicative of a discrete degree of physical stress, are different from those of previous phases and due to a complete change of lifestyle. The men seem to have engaged in agricultural and craft work[36].

Finally, in 2004 all the adult individuals from the first 73 graves already excavated at that time were subjected to paleonutritional analysis by atomic absorption spectroscopy (AAS) at the Laboratory of Paleonutrition of the Department of

Archaeological Sciences of the University of Pisa[41]. Also the organic remains adherent to the metallic finds were analyzed by light microscopy[42].

Skeletal remains are currently stored in the warehouse of the Dipartimento di Biologia dell'Università di Firenze and owned by Soprintendenza Archeologia, Belle Arti e Paesaggio per la città metropolitana di Torino.

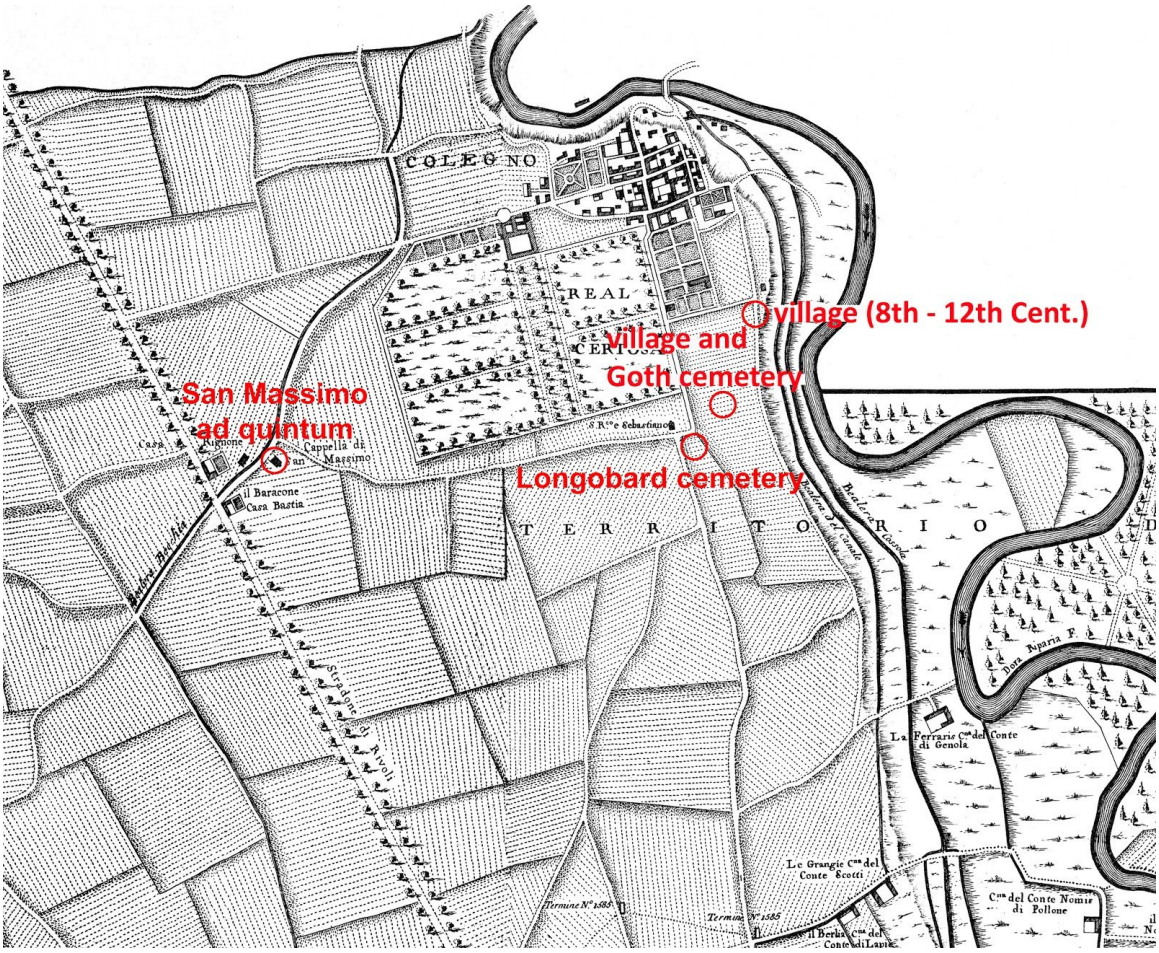

Figure S3.1. Map of the site at Collegno.

Figure S3.2. An artificially modified skull from the Gothic-era cemetery.

Figure S3.3. A sunken-feature building at the settlement in the Longobard period.

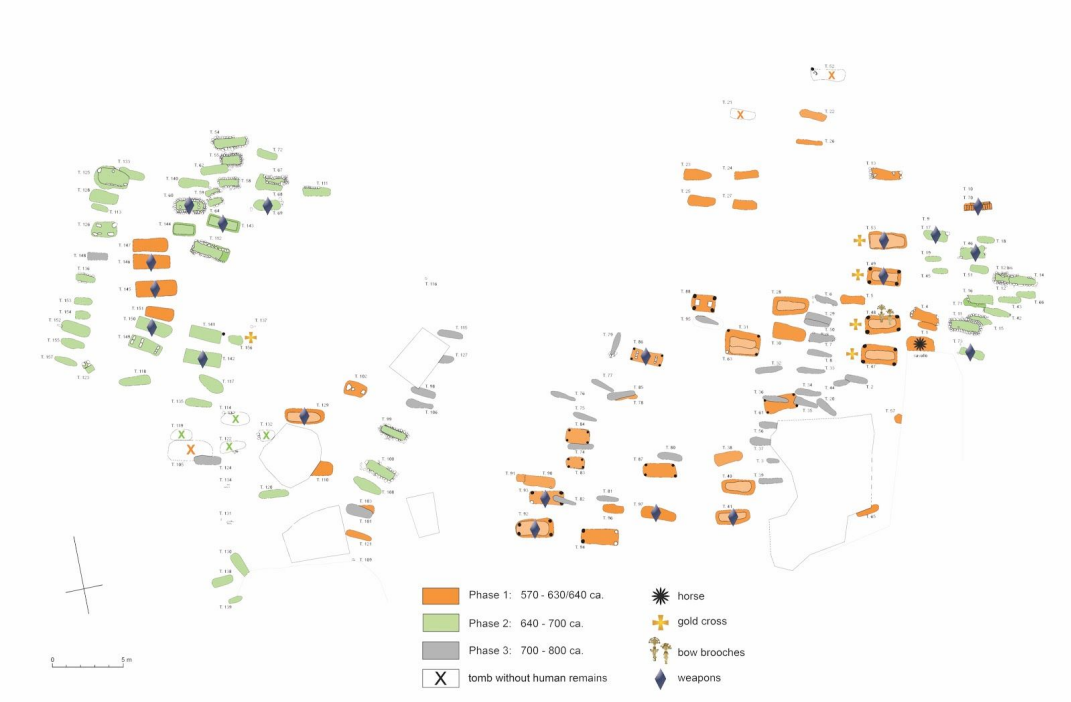

Figure S3.4. Plan of the cemetery of Collegno with three major periods highlighted in colour.

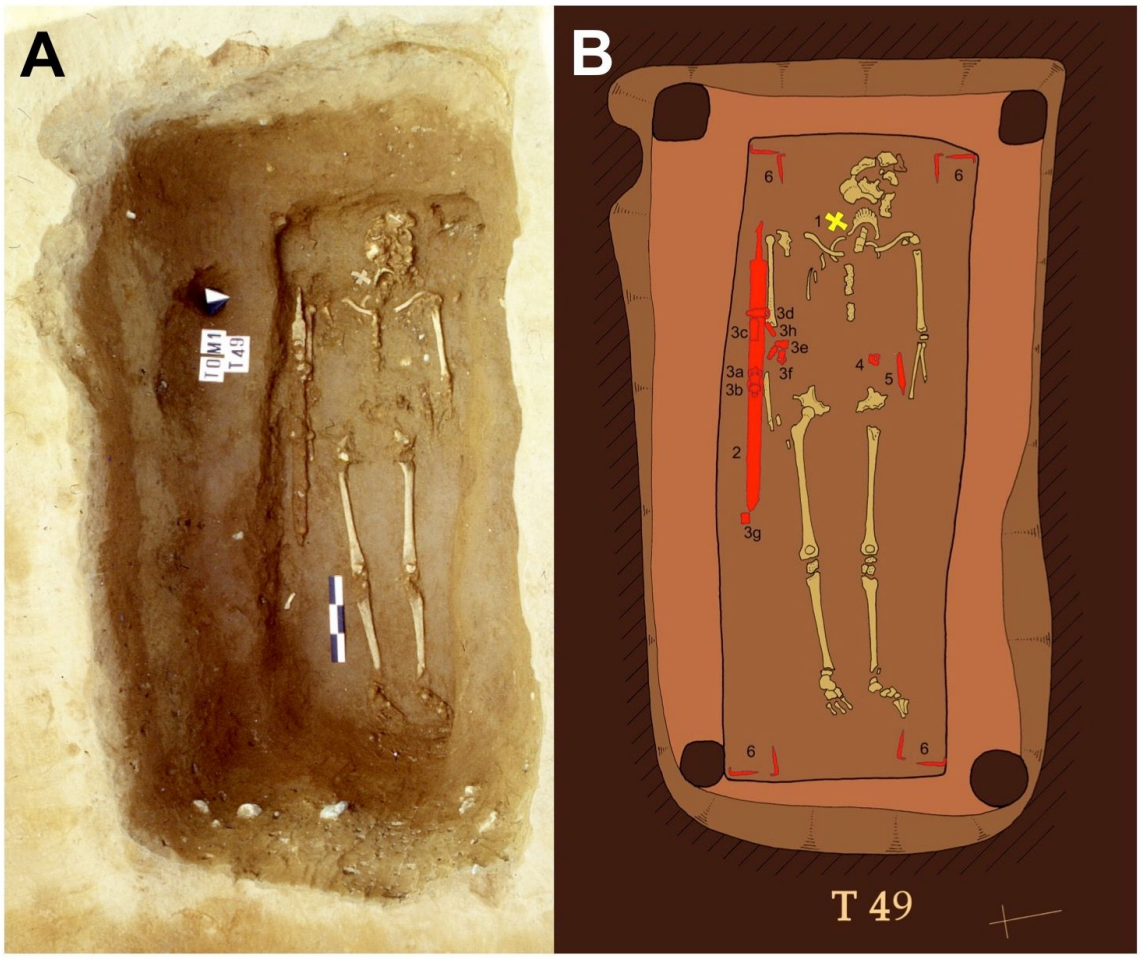

Figure S3.5. Grave 49 during the excavation (A) and plan of the grave (B).

Figure S3.6. The male grave goods for grave 97 (c. 580-600 CE).

Figure S3.7. The male grave goods for grave 53 (c. 600-630 CE).

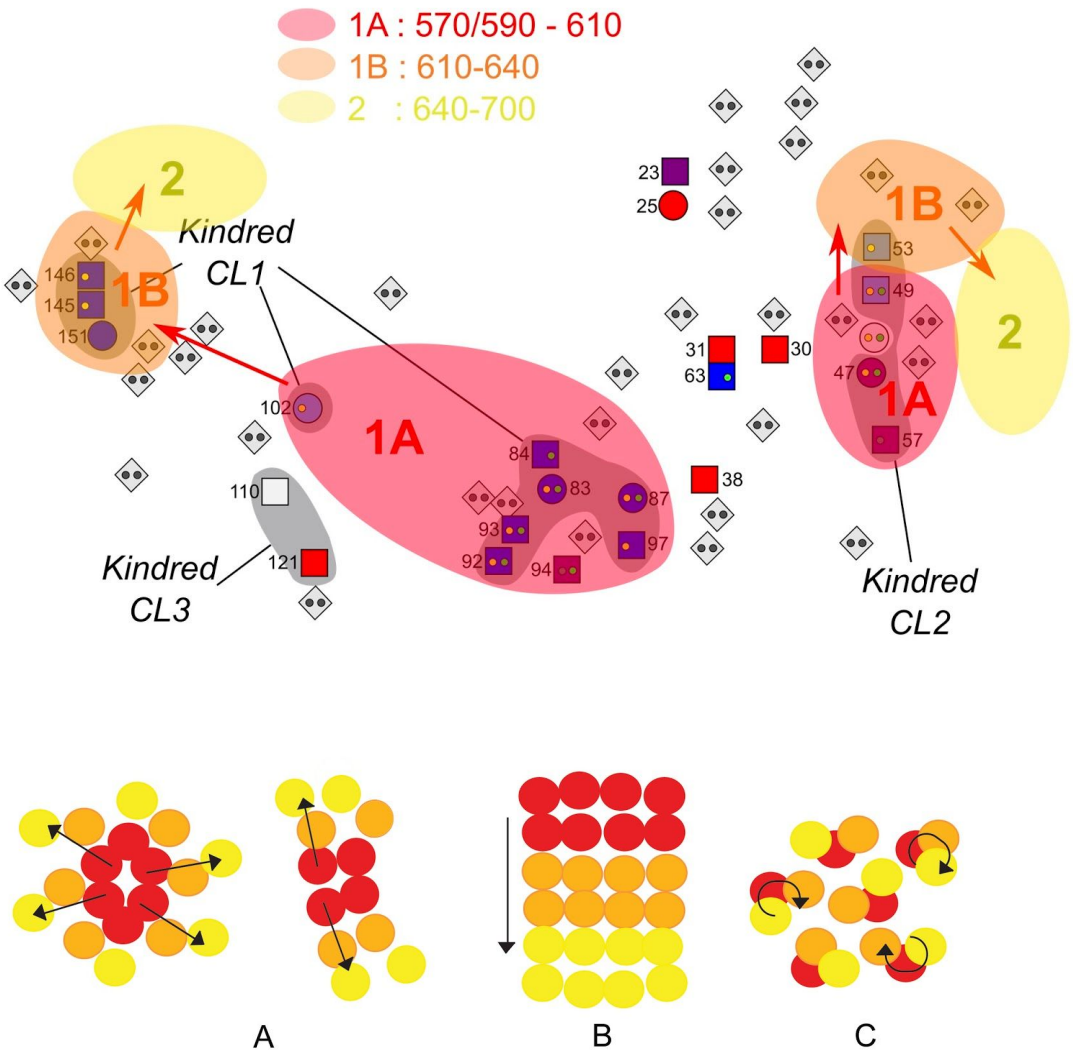

Figure S3.8. The development of the cemetery at Collegno. The two main kindreds occupy a new sector after each generation. They move outwards: one to the west, the other to the east. For phase 1B we have fewer samples. The shift continues afterwards into second period where we currently lack genomic data. Compared to the two main kindred, the *S* individuals have marginal positions between the two main kindred groups. Bottom row shows possible developments of Longobard cemeteries in Italy. (red: phase 1, orange: phase 2: yellow phase 3; the circles are the kindred nucleus)[43].

Figures S3.9: Female grave goods for grave 48, with bow brooch (on the left) and buckle produced north of the Alps.

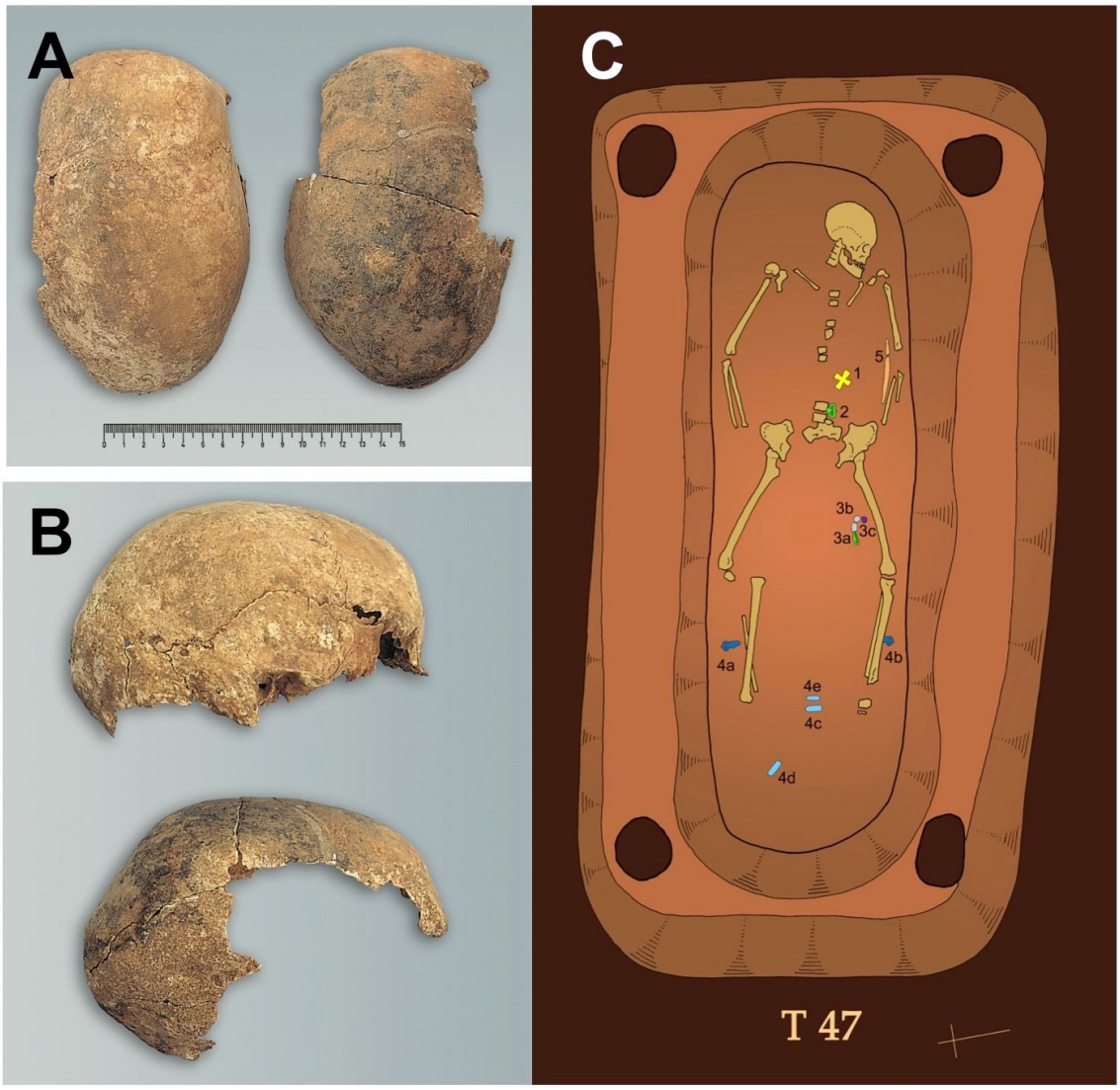

Figure S3.10. Superior and right lateral view of the scaphocephalic female skulls CL47 (left and above) and CL48 (left and below), and the plan of the grave for CL47.

Figure S3.11. Grave 70, an elderly male with two ante mortem cranial wounds caused by an edged weapon on the right temporo-occipital region, and peri mortem wound on the right half of the lambdoid suture caused by a pointed weapon.

S4. DNA ISOLATION, LIBRARY PREPARATION, SCREENING AND GENOME-WIDE CAPTURE

Stefania Vai, Alessandra Modi, Krishna R. Veeramah, Cosimo Posth

Experimental steps of DNA isolation, library preparation and enrichment were carried out at the Laboratory of Anthropology and Paleogenetics at the University of Florence (Italy), the University of Tübingen (Germany) and at the Department of Archaeogenetics at the Max Planck Institute for the Science of Human History in Jena (Germany) in facilities exclusively dedicated to ancient DNA analysis. Appropriate criteria to prevent contamination with present-day DNA were followed. DNA extraction and library preparation reactions included negative controls at all stages.

Bone samples, namely the petrous portion of the temporal bone (henceforth petrous bone), teeth, and long bone fragments, were collected for 47 individuals from Szólád and for 36 individuals from Collegno. To remove potential contamination, the outer layer of the samples was mechanically removed using a dentistry microdrill with disposable tools and irradiated by ultraviolet light (254 nm) for 45min in a Biolink DNA Crosslinker (Biometra^{TM}). Petrous bones were sectioned using a disk saw, and the densest part of inner ear part was selected as proposed in Pinhasi et al.[44]. The dentine portion from teeth and the inner part of dense compact tissue for bones were selected to obtain bone powder using a microdrill with disposable tips. 50-100 mg of bone powder was used for DNA extraction using a silica-based protocol that allows ancient DNA molecules to be efficiently recovered even if highly fragmented[45]. DNA was eluted twice in 50 µl of TET buffer (10 nM Tris, 1 mM EDTA, 0.05% Tween-20).

As a first step, a screening was performed in order evaluate the quantity and quality of the endogenous DNA content. For this purpose, aDNA libraries were prepared from 20µl of extract following a custom double-indexing protocol[46,47] optimized for ancient samples, in order to make the DNA immortalized, barcoded and available for Next Generation Sequencing (NGS) on Illumina platforms. No enzymatic damage repair was performed at this stage in order to preserve and analyze the damage patterns of DNA fragments.

Libraries were shotgun sequenced on Illumina MiSeq and NextSeq runs (either single-end run 75 cycles in Jena or paired-end run 75 cycles in New York). Raw sequence data obtained from the sequencing runs were analyzed using pipelines specific for ancient DNA samples. In Jena the general approach of Peltzer was followed[48]. Adapters were clipped-off and the resulting reads of 30bp or longer were then mapped on to the human reference genome (hg19) using `BWA`[48,49] with the following parameters (`-l 16500, -n 0.01`). Duplicates were removed using `DeDup`, a tool that considers both ends of a DNA fragment to recognize them as clonal. In New York we largely followed the ancient DNA pipeline of Kircher[50], though slight modifications were made to scripts to accommodate our data. The first 50bp of each read was trimmed using the `TrimFastQ.py` script. TagDust[51] was then used to identify potential library artifact sequences based on known Illumina adaptor sequences. The thirty most frequent artifacts for each sample were identified and a pairwise alignment was constructed for each against the adaptor sequences. Pairwise alignments were then manually inspected for evidence of sequence motifs that likely represent artifacts such as forward and reverse

adaptors containing no or very small inserts. This list of motifs was used as input for the `MergeReadsFastQ_cc.py` script in order to merge paired-end reads with substantial sequence overlap into single reads and remove adaptor sequence. Any remaining paired-end reads were discarded. Reads with at least 5 base calls with a Phred-scaled quality score of less than 15 were removed using the `QualityFilterFastQ_gz.py script`. Reads were mapped to the the human reference genome GR37 with `BWA aln`[48,49] using the following parameters: maximum edit distance=1%, number of gap opens=2, l=16500. Read groups were added using the PICARD tool `AddOrReplaceReadGroups` and duplicate reads were marked using `MarkDuplicates`.

After mapping in both Jena and New York, reads with mapping quality below 30 were discarded. Length and deamination patterns were estimated using `MapDamage 2.0`[52]. Endogenous content of at least of 0.075% (though, using petrous bone this value was usually much higher, with a mean 36% and a max of 86%), deamination patterns compatible with the age of the individuals (above 20% C to T substitutions at 5' end) and the absence of contamination as evaluated from mitochondrial genomes were assessed when choosing samples for further processing. Relative coverage of reads mapping to the autosomes, X-chromosome and Y-chromosome were used to provide an initial assessment of sex.

A total of 39 samples from Szólád and 24 from Collegno showed endogenous DNA quantity and quality compatible with further genome-wide analyses. A second library with partial UDG treatment (UDGhalf)[53] was performed for 60 out of 63 selected

samples starting from 30 µl of DNA extract (Table S4.1). Ten libraries from Szólád, obtained from petrous bones genetically assigned to male individuals[54], showed enough endogenous DNA content (between 44% and 86%) to undergo whole-genome sequencing in New York on an Illumina HiSeq (100bp single-end run, 4 lanes per sample). In-solution capture[55] was performed on the remaining 53 individuals targeting ~1,237,207 single nucleotide polymorphisms (SNPs) ("1240K capture")[56] scattered across the nuclear genome. The enriched DNA was then sequenced on a NextSeq (75bp single-end run or 150 cycles paired-end run).

Table S4.1. Summary statistics for samples sequenced in this study.

[See Excel spreadsheet]

S5. BIOINFORMATIC PROCESSING

Cosimo Posth, Carlos Eduardo G. Amorim, Krishna R. Veeramah

S5.1. Mapping and Quality Control

Genome-wide capture read data was processed as described above in Supplementary Text S4 for screening libraries in Jena with the additional step for any paired-end data of merging reads into single sequence using `Clip&Merge` when there was a minimum overlap of 10bp between reads. WGS data was processed as described above in Supplementary Text S4 for screening libraries in New York with the additional step of realigning InDels using the `GATK RealignerTargetCreator` and `IndelRealigner` tools[57] and using `KeyAdapterTrimFastQ_cc_gz.py` to only remove adaptor sequence but not merge reads. All 63 individuals presented damage patterns as expected from the applied library protocol (Table S4.1). Relative fold coverage on the targeted autosomal SNPs was compared to the coverage on the X- and Y-chromosome to confirm genetic sex assignment[58]. Nuclear contamination in males was performed with the tool `ANGSD`[59] by estimating heterozygozity levels on known X-chromosome polymorphic sites. Mitochondrial DNA (mtDNA) off-target reads were used, when possible, to reconstruct complete or partial mitochondrial genomes and estimate mtDNA contamination using `schmutzi`[60]. The online program `Haplofind`[61] was used for mtDNA haplogroup assignment.

S5.2. SNP and Genotype Calling

Genotypes were called at SNPs targeted as part of the 1240K capture for all 63 ancient individuals from Szólád and Collegno. In addition, we called genotypes at the same sites for whole genome shotgun re-sequencing data generated from seven third to seventh century individuals (UDG treated) from the UK associated with the Anglo-Saxon material culture[62] and two fifth century individuals (not UDG treated from Bavaria, Germany[63]. Thus we generated new calls for a total of 72 ancient individuals. We applied two different models for genotype calling (implemented in Python and available from https://github.com/kveeramah/) depending on if genomic libraries were subject to UDG treatment or not.

For the 67 samples that underwent partial UDG treatment (60 from the present work plus seven from Schiffels et al.[62]), we implemented a standard genotype likelihood model described by De Pristo et al[57], but trimming the last and first *B* bases of each read. *B* was set as 3 for the 60 individuals generated in this study and 5 for the 7 Anglo-Saxon-associated samples. By doing so, we sought to eliminate the excess of transitions due to PMD that remain at the end of reads due to partial UDG treatment. For the remaining five samples that did not undergo any kind of UDG treatment (three from the present study and two from Veeramah et al.[63]), we called genotypes using a model taking into account PMG described in Hofmanova et al.[64], but considering a Weibull distribution[65].

Both models produced genotype likelihoods for each of the ten possible genotypes at the targeted 1240K capture SNPS. Because coverage for most samples was

only ~1x, we obtained haploid genotypes for each individual based on the highest homozygote genotype likelihood. When likelihoods for two or more different homozygote genotypes were equal, we randomly picked one allele. We limited genotype calling to those sites with a genotyping Phred-scaled quality score of at least 45. This value represents the highest possible quality score when only one read covers a position (i.e. we discard any SNP calls where there is only one read and does not have the highest possible base quality score . Mean coverage at the captured regions (in samples undergoing 1240K capture only) ranged from <0.01x to 2.9x, with a mean of 1.5x and an average of ~520K SNPs successfully sequenced across these 53 samples from Szólád and Collegno.

We also determined full diploid genotypes at all sites in the genome (not just the targeted SNPs) for the 10 high-coverage genomes from Szólád. Mean coverage for these samples ranged from 6.8x to 14.5x, with a mean of 11.3x.

Finally, for analysis comparing ancient samples to each other directly, in order to not bias against samples with lower coverage (which will have a greater error rate), we obtained haploid calls at the 1240K capture SNPs for each individual by randomly sampling one read per site. Because of the potential effect of PMD, we did not include non-UDG treated samples in this dataset.

S6. MODERN AND ANCIENT REFERENCE DATASET CONSTRUCTION

Krishna R. Veeramah

We assembled SNP data for three modern reference datasets and one ancient reference dataset for comparison to the early Medieval samples generated in this study. Datasets were merged using PLINK[66]. Except when we focused the analyses on the 10 WGS sequences, diploid genotypes for modern samples were transformed into pseudo-haploid calls by picking one allele at random.

POPRES: The original European Population Reference Sample (POPRES) project[67] dataset consists of 3,192 individuals genotyped at 500,586 loci. Novembre et al.[68] identified a subset of 197,108 SNPs in 1,385 European individuals[68] for demographic analysis. We imputed additional SNPs from the original Novembre et al. dataset using the Michigan Imputation Server[69]. After accounting for potential strand flips there were 165,443 usable SNPs that could be orientated with human reference genome build 37. Phasing was performed using Eagle2[70] with the worldwide sample set from 1000 Genomes Phase 3[71] acting as the reference panel. Following imputation, biallelic imputed SNPs were filtered to be at >=5% minor allele frequency with a r^2 imputation of value of >= 0.9, resulting in a final imputed SNP set of 2,113,389 SNPs. 329,386 SNPs overlapped with the autosomal SNPs included in the 1240K capture and were thus used for downstream statistical analyses in this study.

HellBus: The same imputation procedure was carried out on 512,368 SNPs in 1,582 European and Asian individuals from Hellenthal et al.[72] (henceforth the HellBus dataset).

Following imputation, biallelic SNPs were filtered to be >=5% minor allele frequency with a r^2 imputation of value of >=0.9, resulting in a final imputed SNP set of 4,883,514 SNPs. 779,577 SNPs overlapped with the autosomal SNPs included in the 1240K capture and were thus used for downstream statistical analyses.

1000 Genomes and Simons Genome Diversity Project: All SNPs from the 1240K capture were extracted from whole genome sequences generated from European (CEU, FIN, GBR, IBS and TSI, together named EUR), SouthEast Asian (GIH, PJL, BEB, STU, and ITU, together named SAS), East Asian (CHB, JPT, CHS, CDX and KHV, together named EAS) and Yoruban (YRI) populations that are part of the 1000 Genomes Project[71] as well the 290 publically available whole genomes from the Simon Genome Diversity Project (SGDP)[73], giving us 1240 capture SNP data for a total of 1,883 genomes. 1000 Genomes SNPs were obtained using VCFtools[74] and SGDP SNPs were obtained using `cpullout` from the cTools package (https://github.com/mengyao/cTools).

Mathieson: Genotype data from 211 ancient West Eurasians from 6,300 - 300 BC genotyped at the 1240K capture using haploid calls was obtained from Mathieson et al.[75]. We ignored individuals determined to be related or outliers in that study. Depending on the analysis, this dataset was merged with one of the three modern reference datasets.

Each of the three modern datasets provides a certain advantage over the others for downstream population genetic analysis. The POPRES dataset has the greatest sampling density for Europe while having the smallest SNP overlap with the 1240K capture. The HellBus dataset has the greatest sampling density for Eurasia while having only medium

SNP overlap with the 1240K capture. The 1000 Genomes+SGDP dataset has essentially maximum 1240K SNP overlap but has the smallest geographic sampling density.

S7. PRINCIPAL COMPONENT ANALYSIS

Carlos Eduardo G. Amorim, Krishna R. Veeramah

All principal components analysis (PCA) was conducted using `smartpca`[76] unless stated otherwise, with our primary approach involving performing separate PCA analyses via pseudo-haploid calls using some set of reference samples against an ancient sample of interest such that there was no missing data at any SNP. When the number of starting non-missing SNPs for any particular comparison was greater than 100,000 SNPs, `PLINK 1.9` was used to filter for possible linkage disequilibrium via the --indep-pairwise argument, using a window size of 50, a step size of 5 and an r^2 value of 0.2. Individual PCAs were then combined using a Procrustes transformation in R using the vegan package as described previously in Veeramah and Hammer[77].

We first performed PCAs using each of the three modern reference datasets against our medieval samples (Figure S7.1-3). Location of the ancient samples was generally very consistent across reference datasets, the only noticeable difference being the HellBus analysis shifting CL31 towards modern populations from the Caucasus, but this sample showed high levels of contamination and thus the results are unreliable. Otherwise, all other samples appear to be overlap with modern European populations.

Previous work has shown that modern European genetic variation is primarily the result of admixture three major ancestry groups, Paleolithic Hunter-Gatherers, Neolithic farmers from Anatolia and Bronze age Steppe Herders[56,78,79]. In order to explore this effect in the context of our Medieval samples. we next merged the Mathieson dataset with both the POPRES and HellBus European samples. We then performed Procrustes

PCAs using the modern samples as reference as well one genome from Mathieson from each of these three groups with the highest coverage (Loschbour representing Hunter-gatherers, I0707 representing Anatolian farmers and I0231 representing Steppe people), with both the Medieval the remaining Mathieson samples used as the targets (Figure S7.4-5). The Medieval samples showed no strong evidence of being closer to any particular ancestral population compared to modern or Bronze Age samples, with overlap between all three and modern samples reiterating the geographic structure observed previously. It is also noteworthy that samples from Szólád do not appear to be clustered next to Neolithic, Bronze Age or modern samples from Hungary. This lack of overlap with the Bronze Age is made more apparent by performing this analysis only with Bronze age, Medieval and modern samples (Fig 2A, Figure S7.6-7).

Finally, we also performed a PCA analysis on a set of 39 unrelated Medieval samples that maximized the amount of SNP overlap amongst samples and did not include any other ancient or modern reference samples. To avoid biases due to SNP calling quality amongst samples, we applied this to haploid calls generated by randomly sampling a single read from each site for each individidual. As such the five non-UDG samples were excluded from this analysis. When only analyzing SNPs with no missing data amongst samples, we ended up with a set of ~50-60K SNPs. CL31 (Figure SX7), followed by SZ45 (Figure S7) were clear outliers. This is not surprising given that CL31 was shown to have high levels of contamination, while `ADMIXTURE` analysis in the next chapter showed SZ45 to possess a unique ancestry profile. However, analysis of the remaining samples (Figure S7.10) essentially recapitulated the main north-south pattern

of modern genetic variation along PC1, despite no actual modern reference individuals being used.

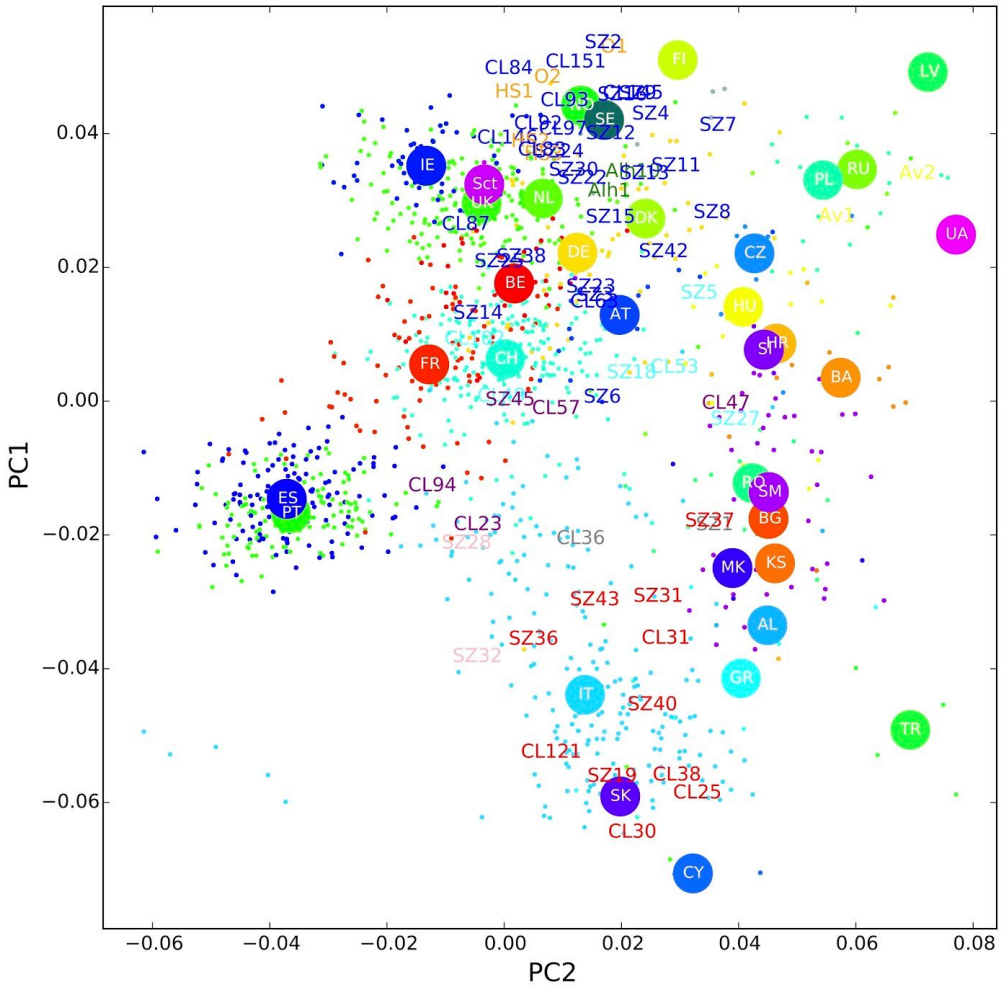

Figure S7.1. Procrustes transformed PCA of medieval ancient samples against POPRES imputed SNP dataset. Color coding of medieval samples is same as in Figs 1 and 2. Two letter and three codes for POPRES samples: AL=Albania, AT=Austria, BA=Bosnia-Herzegovina, BE=Belgium, BG=Bulgaria, CH=Switzerland, CY=Cyprus, CZ=Czech Republic, DE=Germany, DK=Denmark, ES=Spain, FI=Finland, FR=France, GB=United Kingdom, GR, Greece, HR=Croatia, HU=Hungary, IE=Ireland, IT=Italy, KS=Kosovo, LV=Latvia, MK=Macedonia, NO=Norway, NL=Netherlands, PL=Poland, PT=Portugal, RO=Romania, SM=Serbia and Montenegro, RU=Russia, Sct=Scotland, SE=Sweden, SI=Slovenia, SK=Slovakia, TR=Turkey, UA=Ukraine. Three letter codes for SGDP samples: Ber=Bergamo, Bul=Bulgaria, Cze=Czech Republic, Eng=England, Est=Estonia, Fre=France, Gre=Greece, Hun=Hungary, Nor=Norway, Pol=Poland, Sar=Sardinian, Spa=Spain, Tus=Tuscan.

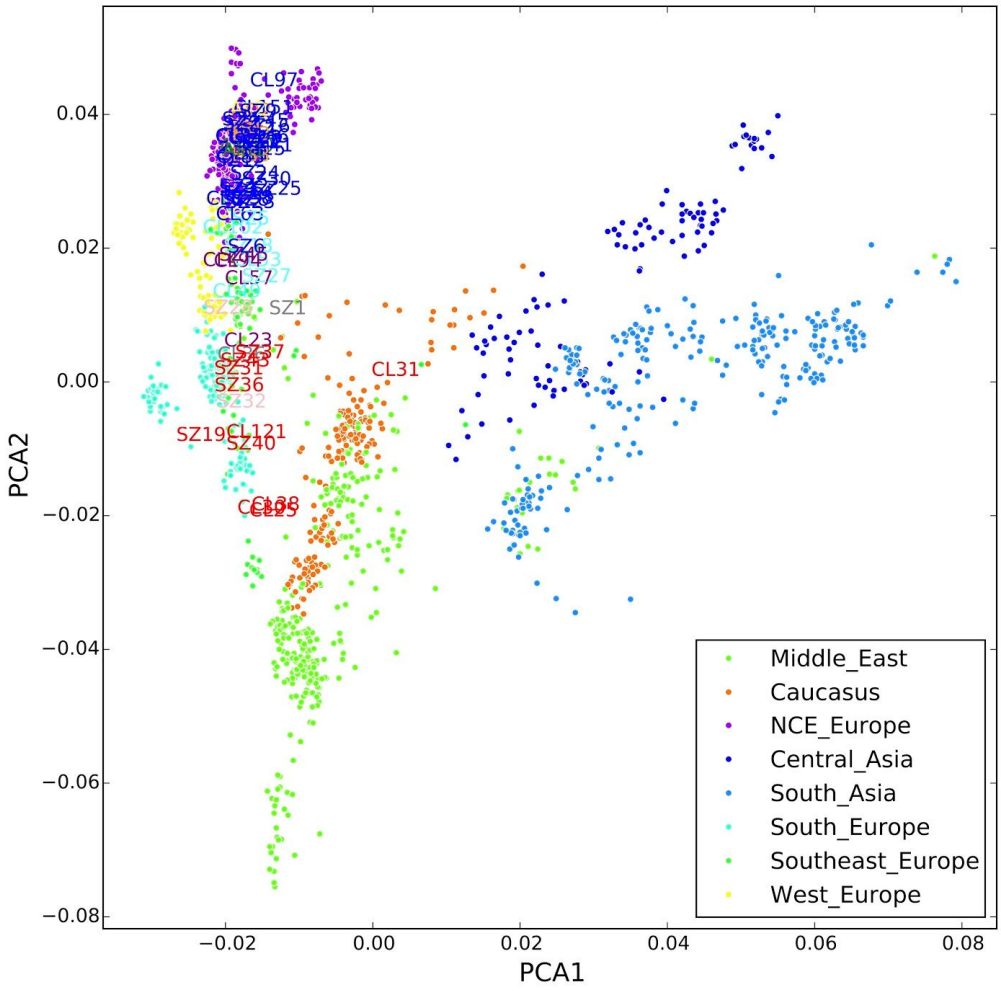

Figure S7.2. Procrustes transformed PCA of Medieval samples against HellBus imputed SNP dataset. Color coding of medieval samples is same as in Figs 1 and 2.

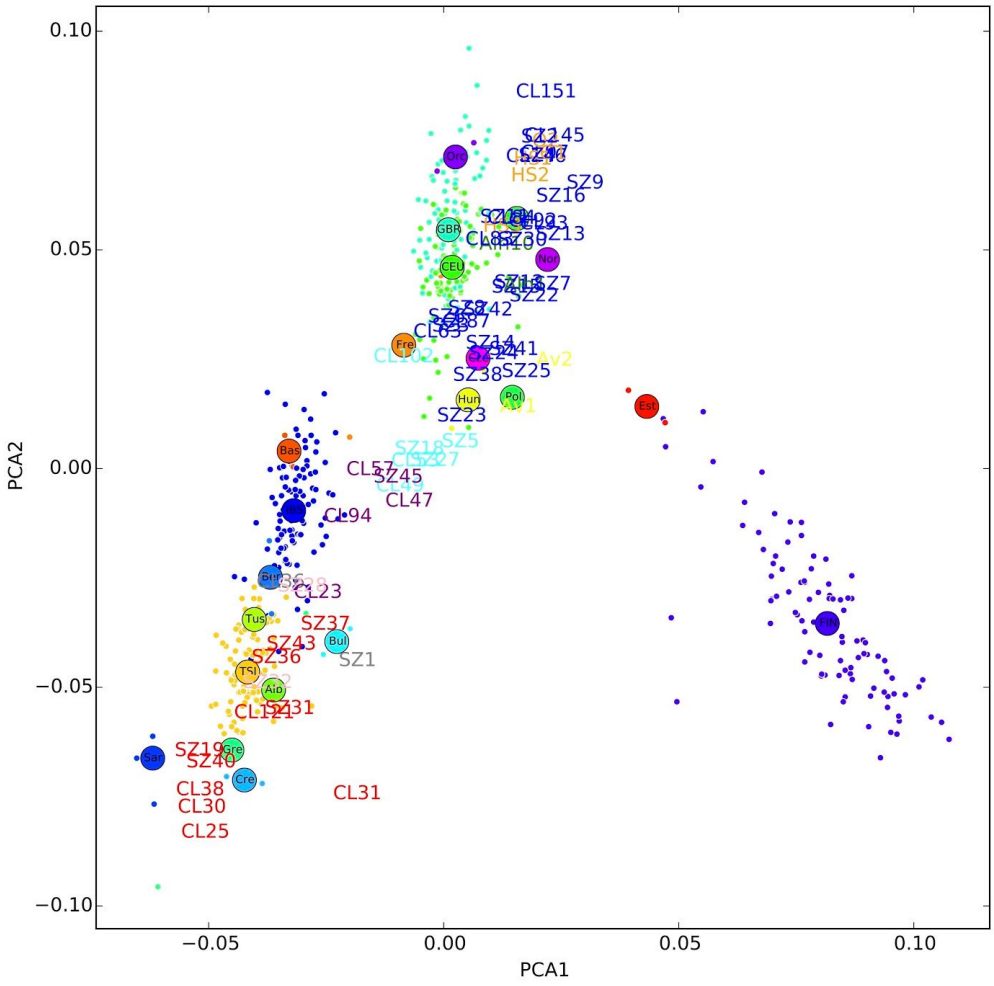

Figure S7.3. Procrustes transformed PCA of Medieval samples against 1000 Genomes + SGDP European samples. Color coding of medieval samples is same as in Figs 1 and 2. Three letter codes: Alb = Albania, Bas=Basque, Ber=Bergamo,Bul=Bulgaria, CEU=Northern and Western European Ancestry from 1000 Genomes , Cre = Crete, Cze=Czech Republic, Est=Estonia, Fre=France, FIN=Finland from 1000 Genomes, GBR=Britain from 1000 Genomes, Gre=Greece, Hun=Hungary, Ice=Iceland, IBS=Iberia from Spain 1000 Genomes, Nor=Norway, Orc=Orcadians, Pol=Poland, Sar=Sardinian, Spa=Spain, Tus=Tuscan, TSI=Tuscany from 1000 Genomes.

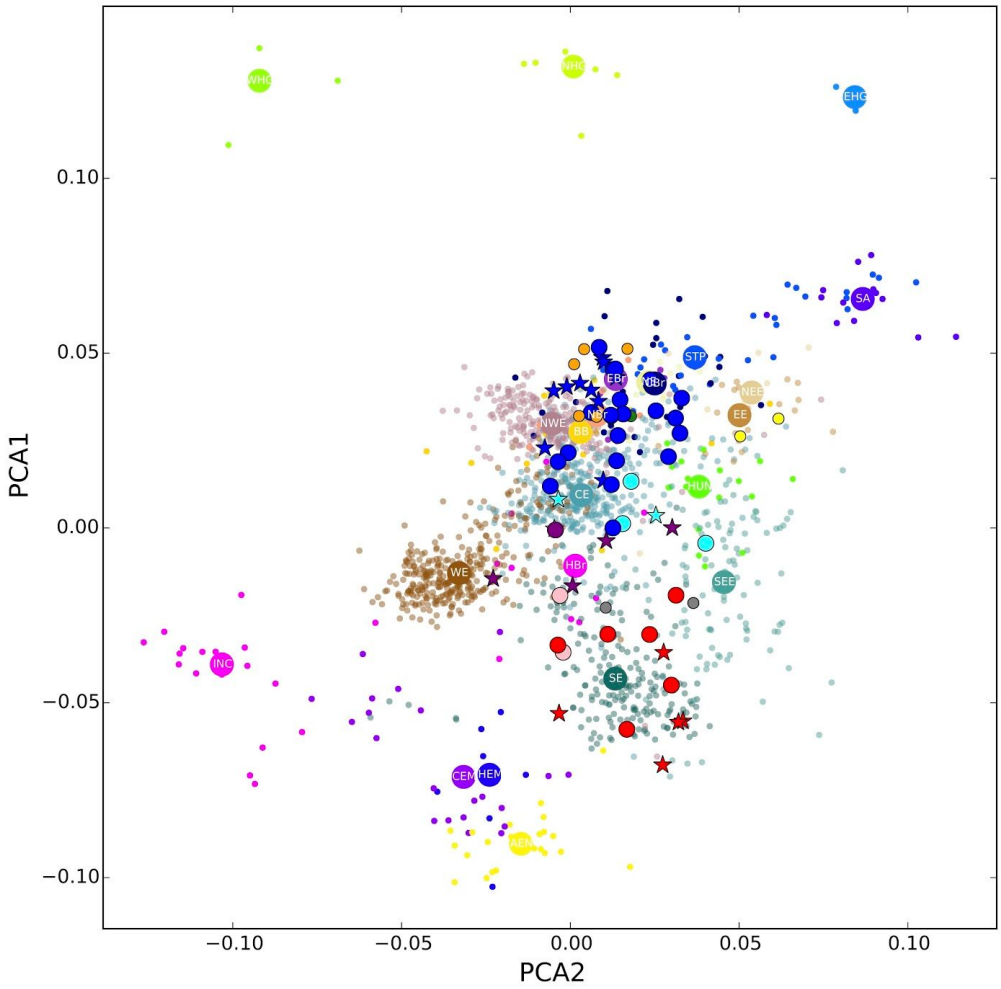

Figure S7.4. Procrustes transformed PCA of Medieval and prehistorical samples from Mathieson et al. against POPRES imputed SNP dataset. Color coding of medieval samples is same as in Figs 1 and 2. Labels for POPRES regions: NWE = northwest Europe, NE = modern north Europe, NEE = modern northeast Europe, CE =central Europe, EE = eastern Europe, WE =Western Europe, SE = southern Europe, SEE = southeast Europe. Labels from Mathieson et al.: WHG=Western hunter-gatherers, NHG=Northern hunter-gatherers, EHG=Eastern hunter=gatherers, NBr=Northern European Bronze Age, EBr=Eastern European Bronze Age, CBr=Central European Bronze Age, HBr=Hungarian Bronze Age, BB=Bell Beaker Europe, CEM=Central European Early and Middle Neolithic, HEM=Hungarian Early and Middle Neolithic, INC=Iberian Neolithic and Chacolithic, AEN=Anatolian Neolithic, SA=Steppe Ancestry.

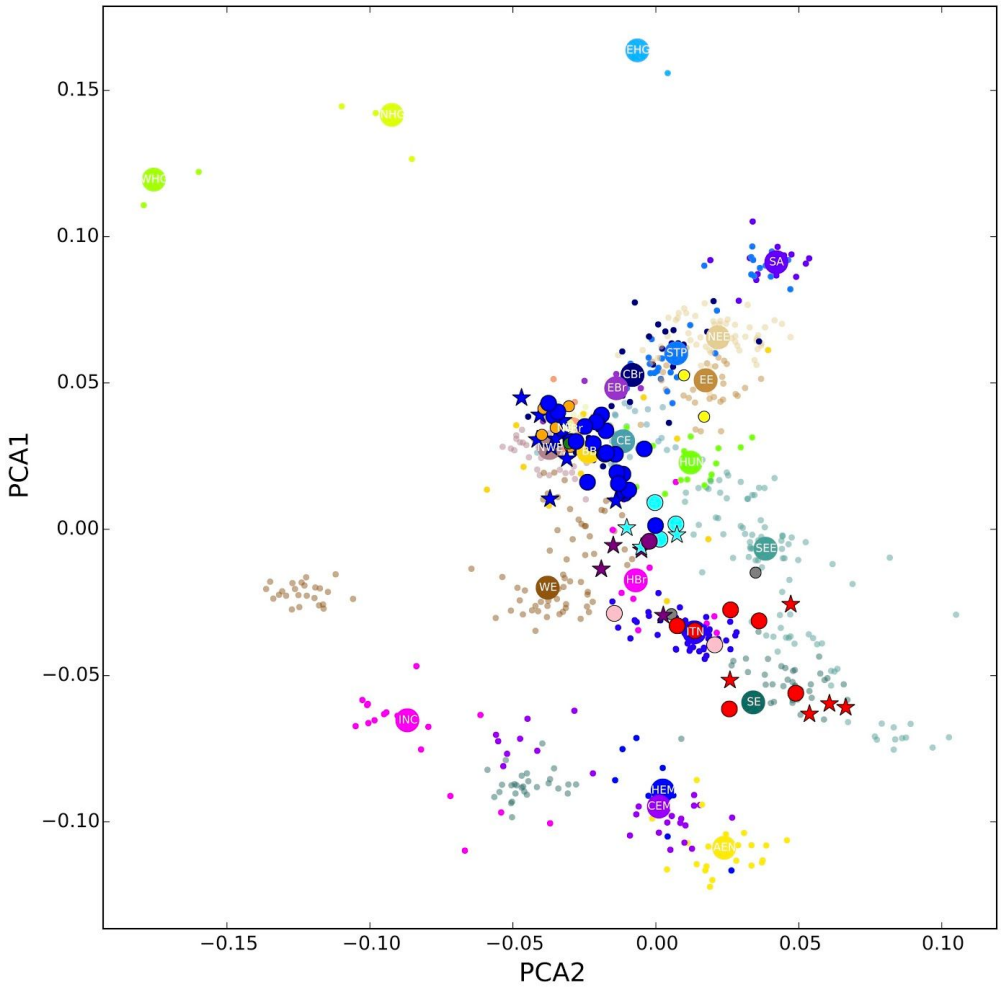

Figure S7.5. Procrustes transformed PCA of Medieval and prehistorical samples from Mathieson et al. against European HellBus imputed SNP dataset. Color coding of medieval samples is same as in Figs 1 and 2. Other coding same as for Figure S7.4.

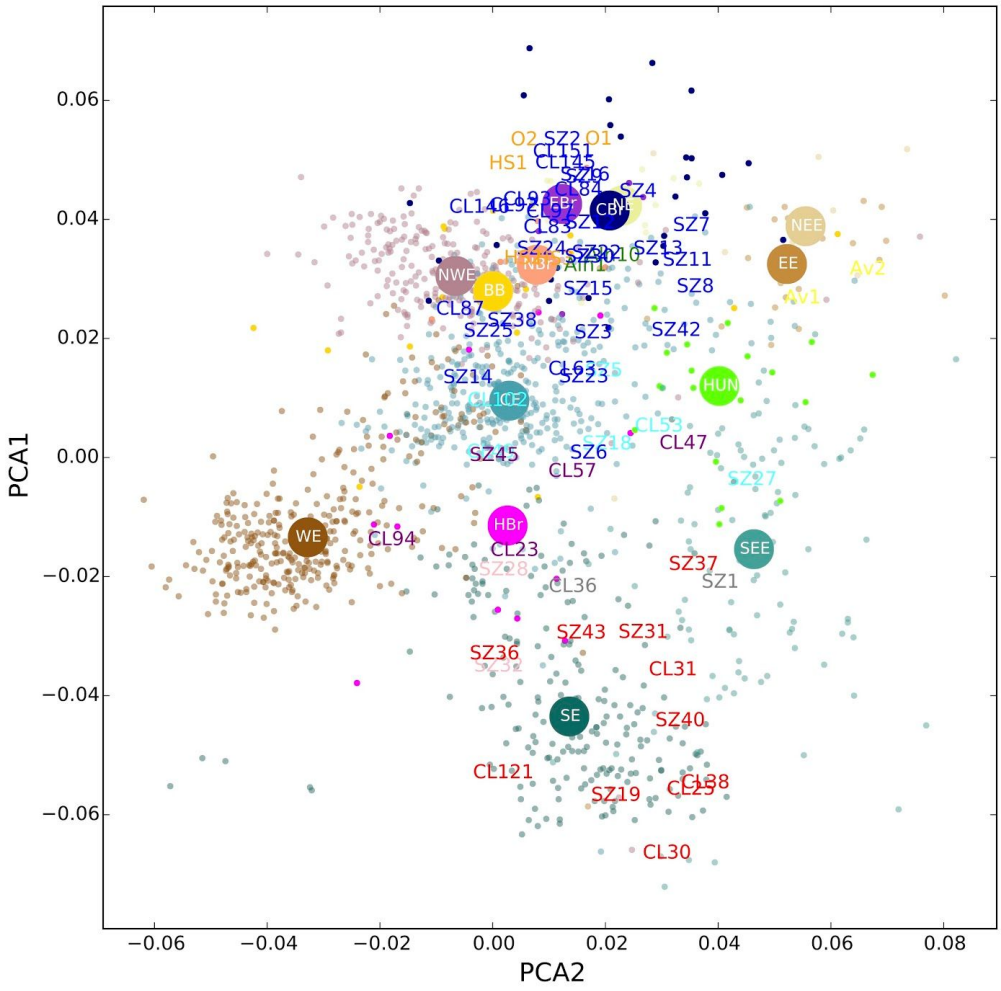

Figure S7.6. Procrustes transformed PCA of Medieval and Bronze Age samples from Mathieson et al. against POPRES imputed SNP dataset. Color coding of medieval samples is same as in Figs 1 and 2. Other coding same as for Figure S7.4.

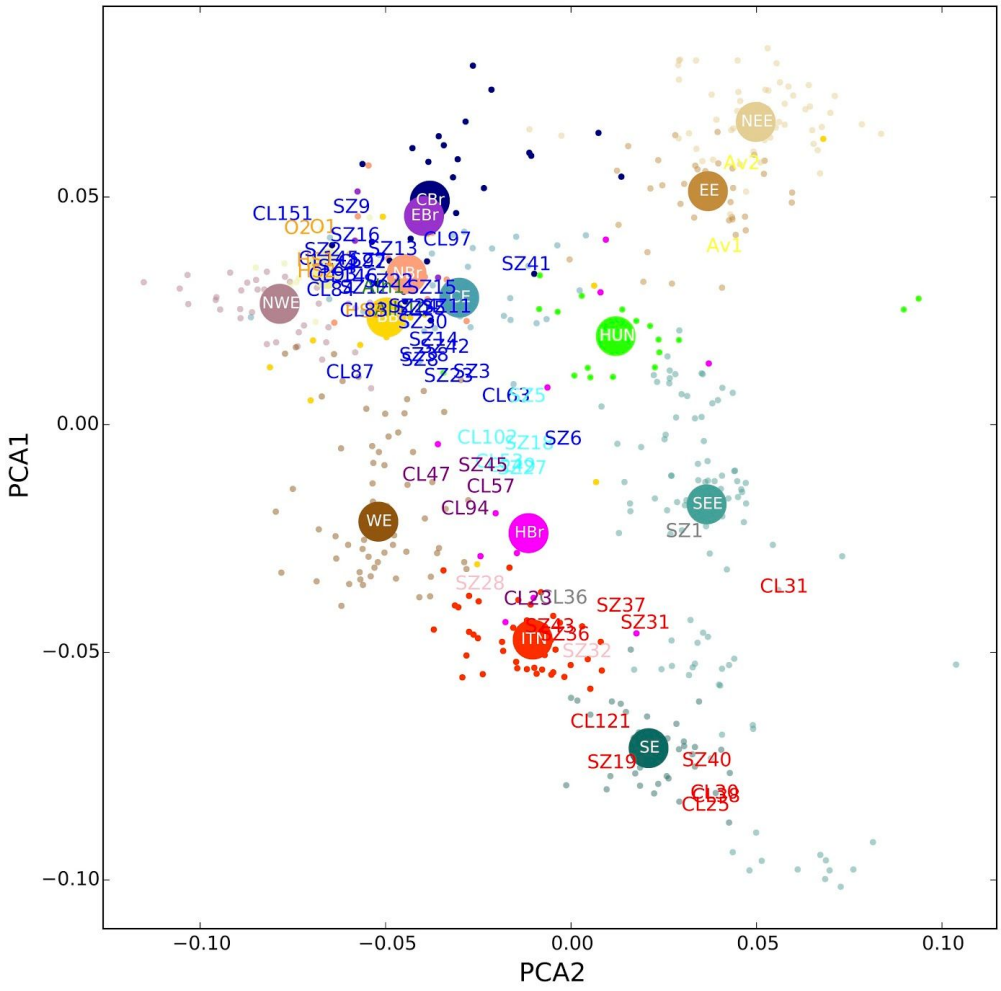

Figure S7.7. Procrustes transformed PCA of Medieval and Bronze Age samples from Mathieson et al. against European HellBus imputed SNP dataset. Colour coding of medieval samples is same as in Figs 1 and 2. Other coding same as for Figure S7.4.

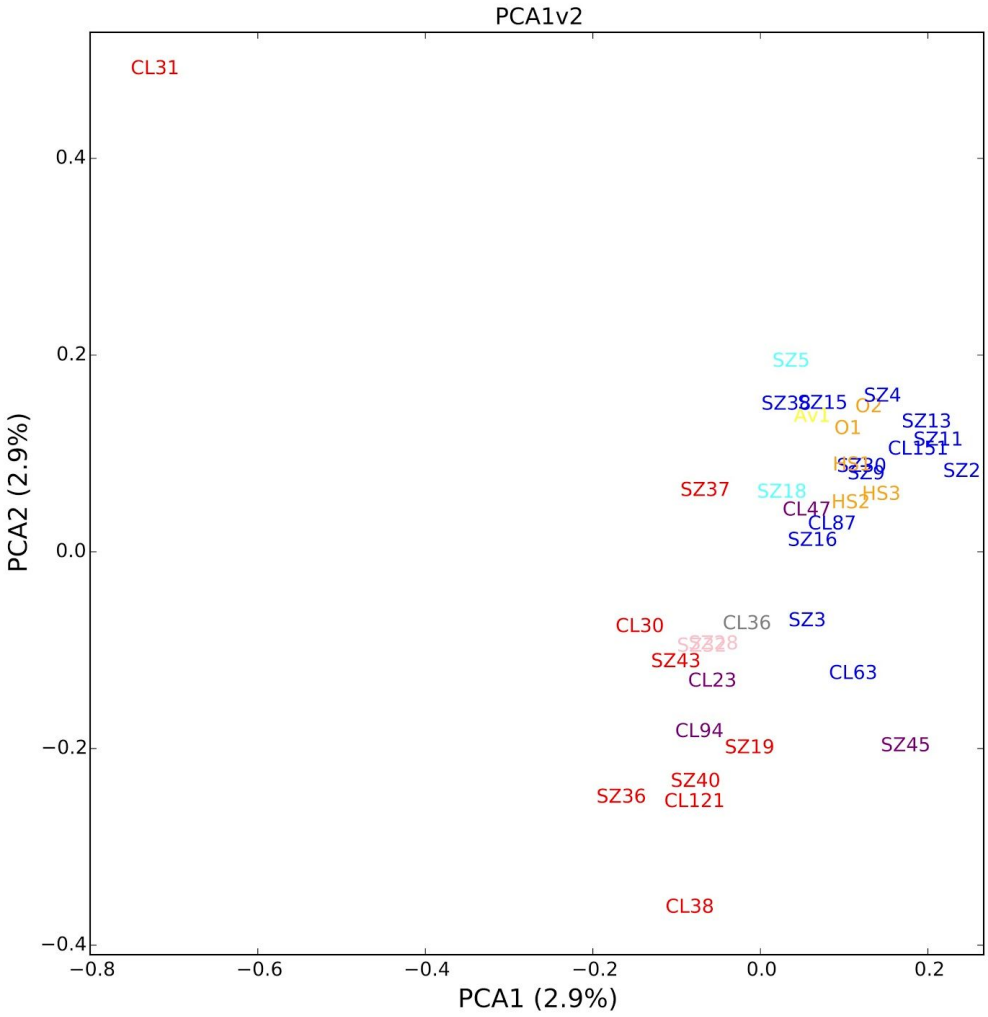

Figure S7.8. PCA of unrelated Medieval samples with no missing SNP positions amongst samples. Colour coding of medieval samples is same as in Figs 1 and 2.

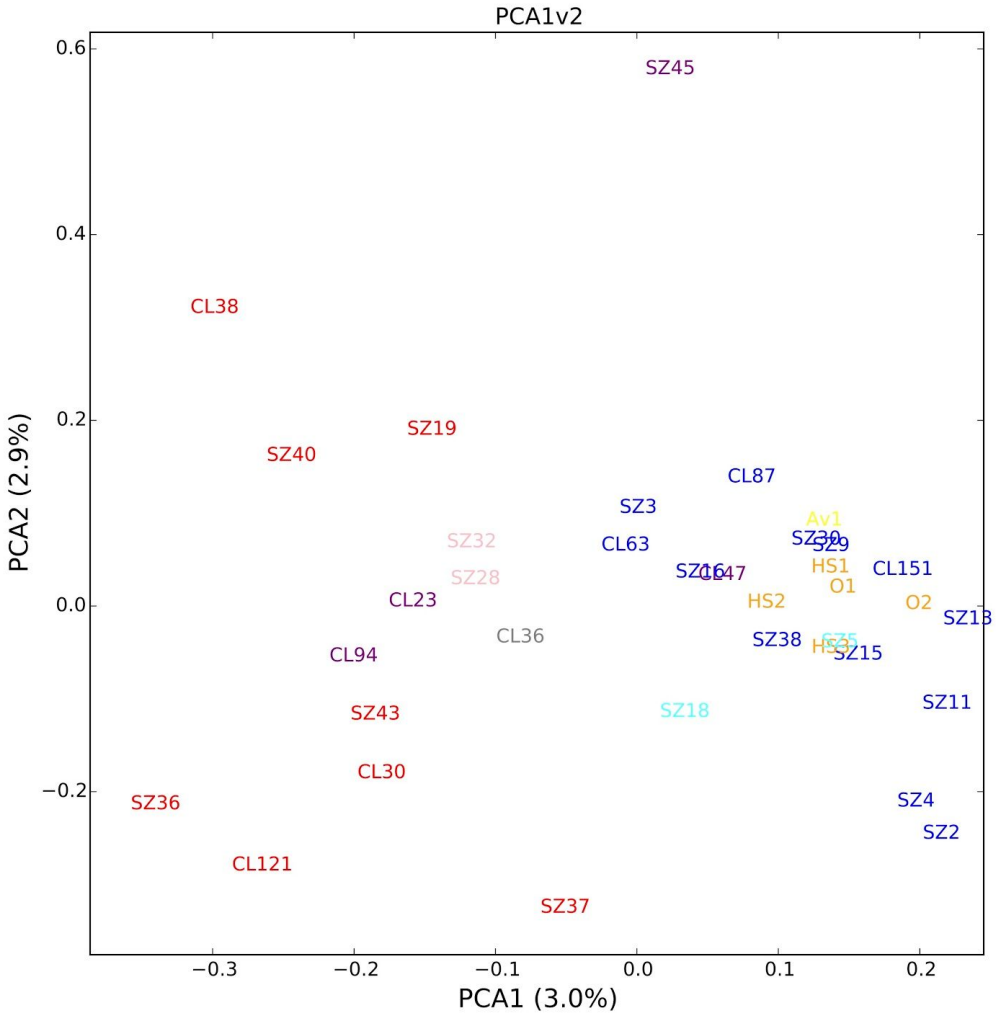

Figure S7.9. PCA of unrelated Medieval samples, excluding CL31, with no missing SNP positions amongst samples. Colour coding of medieval samples is same as in Figs 1 and 2.

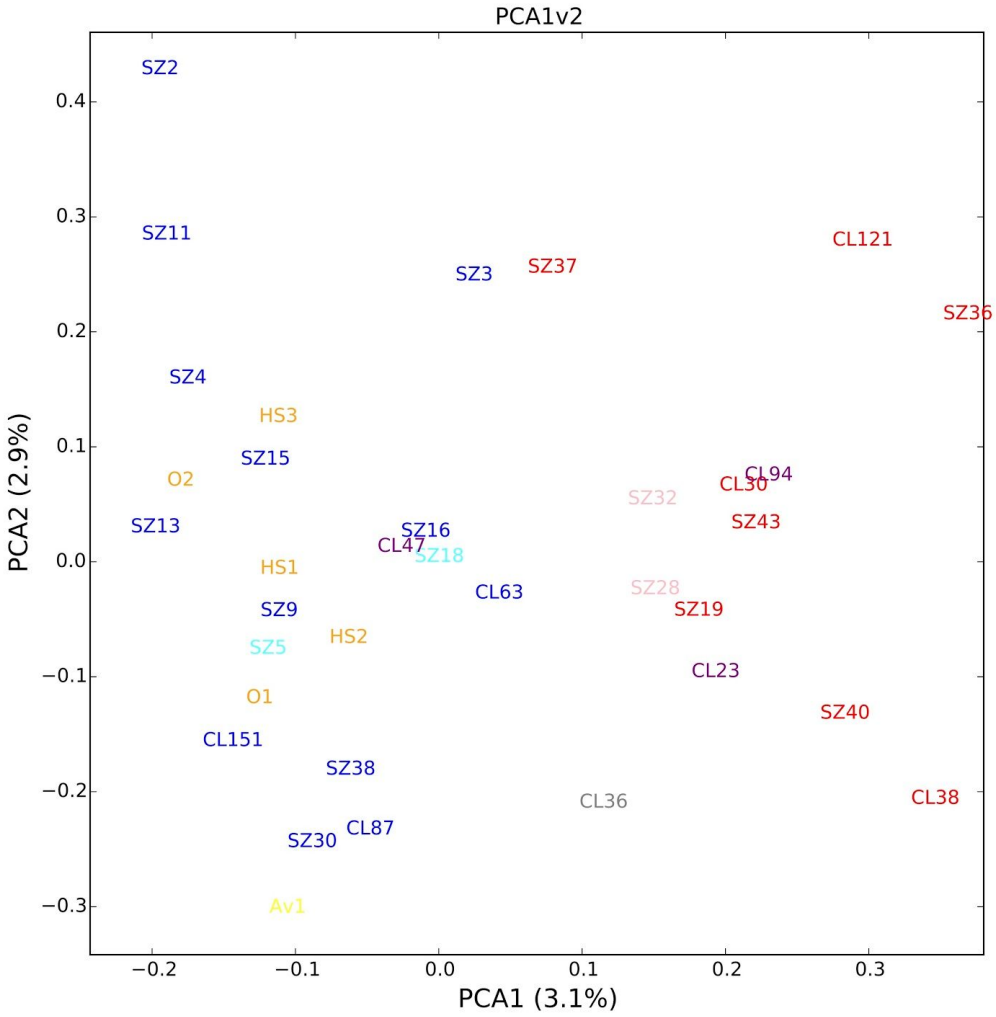

Figure S7.10. PCA of unrelated Medieval samples, excluding CL31 and SZ45, with no missing SNP positions amongst samples. Colour coding of medieval samples is same as in Figs 1 and 2.

S8. MODEL-BASED CLUSTERING ANALYSIS

Carlos Eduardo G. Amorim, Krishna R. Veeramah

All model-based clustering analysis was implemented using ADMIXTURE[80]. We performed two primary analyses, the first to understand how our Medieval samples were related to modern samples, and second to explore to what extent their ancestry was shaped by the three major prehistoric groups.

Given that the PCA showed that all our Medieval samples contained primarily European genetic variation, we performed a supervised ADMIXTURE analysis, treating samples from the 1000 Genomes FIN, CEU, GBR, IBS and TSI populations as 5 distinct parental groups (i.e. K was set to 5). We also performed the analysis using the same groupings as well all South Asian (SAS), East Asian (EAS) and Yoruba (YRI) being treated as 3 additional parental groups (i.e. K=8). Following the procedure for PCAs above, a separate supervised ADMIXTURE analysis was performed for each medieval sample alongside modern reference samples, with no SNPs analyzed with any missing data and LD filtering for cases with more than 100,000 SNPs. For K=5, each sample was analyzed 10 times with different random seeds and the run with the highest likelihood taken as the final result. However, for K=8 we restricted ourselves to a single run per sample due to the extra computational burden (though we note that the best K=5 results are highly concordant with our K=8 runs).

SGDP European (for K=5) and SGDP Eurasian (for K=8) whole genomes were also included in each of these analyses. These acted as control samples, allowing us to examine to what extent ancestry estimates were varying as result of the different SNP

positions potentially used for each Medieval sample. We found that while estimates of FIN, IBS and TSI ancestry were fairly consistent for the SGDP samples (especially when limiting to Medieval samples with at least 50,000 callable SNPs, estimates for CEU and GBR showed much more variation (Figure S8.1-5). However, summing these two ancestry estimates together gave much narrower ranges (Figure S8.6), suggesting that ADMIXTURE was having difficulty distinguished CEU and GBR ancestry because of their low genetic divergence. Therefore we report all results combining estimates for CEU and GBR.

Overall, results were concordant with the PCA analysis, with samples primarily of either CEU+GBR ancestry or TSI ancestry corresponding with samples placed near northern and southern European populations in the PCA (Fig 2A). We devised a crude color-based grouping system based on relative amounts of ancestry to demonstrate this concordance: >70% CEU+GBR+FIN = blue, majority CEU+GBR+FIN = cyan, >70% TSI = red, majority TSI = pink, majority TSI+IBS = purple. We note these are not intended to provide population genetic robust groupings, simply to aid visualizing the connection between the model-free PCA and model-based ADMIXTURE plots. It appears that northern samples in Szólád appear to have greater FIN ancestry than those from Collegno in general, though it is a minor component regardless. Estimates of the four European ancestry coefficients were highly robust when increasing K=5 (Figure S8.7-9) to K=8 (Fig 2B,C, Figure S8.10) using additional non-European parental populations, the major noticeable difference being the 20% EAS component for CL31, though results for this sample are unreliable because of high estimated contamination (Table S4.1).

Given that modern European genetic variation demonstrates a strong isolation-by-distance pattern as seen in PCA rather than distinct clusters, we also estimated ancestry coefficients for K=5 for all POPRES European individuals, and overlaid the relative individual values on the corresponding PCA. This would provide better context for interpreting our Medieval ADMIXTURE ancestry results (for example, what does having high TSI ancestry actually mean given such a strong continuous isolation-by-distance pattern in Europe?). All five 1000 Genomes populations show the strongest signals closest to POPRES populations from their region of interest (Figure S8.11-15). However their specific distributions that are useful indicators of their meaning. Firstly, FIN ancestry is fairly modest, even in North East Europe, with only the Finnish POPRES individual demonstrating 100% ancestry, reflecting this populations high levels of genetic drift/low N_e and historic inbreeding. Northern Western and Northern/Central Europe is dominated by CEU and GBR ancestry, though there is less smoothness to this relationship compared to IBS and TSI. However, while IBS ancestry is highly localized to the Iberian peninsula, TSI ancestry is highest in both southern Italy and parts of South East Europe.

Our use of modern samples as surrogates for ancestral populations for the Medieval samples was guided by the fact that the latter are temporally quite close, and thus we hypothesized that fifth to sixth century European population structure would likely be fairly well approximated by modern European population structure. However, it also might be of interest to examine these patterns within the context of the three major European prehistorical ancestry groups. Therefore we performed a supervised

ADMIXTURE analysis with K=3, with a hunter-gatherer (WHG) ancestral population consisting of all northern and western hunter-gatherers (n=9), an EEF ancestral population consisting of all Anatolian Neolithic farmers (n=24) and an SA ancestral population consisting of 15 samples from the Yamnaya culture. Unlike the previous analysis, because of the limited SNP data in the Mathieson ancient samples because of uneven coverage, we did not perform individual analysis for each Medieval individual. Instead a set of 42 unrelated individuals were identified and analyzed simultaneously with the remaining Mathieson samples as well as either POPRES or HellBus European samples. LD filtering was again performed prior to analysis. Ten runs with random seeds were performed and the run with the highest likelihood used to in the final analysis. There are two sets of results for the Medieval samples, one for the POPRES samples and one for the HellBus samples. We report the latter due to the increased number of SNPs overlapping with the 1240K but the former was very similar.

Almost every individual contains ancestry from each of the three ancestral groups (the exception being CL30 which lacks any WHG ancestry) (Figure S8.16). However, the relative amounts were highly variable amongst individuals. To better visualize these ancestry components we performed PCA using the `prcomp` function in R based on the three `ADMIXTURE` coefficients (not the actual SNP data) for all unrelated Medieval samples, all POPRES individuals and all European HellBus individuals. The resulting plot (Figure S8.17) large recapitulates the PCA analysis based on SNP data, with regard to both modern European population structure and the relative placement of the Medieval samples. However, this analysis also reveals to what extent this pattern is driven by the

three prehistorical ancestry groups. Southern European ancestry is primarily driven by Neolithic farming ancestry, while northwestern and northeastern Europe have increased hunter-gatherer and steppe ancestry respectively. Adding European Bronze Age samples to this analysis again largely matches the PCA analysis, though there is stronger differentiation of some Bronze Age samples from Modern samples along the steppe-dominated space (Figure S8.18). Once again, neither Bronze age or modern Hungarian samples show much overlap in ancestry with samples from Szólád.

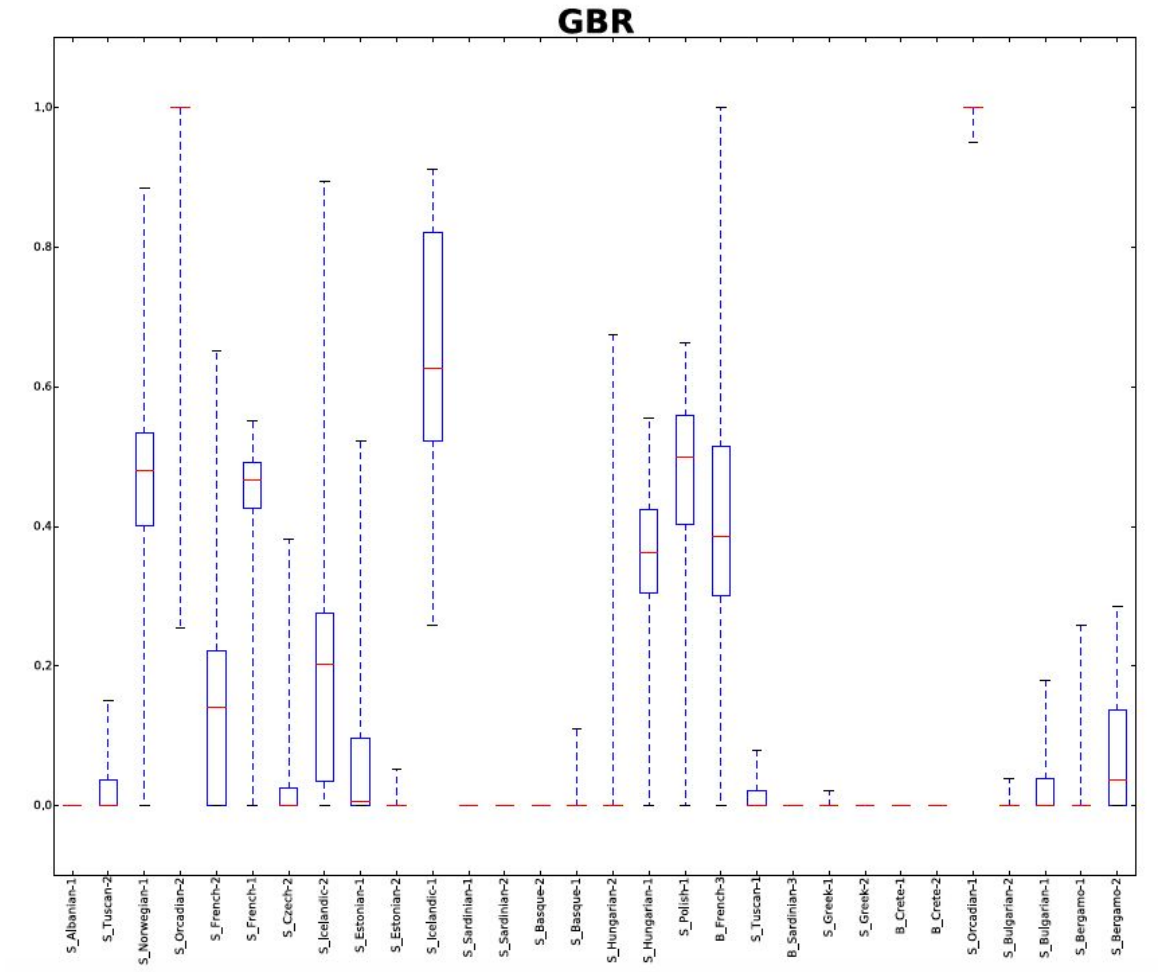

Figure S8.1. Boxplot of GBR Ancestry coefficients for SGDP European samples analyzed alongside individual Medieval samples.

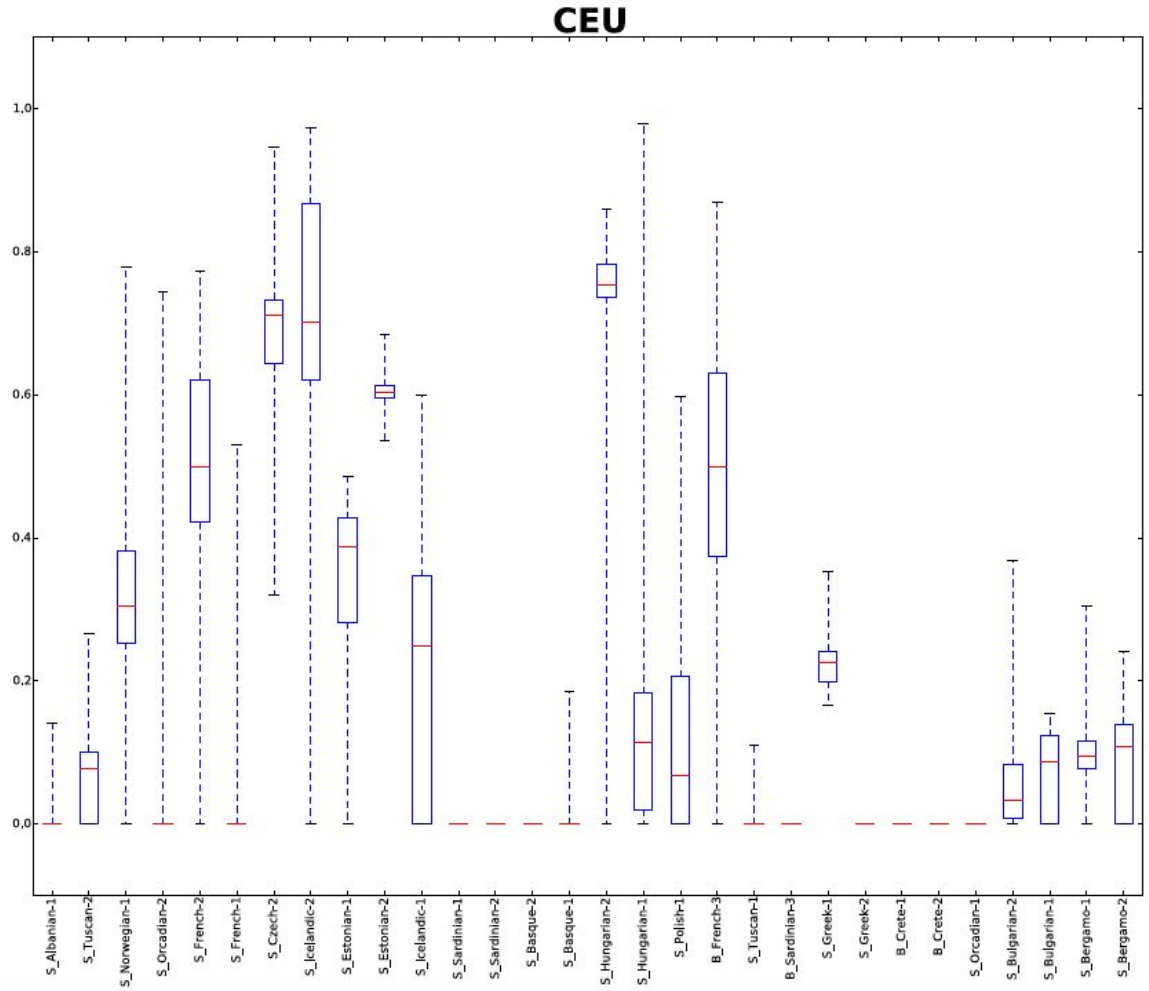

Figure S8.2. Boxplot of CEU Ancestry coefficients for SGDP European samples analyzed alongside individual Medieval samples.

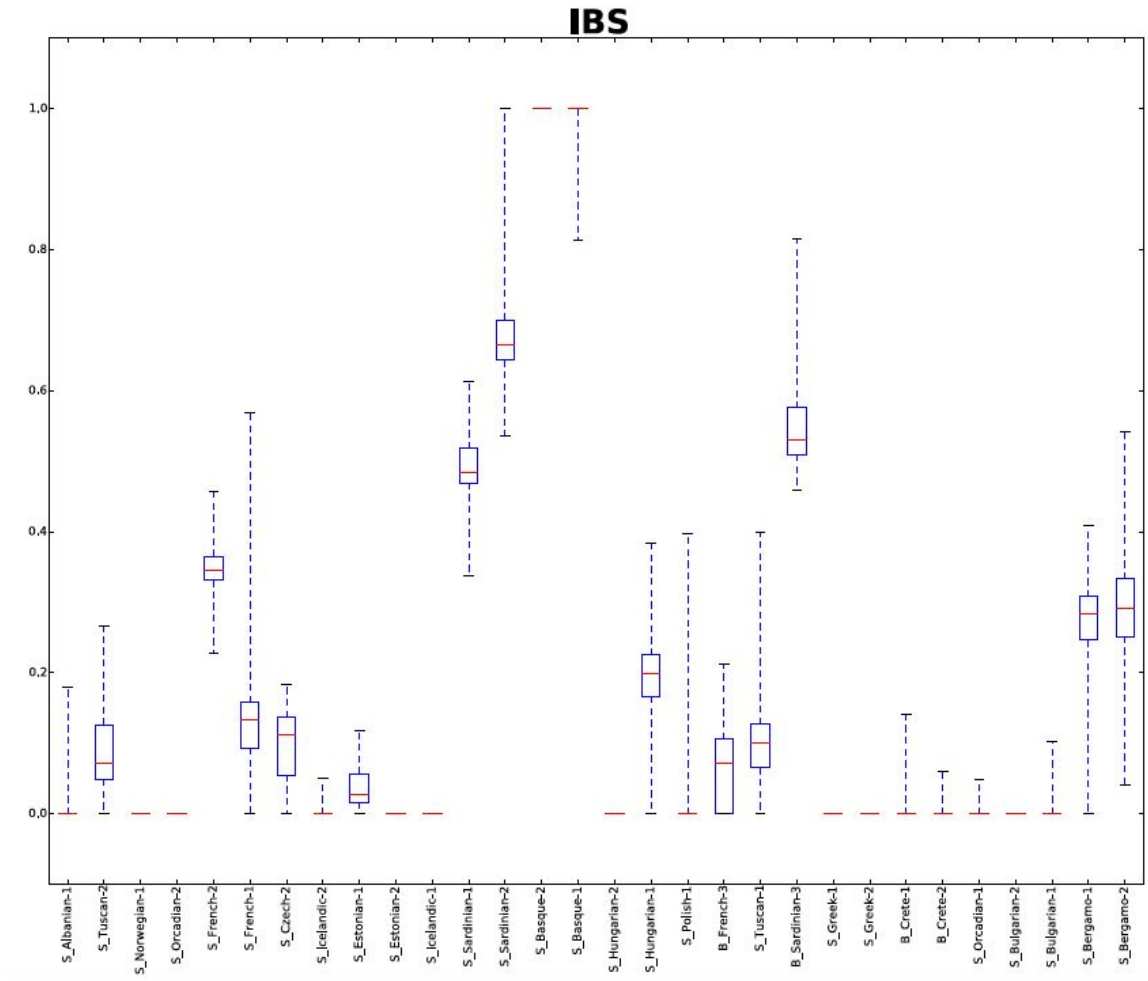

Figure S8.3. Boxplot of IBS Ancestry coefficients for SGDP European samples analyzed alongside individual Medieval samples.

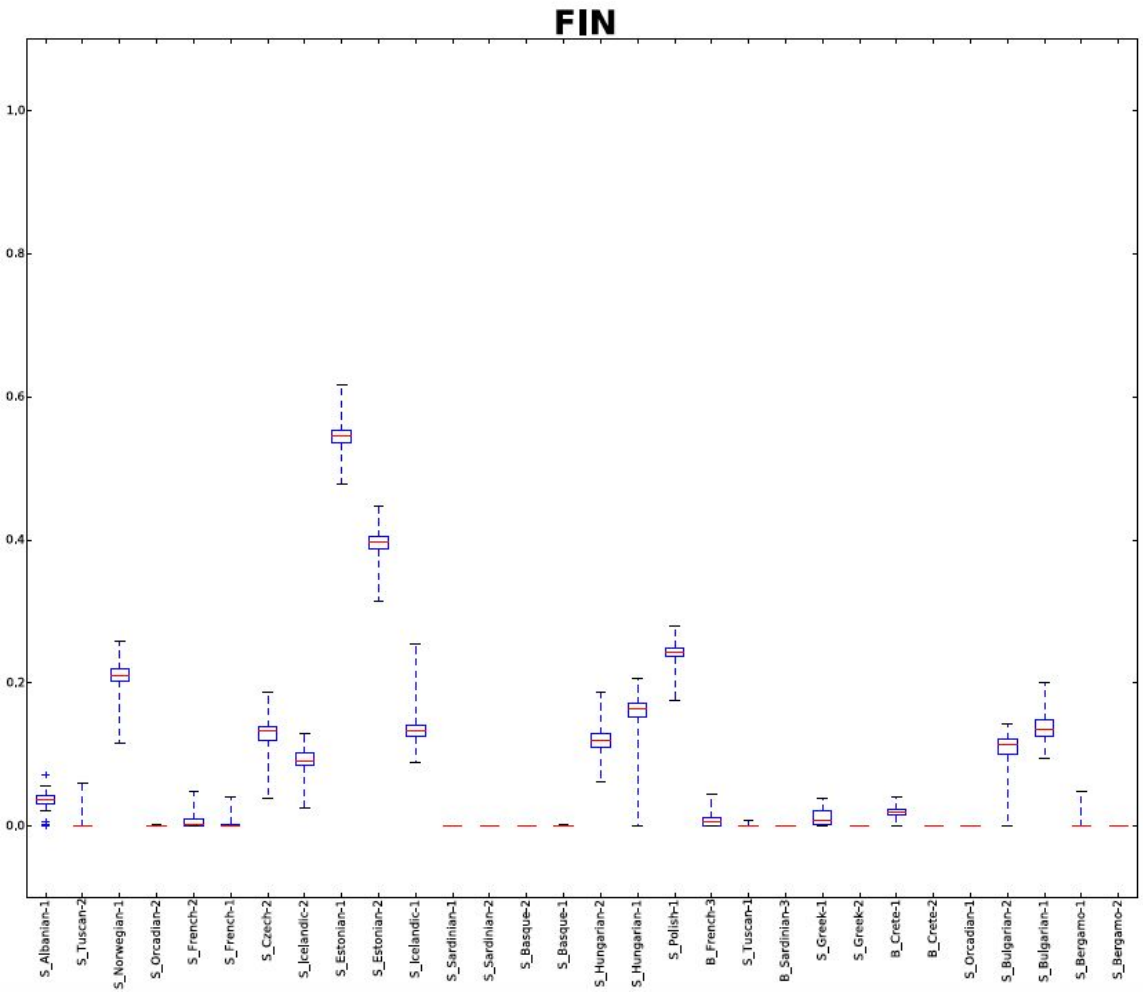

Figure S8.4. Boxplot of FIN Ancestry coefficients for SGDP European samples analyzed alongside individual Medieval samples.

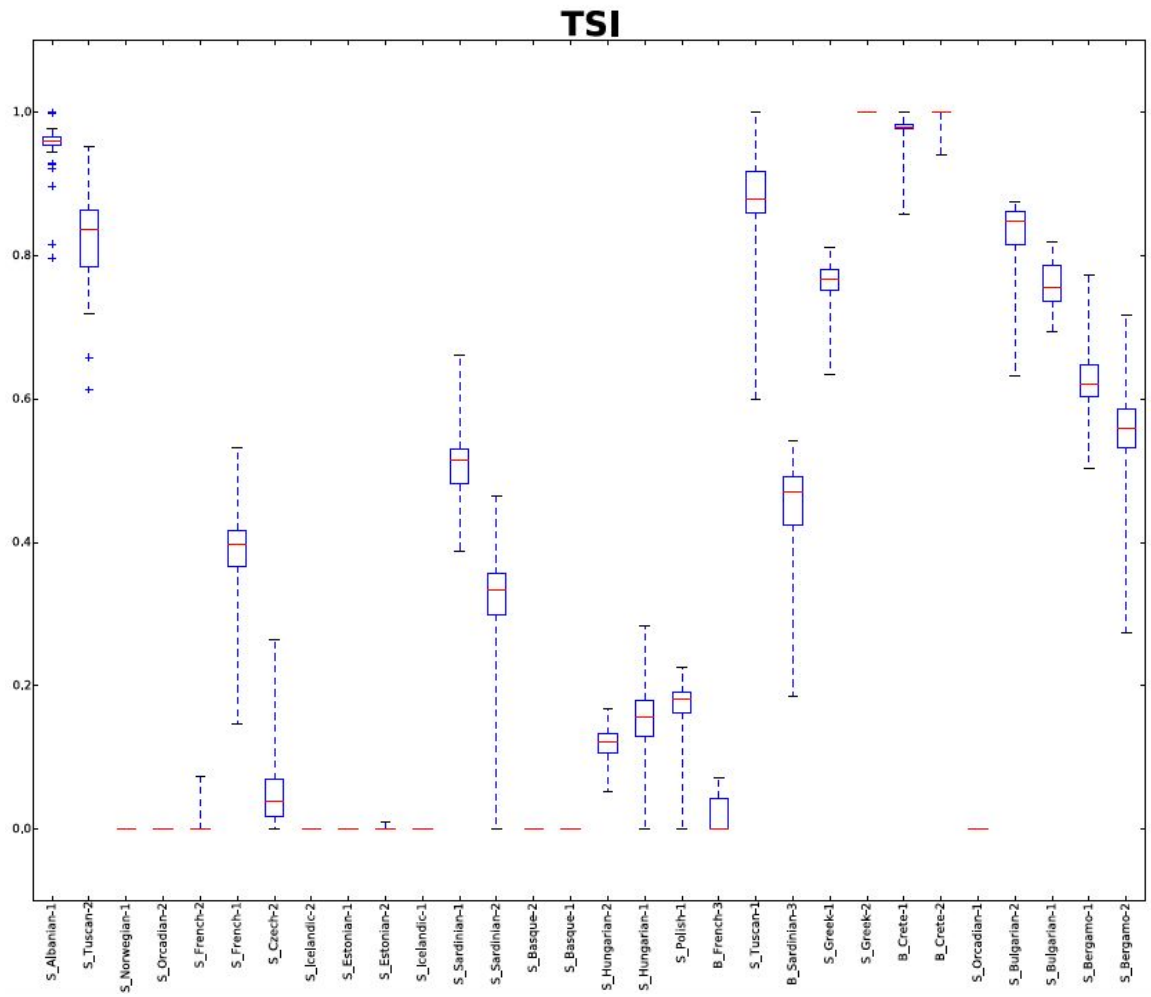

Figure S8.5. Boxplot of TSI Ancestry coefficients for SGDP European samples analyzed alongside individual Medieval samples.

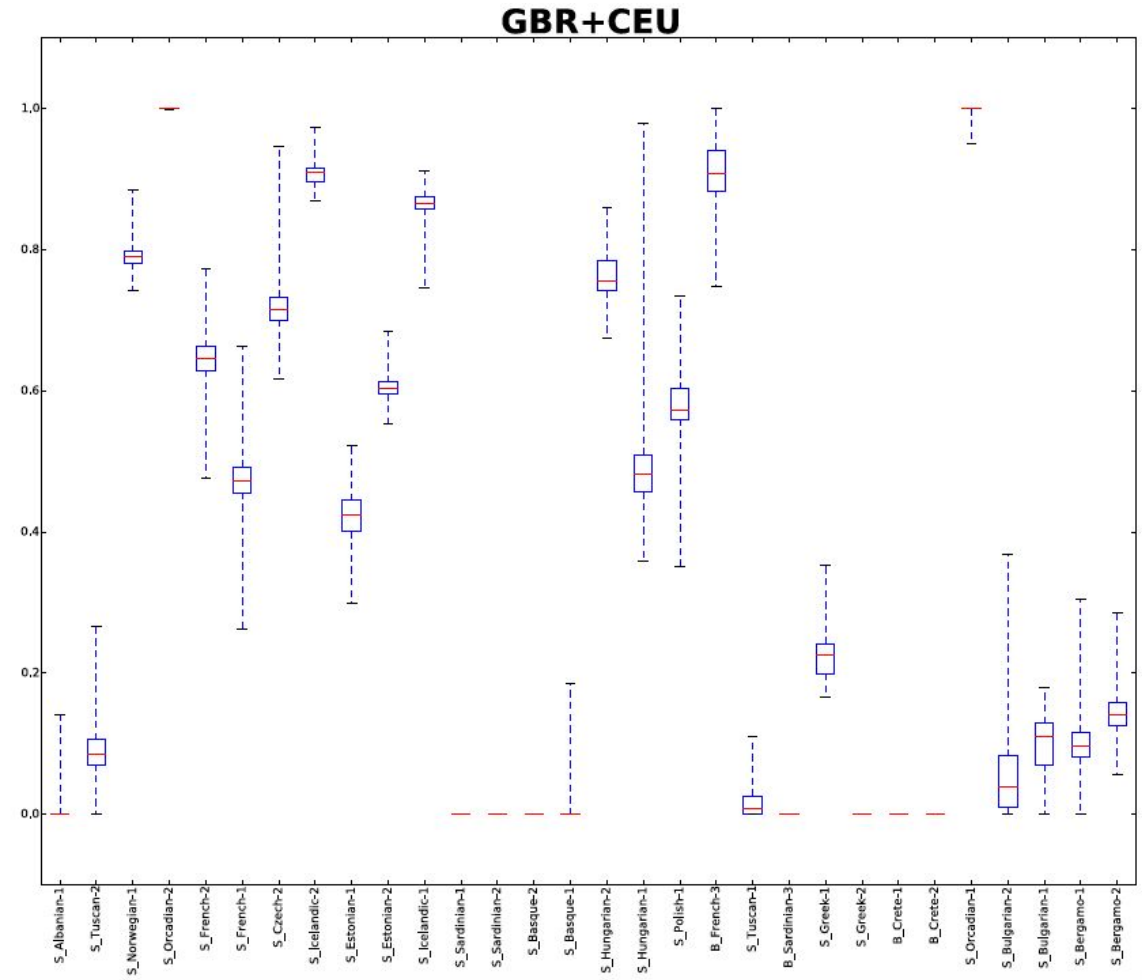

Figure S8.6. Boxplot of GBR+CEU Ancestry coefficients for SGDP European samples analyzed alongside individual Medieval samples.

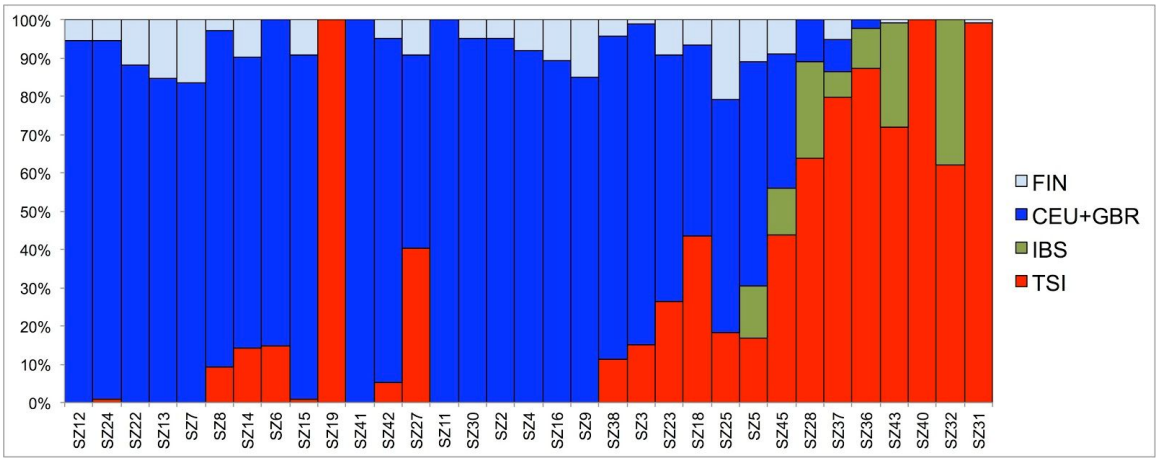

Figure S8.7. Supervised ADMIXTURE ancestry estimation for K=5 for Szólád sixth century samples.

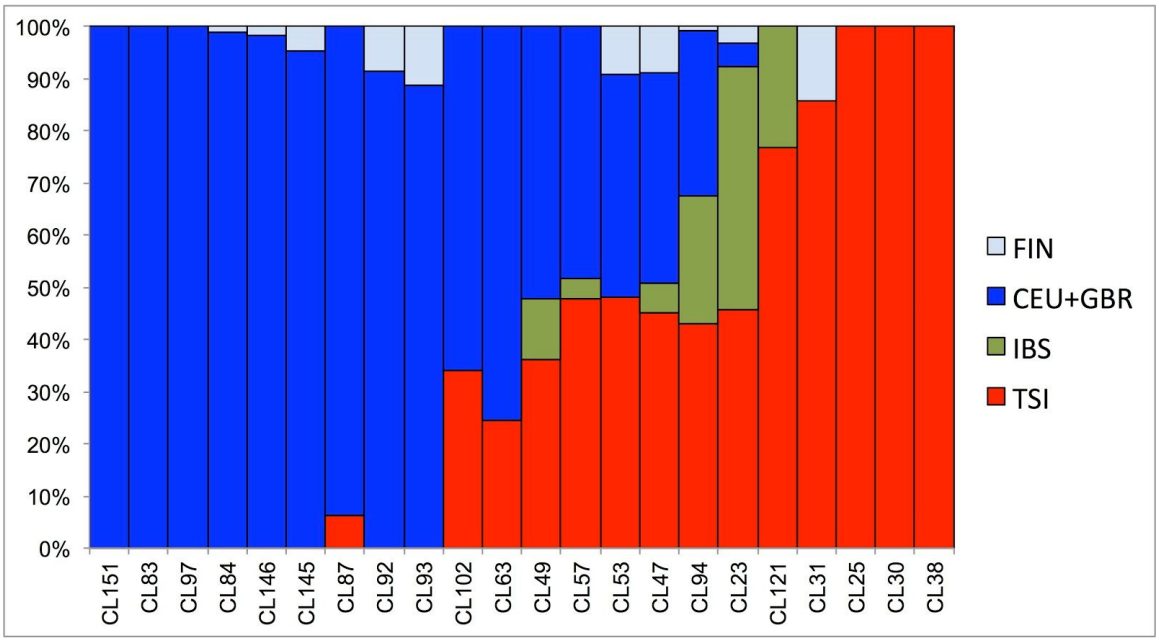

Figure S8.8. Supervised `ADMIXTURE` ancestry estimation for K=5 for Collegno first period samples.

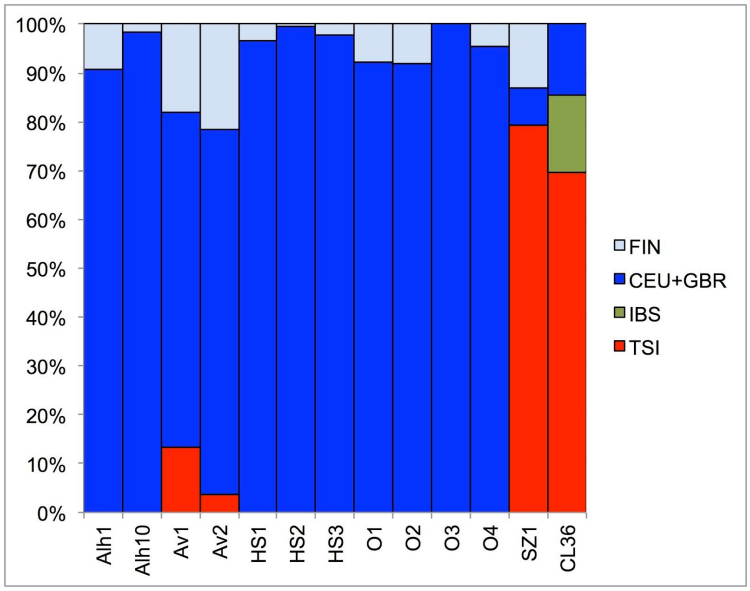

Figure S8.9. Supervised `ADMIXTURE` ancestry estimation for K=5 for other Medieval samples and SZ1.

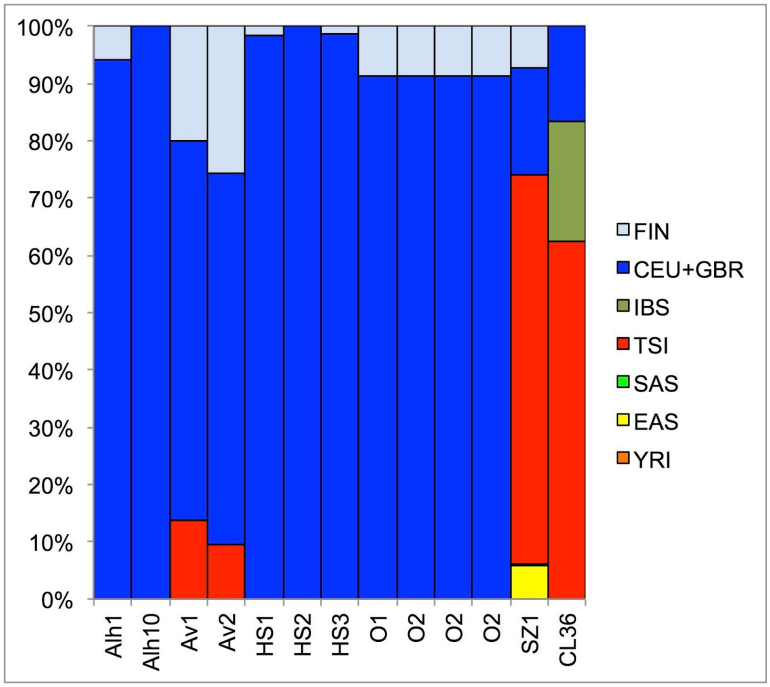

Figure S8.10. Supervised ADMIXTURE ancestry estimation for K=8 for other Medieval samples and SZ1.

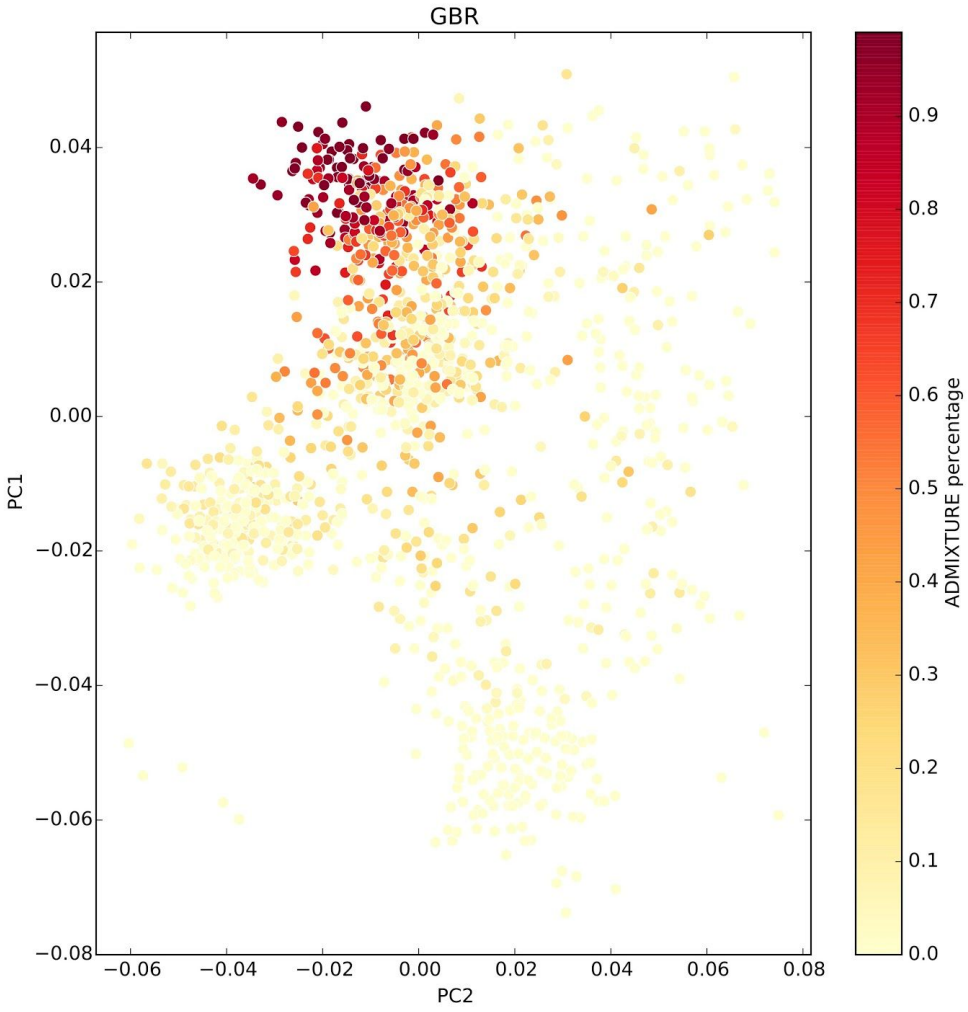

Figure S8.11. Supervised `ADMIXTURE` estimates for GBR when K=5 for POPRES samples overlaid on PCA.

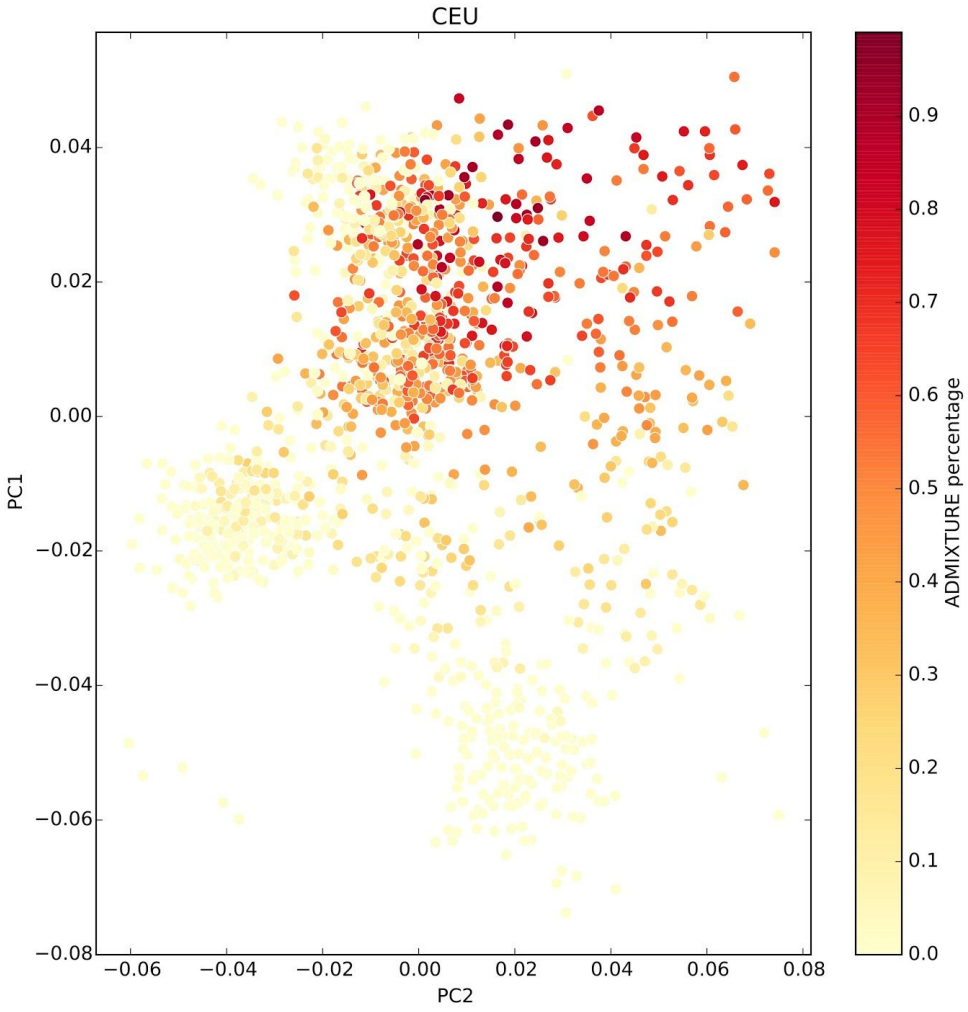

Figure S8.12. Supervised `ADMIXTURE` estimates for CEU when K=5 for POPRES samples overlaid on PCA.

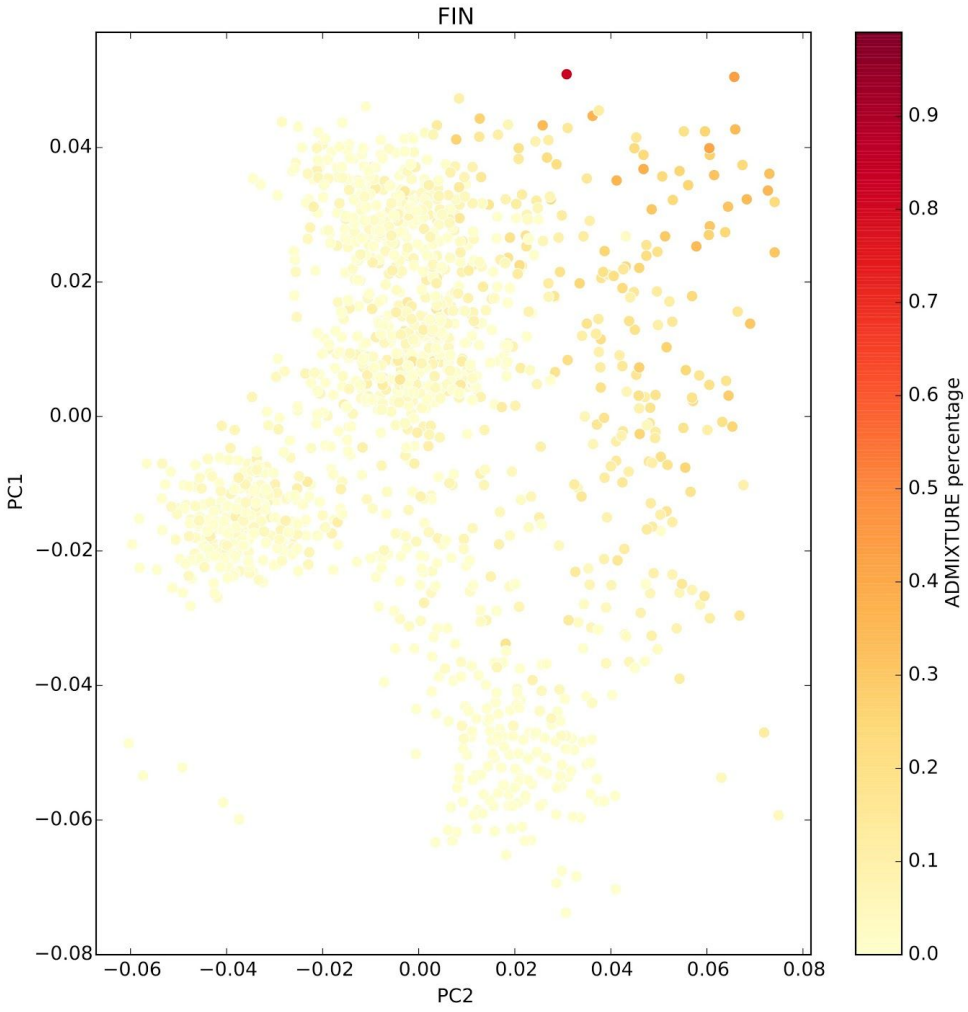

Figure S8.13. Supervised `ADMIXTURE` estimates for FIN when K=5 for POPRES samples overlaid on PCA.

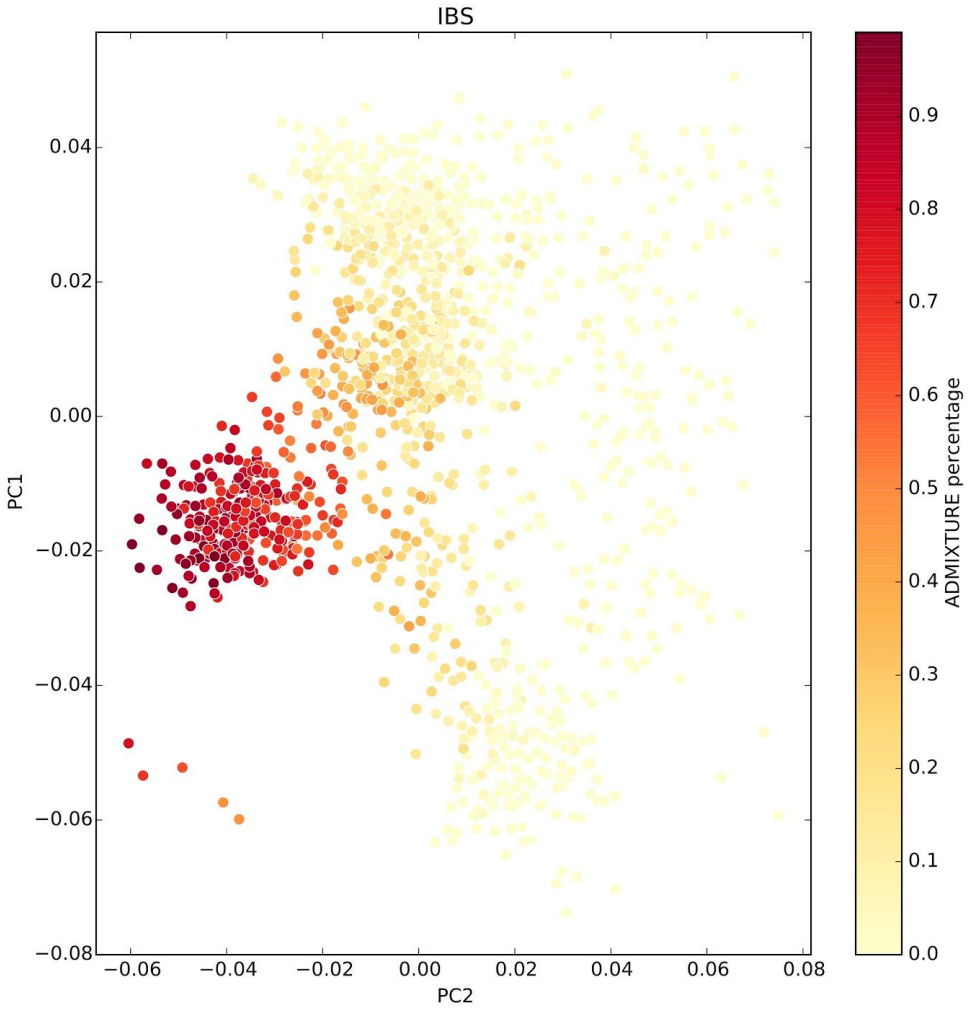

Figure S8.14. Supervised `ADMIXTURE` estimates for IBS when K=5 for POPRES samples overlaid on PCA.

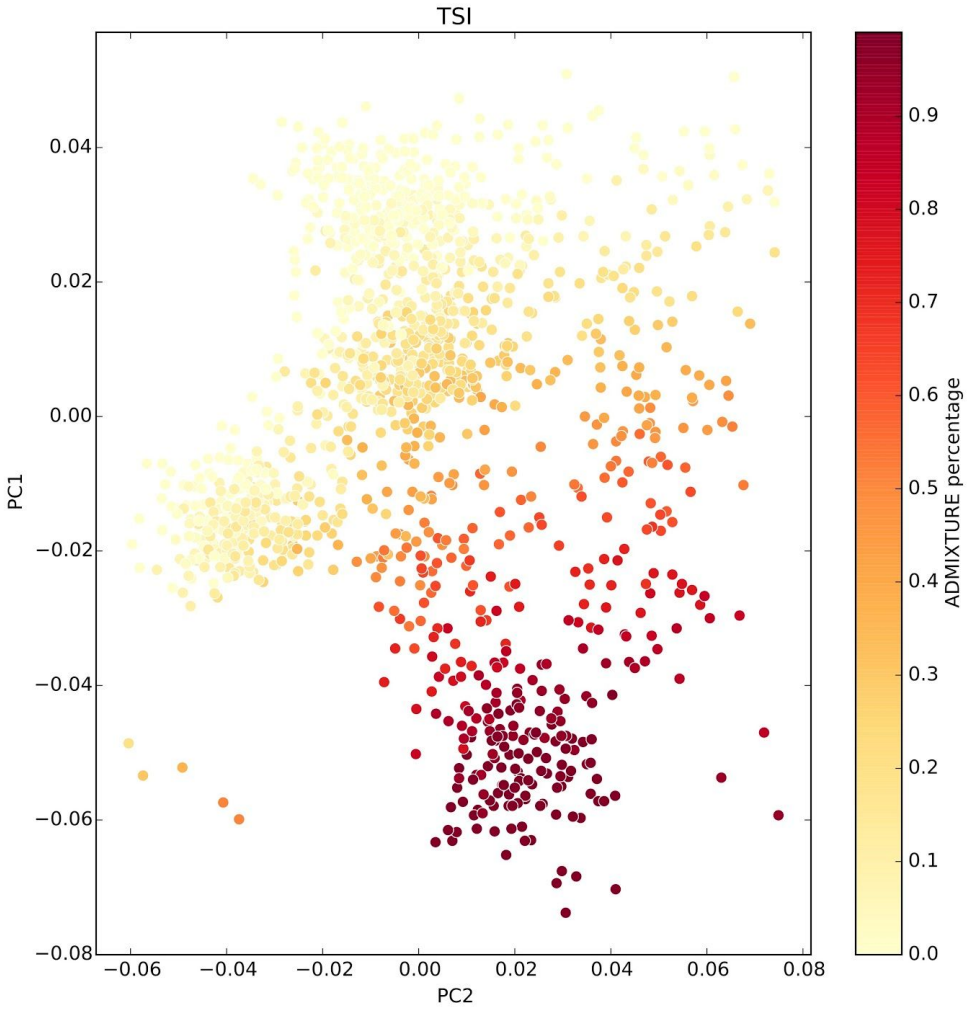

Figure S8.15. Supervised `ADMIXTURE` estimates for TSI when K=5 for POPRES samples overlaid on PCA.

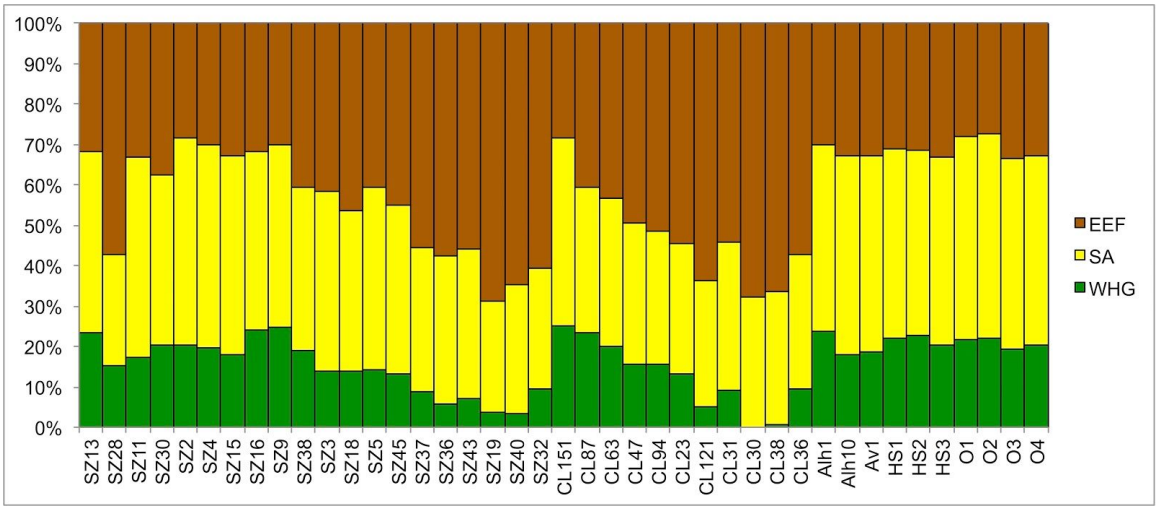

Figure S8.16. Supervised `ADMIXTURE` estimates for unrelated Medieval sample for K=3 using prehistorical parental populations.

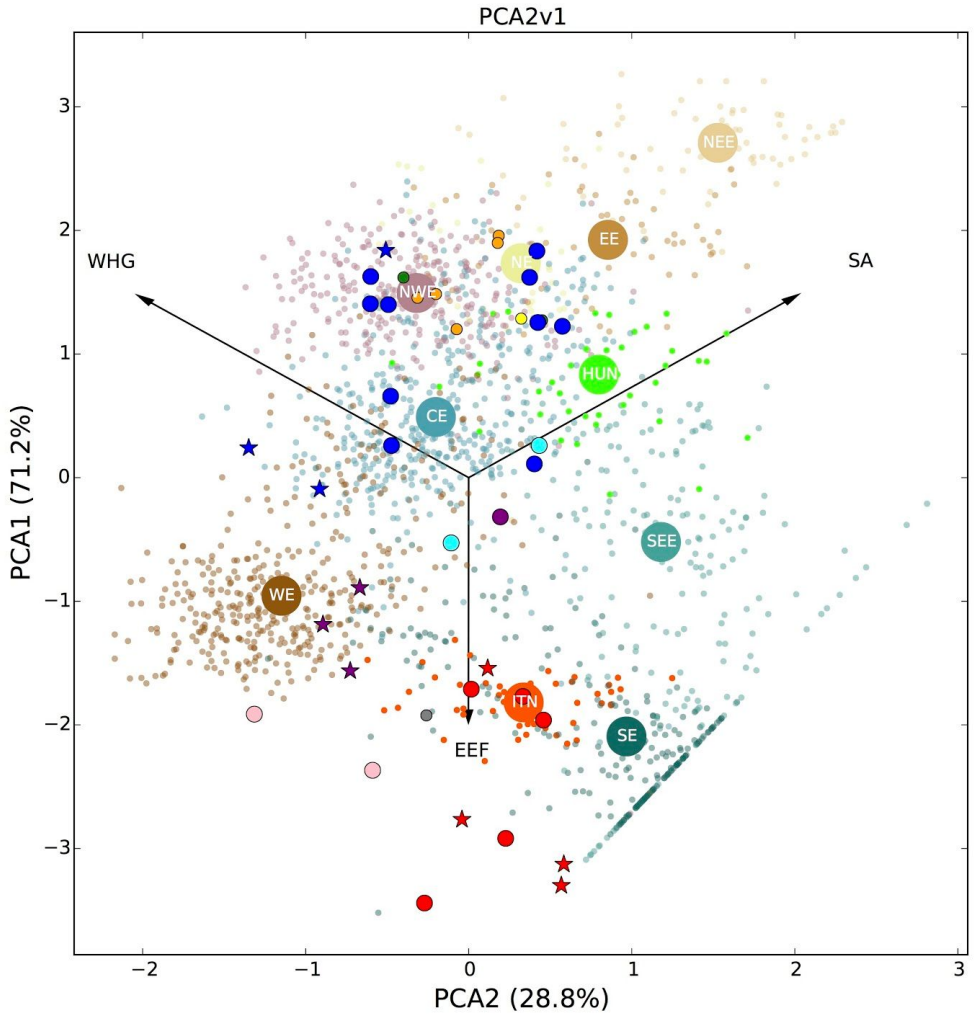

Figure S8.17. PCA of supervised `ADMIXTURE` estimates for unrelated Medieval samples and POPRES and European HellBus individuals for K=3 using prehistorical parental populations. Colour coding of medieval samples is same as in Figs 1 and 2.

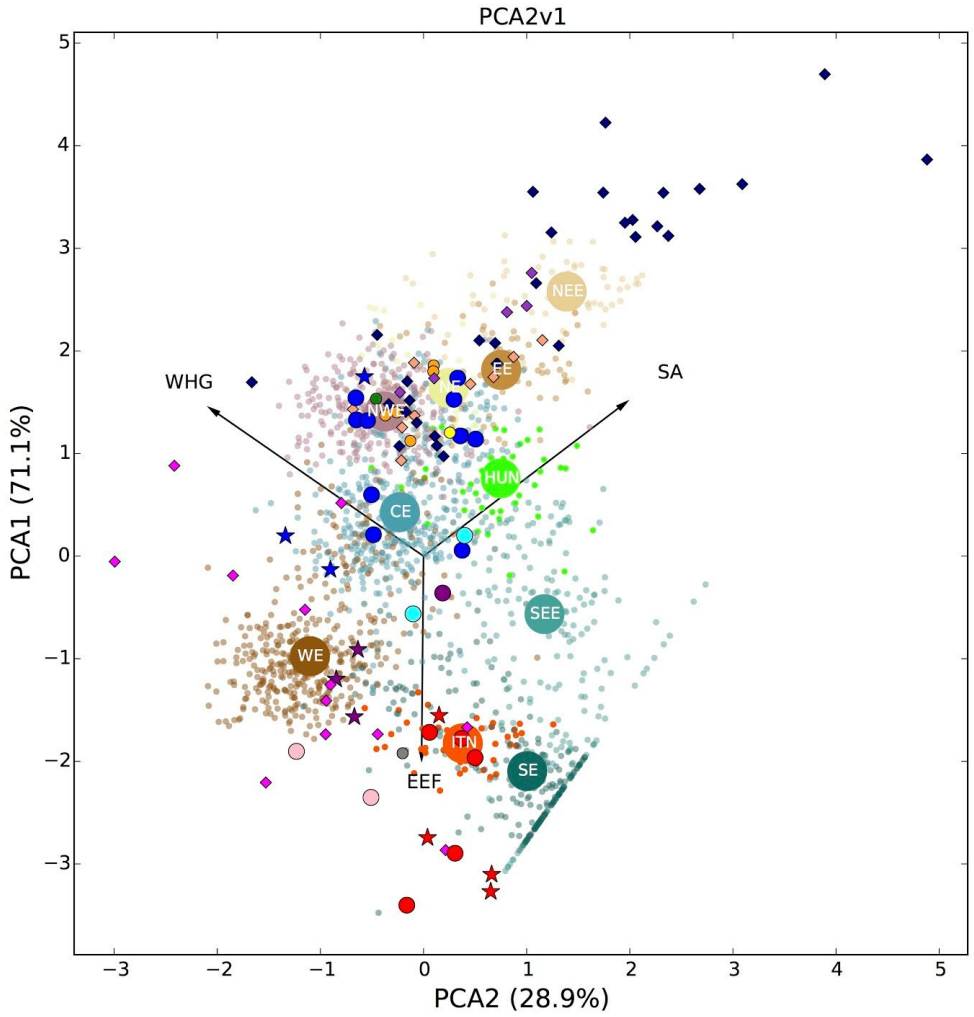

Figure S8.18. PCA of supervised ADMIXTURE estimates for unrelated Medieval samples, POPRES and European HellBus individuals, and Bronze Age European samples. for K=3 using prehistorical parental populations. Colour coding of medieval samples is same as in Figs 1 and 2. Magenta diamond = Hungarian Bronze Age, light salmon diamond = Northern European Bronze age, navy diamond = Central European Bronze age, dark orchid diamonds = Eastern European Bronze age.

S9. CHROMOSOME-Y HAPLOGROUP INFERENCE

Paolo Francalacci

S9.1 METHODS

Sequencing data were provided for the Y chromosome of 39 individuals and the respective VCF files reported information for 32,126 biallelic Single Nucleotide Polymorphisms (SNPs). The VCF data were imported in an Excel spreadsheet, where, for each sample and for each physical position (in build37), the number "0" refers to a nucleotide identical to the reference, the number "1" the alternative and the sign "." indicates a missing nucleotide call. Two individuals (SZ6 and SZ20) showed poor quality calls (both 0 and 1) and were excluded from further analysis. The remaining 37 individuals showed an average of 15,913.5 calls out of the 32,126 positions (52.2%). However, the ratio between positive vs. no calls was not homogeneous in the database, since the 9 individuals for which we had whole genome sequences yielded a positive call for most of the 32,126 SNPs, with only 1.4% of no calls, while 28 individuals for which we had SNP capture data showed an average of 32.2% of positive calls.

Among the 32,126 SNPs analysed, 27,904 were not polymorphic across the samples and were identical to the reference in all the samples showing a positive call, 2,049 were singleton (presenting the alternative nucleotide in only one individual) and 2,173 were polymorphic sites that occurred in at least two individuals.

Polymorphic nucleotide positions and respective genotypes were listed and the variants were assigned according to their association to known haplogroups (groups of haplotypes sharing one or more common ancestral SNPs). The phylogenetic position of

each SNPs was established according to its occurrence in public database or in published literature[81–85].

The reference genome is a chimera of at least two individuals and contains a major portion belonging to haplogroup R, with about 1Mb (from 14.3Mb to 15.3Mb) belonging to haplogroup G. To overcome this confounding factor, we referred to the ancestral allelic status, inferred by parsimony, to describe each SNP, rather than to the allele reported in the reference.

A total of 1,087 variants univocally associated with a known haplogroup, sub-haplogroup or phylogenetically related haplogroups were considered informative. The lack of base calls due to the absence of reads at a position in a particular sample was resolved either as an ancestral or derived allele by a hierarchical inferential method according to the phylogenetic context based on a cladistic approach. In fact, the absence of recombination and the low recurrence and reversion rates of the Male Specific portion of the Y chromosome (MSY) implies the sequential accumulation of mutations over time, so that the presence of a derivate recent (apomorphic) allele allows the attribution to the derivate status to all the ancestral (plesiomorphic) alleles present upstream in the haplogroup, regardless of being directly observed or not. Hence, the allelic status of a specific SNPs is not always experimentally determined for each sequenced individual, but we report an average of 53.7% directly detected and 46.3% inferred SNPs for each sample (closely reflecting the analogous positive/missing call ratio for the total 32,126 SNPs).

A total of 1,066 polymorphic sites that were discovered in multiple individuals but could not be unequivocally assigned to any of the haplogroups were discarded.

In addition to these 1,087 informative SNPs detected in at least two individuals, there were 2,049 detected in only one individual (singletons). Since in this case it is not possible to apply a phylogenetic criterion, only 226 SNPs already observed in other databases and coherent with the previous haplogroup assignment made with the informative SNPs were considered. Considering both informative SNPs and known singletons, the database yielded a total of 1,313 variants (Table S9.1) which allowed the classification of the 38 individuals according to the nomenclature defined by the Y-Chromosome Consortium[86] and further detailed in the site of the ISOGG[85].

The 1,313 phylogenetically informative SNPs were used to build a parsimony-based phylogenetic tree using the `Phylip v3.69` package[87], using the Pars application (Discrete character parsimony algorithm). `FigTree v1.4.2` software was used to display the generated tree[88] (Figure S9.1).

The Collegno (COL) and Szólád (SZO) samples were compared with sequences coming from 5 European (Tuscans=TSI; GBR=Britons; Iberians=IBS; Finnish=FIN; Sardinians=SAR) and one American of European origin (Central European from Utah = CEU) populations from published databases[81,82,84]. For sake of clarity, only the 428 individuals belonging to the haplotypes identified in the ancient samples were included in the analysis. The phylogenetic analysis and the resulting tree were carried out as above (Figure S9.2, S_Doc_B).

A bar plot showing the relative frequencies for all the haplogroup and relevant sub-haplogroup observed in the above-mentioned populations was drawn using Excel (S_Fig_Y2).

S9.2 RESULTS

The analysis of the SNPs detected by sequencing the ancient DNA extracted from 37 samples from Szólád (N=21) and Collegno (N=16) (Tab. 1) allowed the attribution to their respective haplogroup and sub-haplogroup (Table S9.2). In spite of the presence of missing data and false positive results for some polymorphic sites, as expected for sequences derived from aDNA, about a half of the polymorphic sites (1,087 out of 2,173) can be used for constructing a robust phylogenetic tree encompassing the 37 samples (Figure S9.1). In fact, because of the features of the non-recombining portion of the Y chromosome, the lack of base calls due to the absence of reads at a position in a particular sample can be resolved either as an ancestral or derived allele by a hierarchical inferential approach (see Methods in this supplementary section above), which allows the correct attribution of the allelic status of a polymorphic site to all the individuals belonging to a clade (even in the case of a missing call for most of the samples) if they show subsequent derivate SNPs. It should be noted that such a phylogenetically based inference strategy is inherently less accurate for the rarest lineages, where the chance is higher of missing a polymorphic site in all the individuals. As a consequence, all the haplogroups encompassing one or two individuals show a shorter branch length. Moreover, the individuals with a poor yield in terms of positive calls tends to root in the basal position

of their respective haplogroup or sub-haplogroup (Figure S9.2). This is due to the higher probability of having a missing call for all the downstream position and, consequently, they cannot be further assigned to any subclade of the main haplogroups.

We excluded sample SZ1 from further analyses because this sample was found to belong to a different era of occupation of Szólád.

The samples do not appear to be paternally related in most of the cases, as the shared haplotypes are generally rooted in the basal position of each haplogroup, suggesting it could be due to the incomplete detection of derivate alleles for individuals with poor sequencing coverage, as mentioned above, and not necessarily to biological kinship (though we note haplogroup assignment makes sense in light of kinship inferred from autosomal loci.

While most of the haplogroups observed in Szólád and Collegno are also present in Africa, the Middle East, Central Asia and the Indian subcontinent, the sub-haplogroups shows a typical European distribution (Figure S9.3), although with different frequencies at a subregional level (see the review Francalacci and Sanna[89] and references therein). The haplogroups detected in the samples show a prevalence of R1b (55.3%), which is the most common sub-haplogroup in western Europe, with a peak in the Iberian Peninsula and in the British islands and a west-east gradient in central Europe[90]. A consistent percentage of haplotypes belongs to the I haplogroup (26.4%), both in the I1a and, more abundantly, in I2a2 sub-haplogroups. They are particularly frequent in the northern Balkans with a westward gradient in central and western Europe, with some lineages belonging to I2a2a1b particularly common in the Germanic region[91]. Rarer lineages

included R1a, which is possibly related to the Indo-European diffusion and shows its higher occurrence in eastern Europe [90], and G2a for CL31, which probably has its origin is in the Caucasus and followed the Danubian route of the spread of agriculture in central Europe and in Italy until the islands of Corsica and Sardinia[92,93]. Two sub-haplogroups, E1b1 and T1a (both at 5.3%) show a Mediterranean distribution with a prevalence in southern Europe, in particular in the Iberian and Italian peninsulas[90,94].

The comparison of Szólád and Collegno, considered as a whole, with other European populations (Figure S9.3) shows a marked resemblance with the CEU (Central Europeans) because a similar ratio between R1a/I haplogroups, with a certain influence of lineages present in the TSI (Tuscans), indicating a major Central/Northern European component, with a noticeable contribution from Southern European populations (in agreement with the results for the autosomes). However, even with the limitation due to the low sample size, the Central European/Balkan influence is more apparent in the Szólád sample, which shows a relevant presence of the lineages belonging to the haplogroup I, than in the Collegno sample, with a prevalence of Southern/Western European haplotypes.

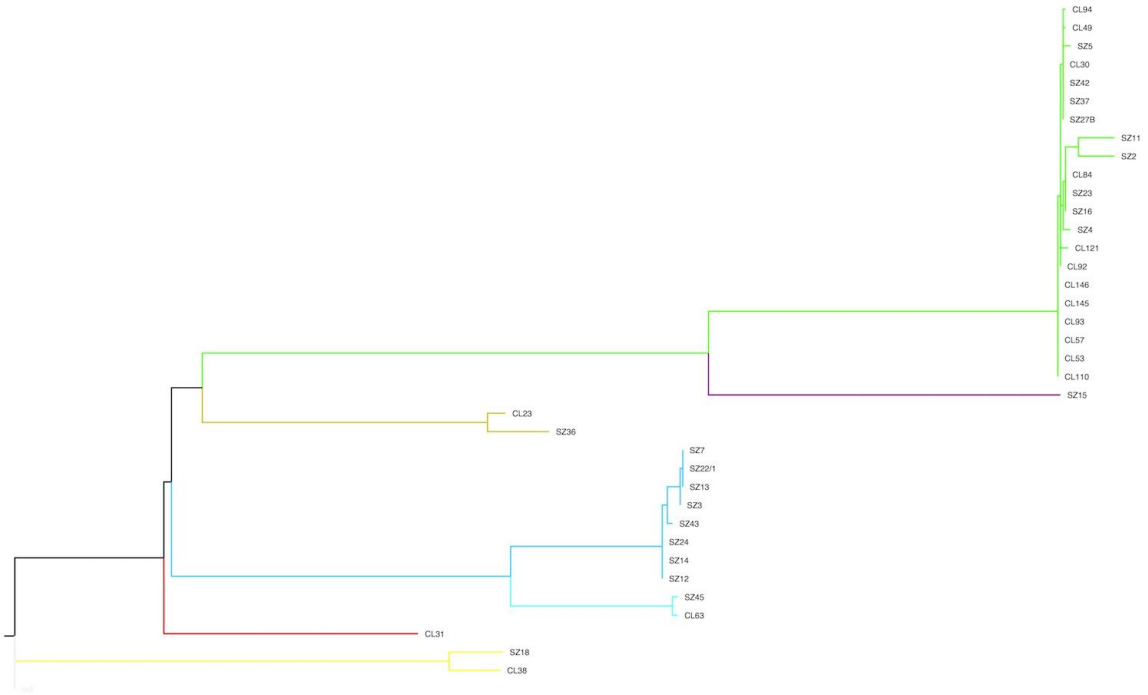

Figure S9.1. Parsimony-based phylogenetic tree of 37 ancient (CL = Collegno; SZ = Szólád) Y-chromosome sequences. Colored branches represent different Y-chromosome haplotypes: E1b = yellow; G2a = red; I1a = light blue; I2a = blue; T1a = light green; R1a = purple; R1b = green.

[See S_Doc_B]

Figure S9.2. Parsimony-based phylogenetic tree of 37 ancient samples (CL = Collegno; SZ = Szólád) and 428 modern European (CEU = Central Europeans from Utah; FIN = Finnish; GBR = Britons; IBS = Iberians; SAR = Sardinians; TSI = Tuscans) Y-chromosome sequences. Colored branches represent different Y-chromosome haplotypes: E1b = yellow; G2a = red; I1a = light blue; I2a = blue; T1a = light green; R1a = purple; R1b = green.

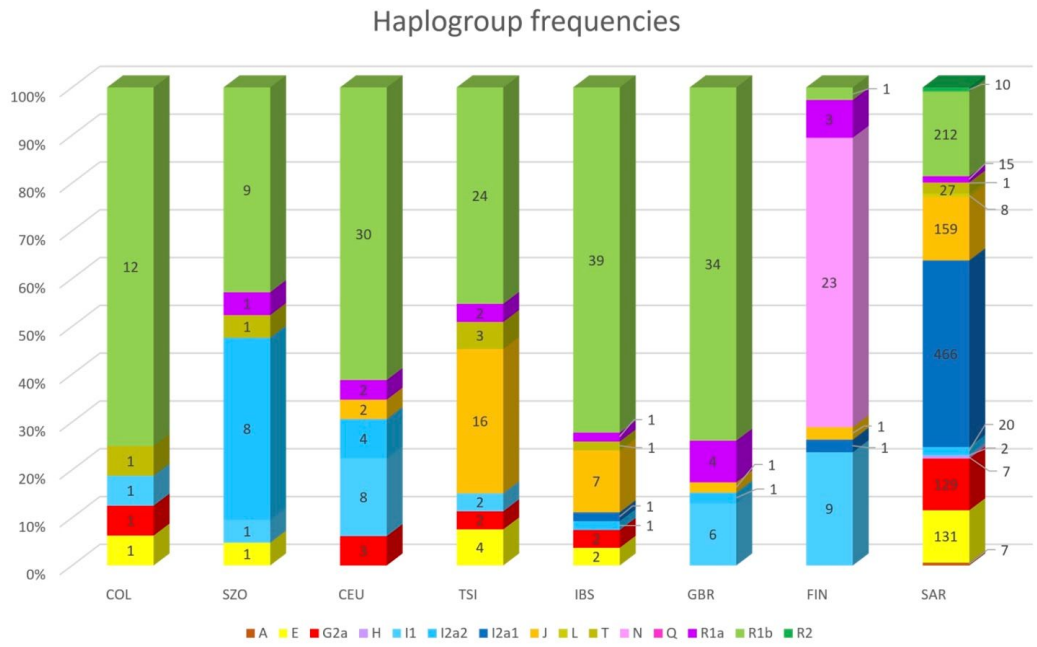

Figure S9.3. Relative and absolute haplogroup frequencies: COL = Collegno; SZO = Szólád; CEU = Central European from Utah; FIN = Finnish; GBR = Britons; IBS = Iberians; SAR = Sardinians; TSI = Tuscans.

Table S9.1. Alignment of the variable SNPs from 37 Medieval and 1 Bronze age individuals

Table S9.2. Haplogroup attribution for 37 Medieval and 1 Bronze age individuals

[See Excel spreadsheet]

S10. POPULATION ASSIGNMENT ANALYSIS

Krishna R. Veeramah

In order to obtain a more precise estimate of the modern population most closely resembling our ancient samples, we applied the following likelihood framework to our Medieval ancient sample data using either the POPRES or HellBus datasets as reference populations in what we call a Population Assignment Analysis (PAA)[63].

For every reference population, k, with at least $n/2$ individuals we estimated for every SNP, i, the allele frequency of an arbitrary allele (q_{ik}) for a randomly drawn set of n chromosomes (so sample sizes were equal across populations). Then, for each ancient sample we determined the most likely population of origin by estimating the log-likelihood of observing the pseudo-haploid call, D_i, given a particular reference population for each SNP position, which is simply the log of q_{ik} for the observed allele, and summing across loci. In order to account for a reference population being fixed for the allele not observed in a particular ancient sample (which may happen because of either the low sample size of the reference population or a sequencing error for the ancient sample), we allowed an 0.1% error rate, e, such that the log likelihood for each SNP used was:

$$lnLL(\, k \mid D_i) = ln[q_{ik} \text{ X } (1\text{-}_e)) + ((1\text{-}q_{ik}) \text{ X } e)] \quad ,$$

where q_{ik} is the frequency of the observed allele, D_i. However, the results were robust to different choices of e (both smaller and larger).

In order to obtain an estimate of uncertainty in our most likely reference population and take into account correlation amongst neighbouring SNPs, we performed

100 bootstrap iterations, where for each iteration we resampled with replacement 5 Mb non-overlapping windows of SNPs from across the genome. For each bootstrap iteration we noted the reference population with the highest likelihood using the above expression and scored the total number of times each population obtained the highest log likelihood across the 100 iterations.

We performed this assignment both at the level of countries which could be assigned a latitude and longitude and region (see Figure S10.1 for European region definitions based on grouping modern countries). When performing the analysis at the level of regions, we applied two different cut offs for *n*. The reason for this was that increasing *n* to a larger number should in theory improve resolution, but because of the limitations of our sampling database, this also leads to not having enough samples to represent Northern Europe (NE).

The most likely reference population for POPRES and HellBus samples is shown in Table S10.1. In general there is high concordance between population assignments, PCA position and ancestry estimation. Notably, southern ancestry individuals from Collegno tended to be assigned to Southern Europe (SE, essentially Italy) with high probability, while those from Szólád were more diverse, with greater weight towards South East Europe (SEE) assignments. The average SE/SEE probability for the four individuals with >70% TSI ancestry in Collegno (excluding CL31) using the POPRES and HellBus datasets (highest *n* cutoff) was 1.0/0.0 and 0.80/0.20 respectively. For the five individuals with >70% TSI ancestry in Szólád the pattern was reversed, with values of 0.31/0.43 and 0.36/0.49 (i.e. a higher SEE probability overall).

For the 17 individuals assigned to the NE region using the lower cutoff for *n* for the POPRES dataset, 9 and 8 were assigned to CE and NWE respectively at the higher cutoff. For the 13 individuals assigned to the NE region using the lower cutoff for *n* for the HellBus dataset, 6, 6 and 1 were assigned to CE, NWE and WE respectively at the higher cutoff. When comparing the two major kindred (see Supplementary Text 12), the POPRES data assigned 5 of the 10 individuals to NWE for *Kindred CL2*, but only 1 individual for *Kindred SZ1* (SZ15, who is only peripherally connected to the family via SZ6). This appears to correspond with the slight shift of *Kindred CL1* to NWE in the PCA and SPA analysis, and the increased FIN ancestry in *Kindred SZ1*. This effect is not as apparent using the HellBus dataset, but this reference population is not as well represented for NWE individuals (Table S10.2)

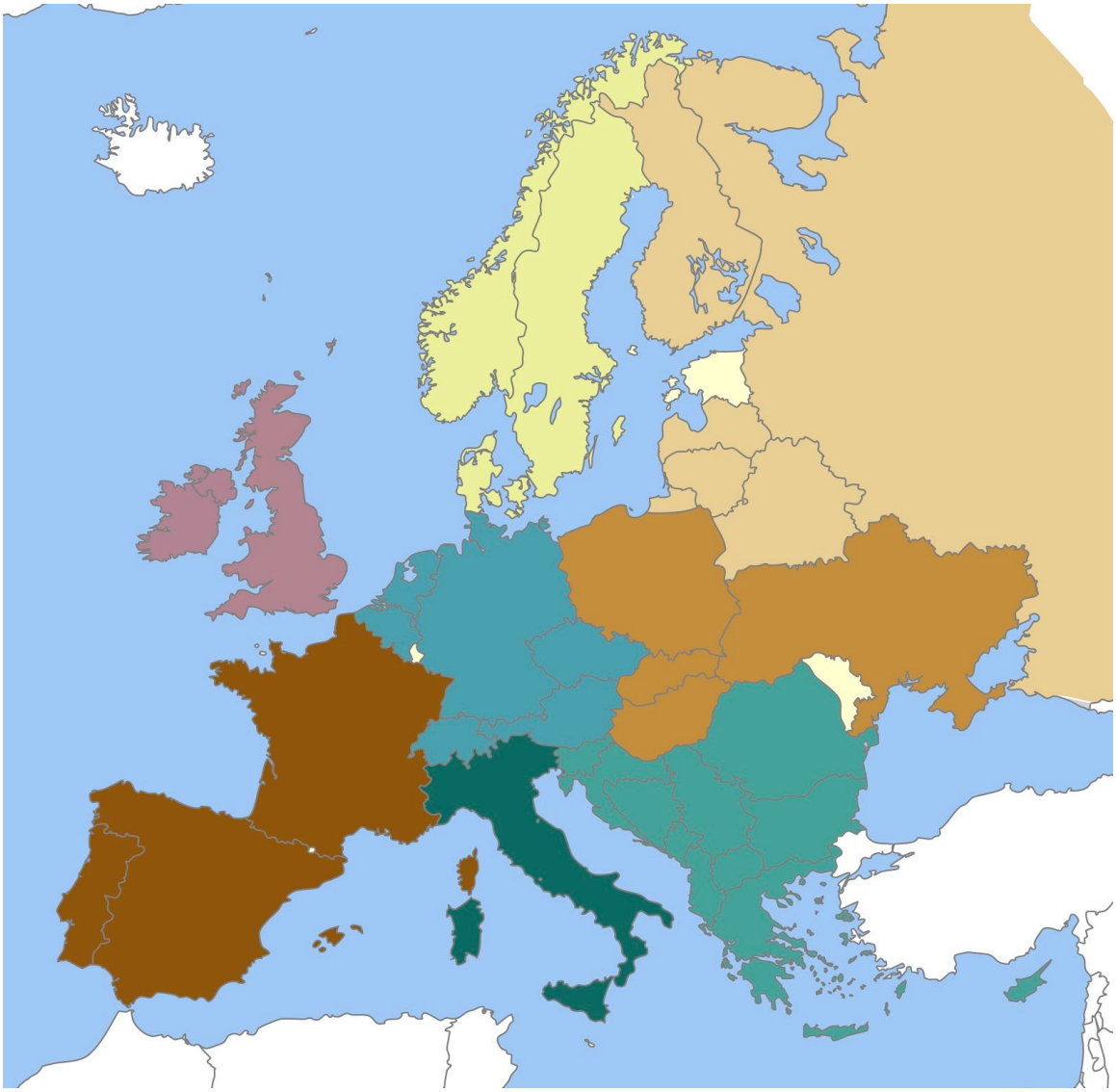

Figure S10.1. Correspondence between modern political borders and European region definition utilized in this study. See Figure 1 for color key.

Table S10.1. Most likely modern population assigned to each ancient sample test using PAA.

[See Excel spreadsheet]

Table S10.2. Numbers of samples in reference populations for regional groupings.

	HellBus	**POPRES**
CE	34	378
EE	57	43
NE	18	14
NEE	61	8
NWE	41	266
SE	116	219
SEE	99	104
WE	88	353
Caucasus	194	0
Middle East	321	0
South Asia	262	0
Central Asia	110	0

S11. RARE VARIANT ANALYSIS

Krishna R. Veeramah

While the majority of our analysis involves the use of methods that examine specific SNPs in the 1240K capture, our medium-high coverage WGS of 10 samples from Szólád (even though one would later be found to have origins from an earlier period) allowed us to make inferences using so called rare-variants, as previously applied to the Anglo-Saxon-era samples from the UK by Schiffels et al.[62].

As in Schiffels et al.[62] we assembled allele frequencies for four 1000 Genomes European populations (GBR, FIN,IBS and TSI), as well 200 unrelated Dutch (NED) chromosomes[95] (randomly downsampled from 998) and 40 unrelated Danish (DAN) chromosomes[96] for every autosomal position on human reference genome build GR37, restricting to mappable regions determined by the 1000 genomes Phase 3 mask. We then called both pseudo-haploid and diploid genotypes as described in S5 for our Medieval whole genomes in the same regions, restricting to sites with 7x depth or greater. Any analysis involving a particular Medieval sample was restricted to these regions across all samples. Alleles were determined as ancestral or derived using the 1000 Genomes ancestral sequence.

In an initial analysis we identified a set of sites with a derived allele count of <10 across both NED and TSI. Then for each of the nine Medieval individuals we scored whether they possessed the derived allele at theses sites using the pseudo-haploid calls. For each total derived count bin, we then estimated the ratio of number of sites shared with NED and TSI. We then plotted this following Schiffels et al.[62], with error estimated

using standard error propagation (Figure S11.1). Samples were color coded based on their relative NED (blue) versus TSI (red) ancestry at singleton sites. Despite being based on rare variants rather than SNPs with more common allele frequencies, the relative sharing of these 9 WGS highly concordant with their position in a PCA of modern POPRES samples using 1240K capture SNPs (Figure S11.2), demonstrating that these sixth century samples are closely related to modern populations (i.e. a Medieval sample with northern ancestry shares more private variants with modern northern European samples than a modern southern European would do).

In order to more formally model these relationships we analyzed our nine Medieval WGS using the software `rarecoal`. We first re-estimated parameters for the population genetic model for the six modern reference populations using the Monte Carlo Markov Chain method while modelling rare variants with a total count of 4 or less across all populations. Our estimates were generally similar to that of Schiffels et al.[62], though we estimated a deeper split time for TSI and IBS, lower ancestral N_e and higher modern day N_es. Schiffels et al.[62] previously noted these parameters were problematic because of possible post-divergence gene flow (Table S11.1). For consistency, we performed our analysis using the original Schiffels et al.[62] model.

We then attempted to place each of the nine WGS on to one of branches of this model, ignoring any derived site that was only found in the ancient sample to guard against false positives (Figure S11.3). The three most extreme northern samples (SZ2, SZ4 and SZ11) were placed on either the Danish or Dutch branches (with high relative likelihood for both). SZ3, the fourth most northern sample was found close to the root of

GBR, DAN, NED, and FIN branch point, while SZ36 and SZ43 were placed closest to the root of the tree separating northern and southern Europe, presumably because of their increased southern ancestry. SZ5 and SZ45 had a likelihood space across most of the tips of the branches, perhaps as a result of their intermediate ancestry. Using diploid calls (still ignoring singletons) appeared to improve our ability to place samples on the southern portion of the tree (Figure S11.4), with SZ36 placed on the shallow TSI branch, and the likelihood distribution being much sharper across the tree space, though we must be cautious in interpreting these results due to the variable WGS coverage that may result in overconfident placement due to unnaccounted diploid calling error.

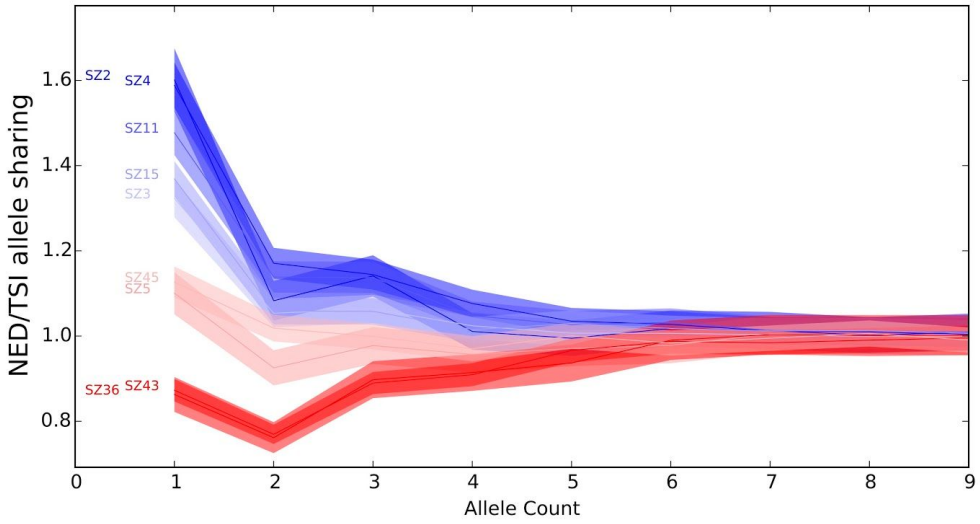

Figure S11.1. Relative NED/TSI allele sharing for Medieval whole genomes for rare variants (derived allele count <10).

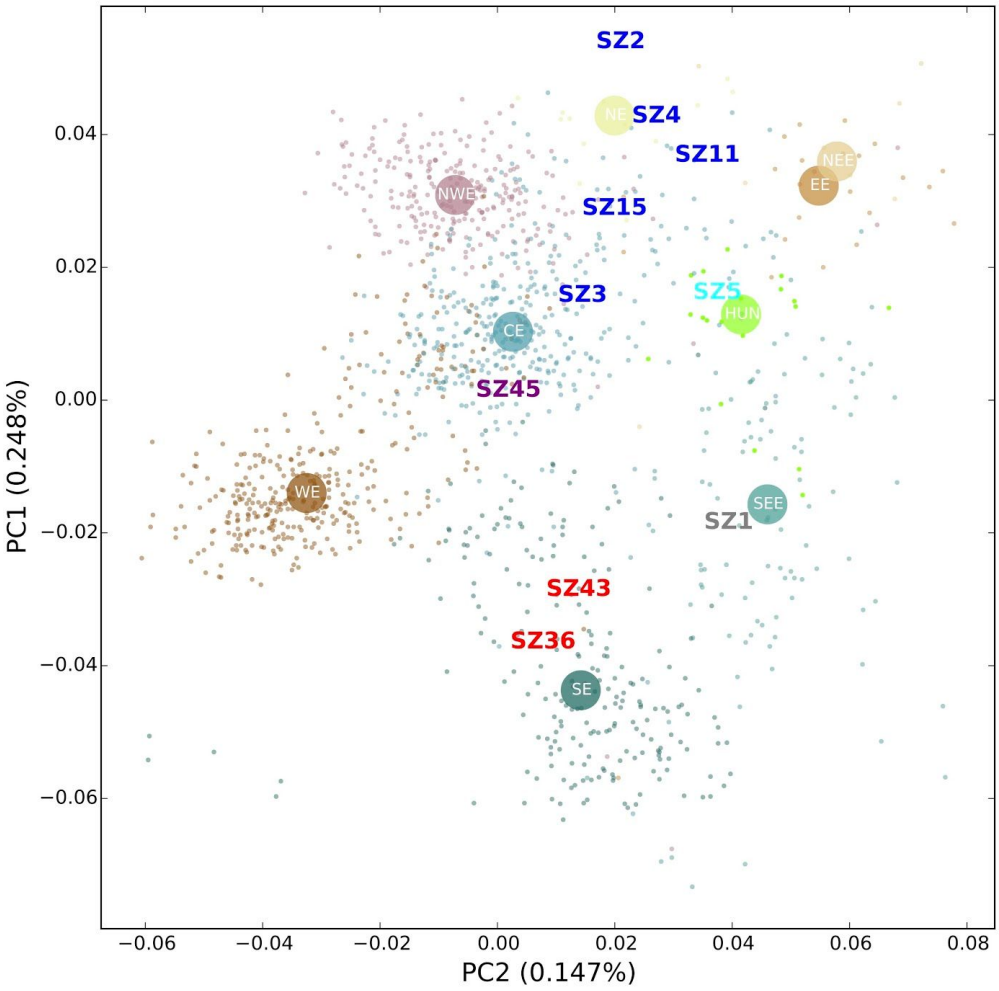

Figure S11.2. PCA of POPRES samples and 10 whole genome sequences generated in the study. Color coding of medieval samples is same as in Figs 1 and 2.

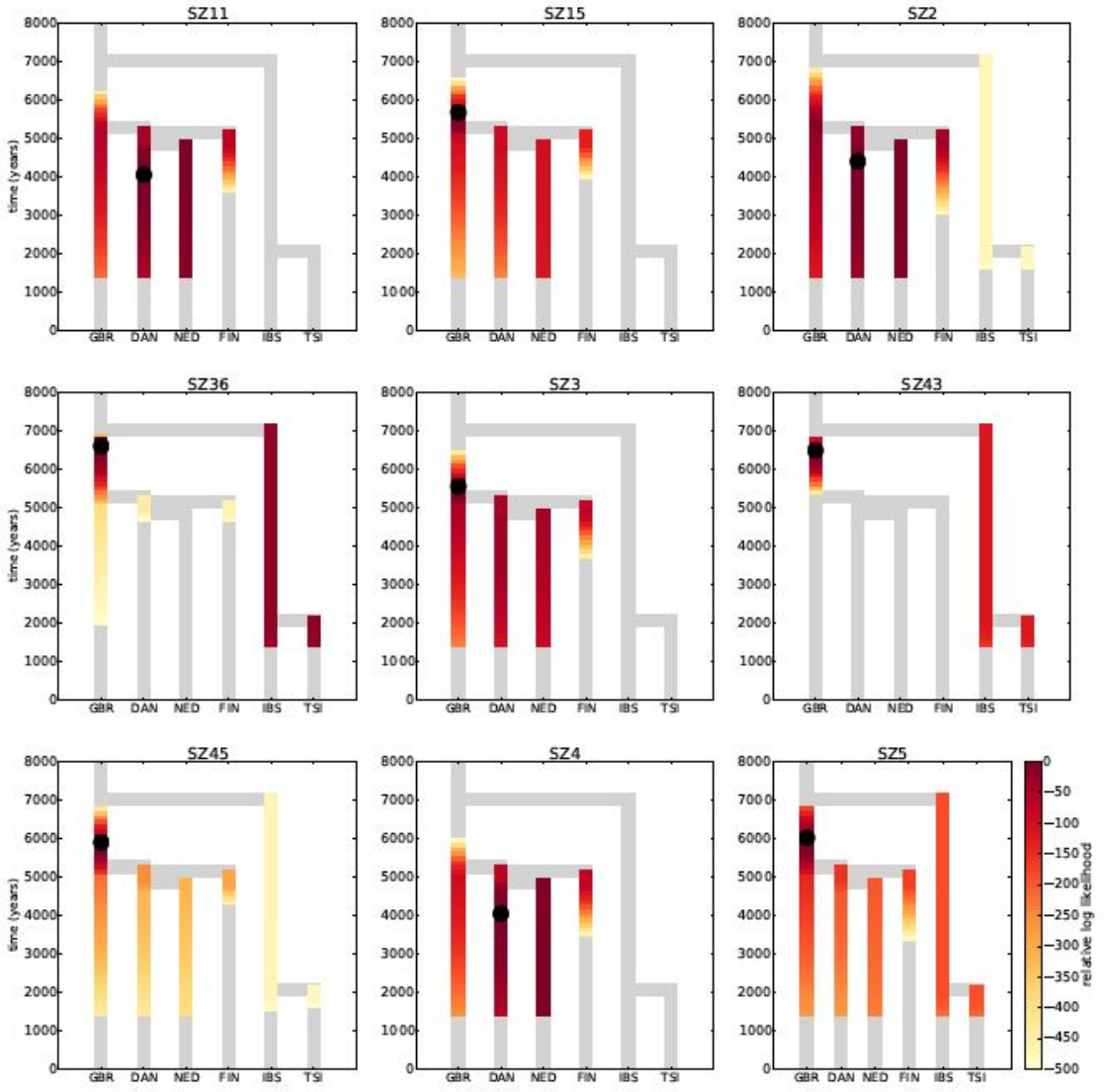

Figure S11.3. `rarecoal` analysis, placing each of the 9 Medieval whole genomes with pseudo-haploid calls on a branching model of European demographic history. Black dot represent ML estimate. Scaled time from `rarecoal` converted to years assuming mutation rate of 1.25 x 10^{-8} per generation and generation time of 29 years.

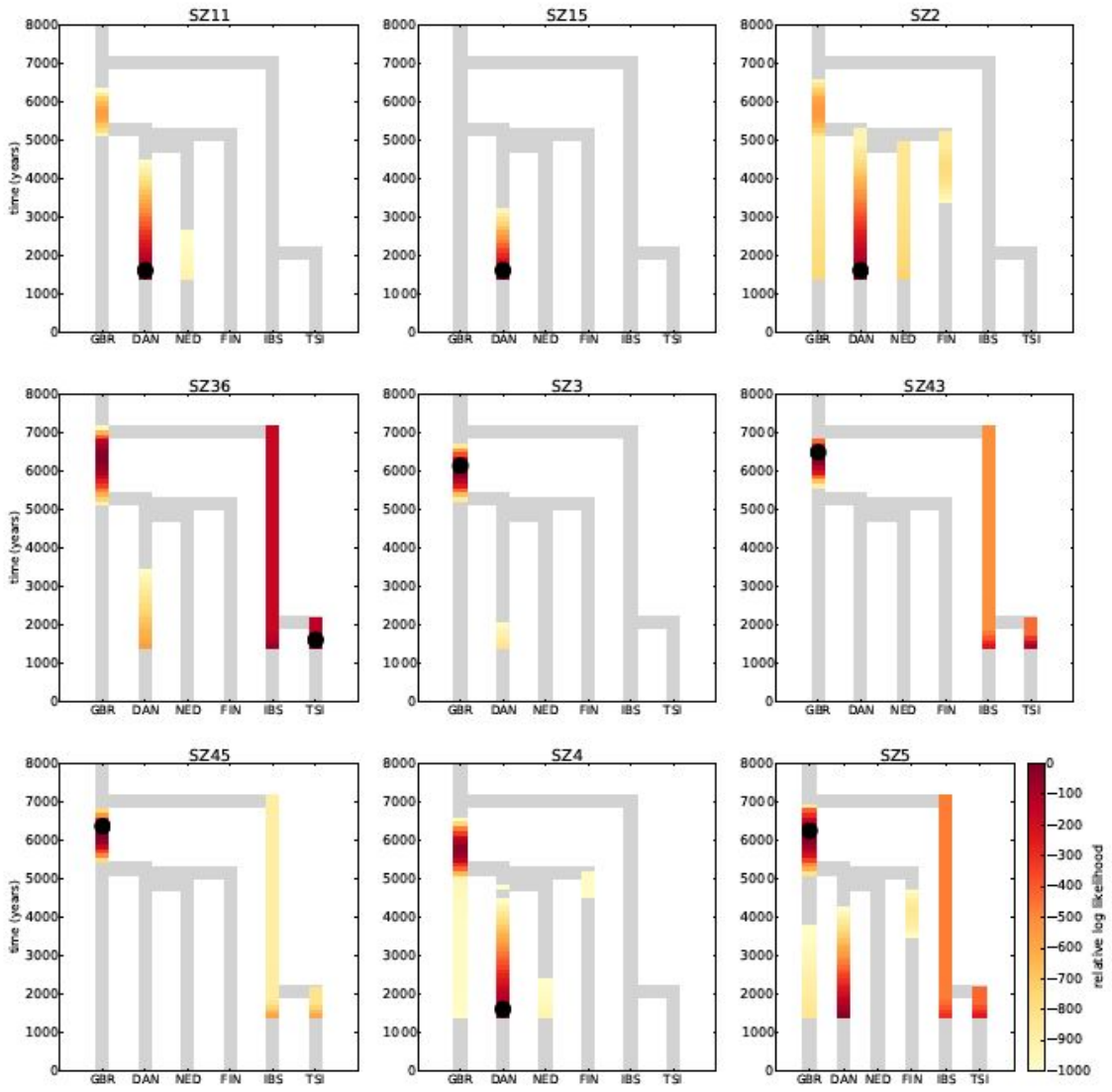

Figure S11.4. `rarecoal` analysis, placing each of the 9 Medieval whole genomes with diploid calls on a branching model of European demographic history. Scaled time from `rarecoal` converted to years assuming mutation rate of 1.25 x 10^{-8} per generation and generation time of 29 years.

Table S11.1. Comparison of Schiffels et al. and our estimates of demographic parameters for modern European populations using `rarecoal`.

Parameter	Schiffels ML estimate	Our ML estimate	Lower 95% CI	Upper 95% CI
$t_{(NED,DAN)}$	4.13E-03	3.72E-03	3.70E-03	3.73E-03
$t_{FIN(NED,DAN))}$	4.38E-03	4.00E-03	3.97E-03	4.01E-03
$t_{F(FIN,(NED,DAN)),GBR)}$	4.49E-03	4.05E-03	4.05E-03	4.08E-03
$t_{(IBS,TSI)}$	1.74E-03	5.54E-03	5.52E-03	5.55E-03
$t_{(((FIN,(NED,DAN)),GBR,(IBS,TSI))}$	6.01E-03	5.55E-03	5.53E-03	5.56E-03
N_{FIN}	0.60	0.53	0.53	0.53
N_{GBR}	4.87	4.21	4.15	4.25
N_{IBS}	3.93	9.23	9.15	9.32
N_{TSI}	3.26	7.44	7.39	7.52
N_{NED}	9.96	9.50	9.20	9.68
N_{DAN}	1.95	2.42	2.36	2.50
$N_{(NED,DAN)}$	0.57	0.68	0.66	0.72
$N_{FIN(NED,DAN))}$	0.71	0.65	0.62	0.71
$N_{(FIN,(NED,DAN)),GBR)}$	0.64	0.65	0.65	0.65
$N_{(IBS,TSI)}$	997.00	5.62	1.17	6.33
$N_{(((FIN,(NED,DAN)),GBR,(IBS,TSI))}$	1.02	0.91	0.91	0.91

S12. BIOLOGICAL KINSHIP INFERENCE

Carlos Eduardo G. Amorim, Krishna R. Veeramah

To infer biological kinship between each pair of individuals, we used `lcMLkin`[97], a software implemented in C++ and with modifications implemented in Python. The method implemented in this software considers genotype likelihoods instead of a single best genotype for each individual to infer biological kinship, and so it is optimal for use with ancient DNA (aDNA) and other potentially low coverage DNA samples (e.g. in forensics), for which an excess of false homozygotes is usually an artifact. `lcMLkin` can infer biological kinship down to 5th degree relatives (e.g. second degree cousins), even when coverage is as low as 2x[97]. The software uses population frequencies to estimate the probability of identity-by-descent (IBD) given the observed genotypes likelihoods, and outputs the k probabilities that two diploid individuals share zero (k_0), one (k_1) or two (k_2) alleles at a given loci IBD, such that $k_0 + k_1 + k_2 = 1$. Individual SNP log likelihoods are summed for a given pair of individuals. If the three k parameters can be estimated, one can infer the degree of relationship between each pair of individuals and calculate the kinship coefficient ϕ. See Table 1 in Weir et al.[98] for a list of expected values for k_0, k_1, and k_2, for different degrees of relationship.

Population allele frequencies will determine the probability of IBD given identity-by-state (IBS). `lcMLkin` implements two methods: (a) one that considers allele frequencies in an external reference population and (b) another that uses the target samples themselves to estimate the frequencies. Though we have further developed `lcMLkin` incorporate drift based on a specific F_{ST} via a Balding-Nichols model[99], we

find that kinship inference will generally be robust for inferring major degrees of relatedness when the assumed population allele frequencies are diverged from the true frequencies for realistic levels of genetic drift occurring within European populations such as in this study[97].

We implemented four types of runs in `lcMLkin` using different samples to estimate the population allele frequencies: (*i*) CEU, (*ii*) TSI or (*iii*) merged CEU and TSI as reference populations (since these can account for the major genetic component in our Medieval samples according to Fig 2A), and (*iv*) without a reference population set. Allele frequencies for the latter case were estimated without individuals identified as relatives based on a preliminary run.

The values for the kinship coefficient ϕ between all possible pairs (both within and across cemeteries) using no reference set (run *iv*) were very similar to the other three types of runs (Figure S12.1). r^2 for ϕ in run *iv* versus runs *i*, *ii*, and *iii* are 0.81, 0.79, and 0.81 respectively, with p-value < 1 x 10e-15 in all cases. This suggests that kinship inference was be robust to our assumptions regarding the population allele frequencies for our data (indeed, all major relationships identified in this study were observable using all four runs).

The value of k_0 describes the probability of two individuals not sharing an allele in a given site by IBD. If this value is next to 1, then individuals are not related. Based on the value of k_0 associated with the kinship coefficient ϕ, we arbitrarily subset the dataset in two groups: one with individuals that we could discard as relatives (i.e. those that had k_0 close to 1 and ϕ close to 0), regardless of them being from the same cemetery or not;

and another with potential relatives. Since we have no reason to believe that individuals coming from distinct cemeteries are actual relatives, we used the distribution of ϕ in that group (which is centered around zero) as a benchmark for ϕ values among non-related individuals. The distribution of ϕ for putative non-relatives coming from the same cemetery closely matched that for different cemeteries (Figure S12.2), suggesting this former group is mainly composed by unrelated individuals as well. The distribution of ϕ for the putative relatives is broader, with a peak at zero (for individuals that are potentially unrelated or not closely related) and other smaller ones at 0.2 and 0.45 (Figure S12.2). The density away from zero should largely reflect ϕ for individuals that are first, second or third degree relatives. We focused on the subset of potentially related individuals (see Table S12.1 for kinship coefficients for each of these pairs) to infer pedigree structures, as follows.

We started by identifying non-ambiguous relationships (e.g. parent and child) and then extended the family tree to the more ambiguous cases (e.g. $k_0 = 0.5$, $k_1 = 0.5$, and $k_2 = 0$ may be of the type avuncular, first cousins and grandparent-grandchild). When a parent-child relationship was inferred, we defined the parent as the individual who was the oldest at the moment of death. The same is valid for grandparent-grandchild. In large pedigrees (e.g. *Kindreds SZ1, CL1,* and *CL2*), the relationship between one pair of individuals was always corroborated by the relationship of each one of the individuals in this pair to a third individual (except for individual SZ6, see below). For example, CL146 and CL145 are brothers and both can be assigned as nephews of CL93 (Fig 3B). The

various possibilities in the ambiguous cases were examined one by one, by two of the investigators in this work until consensus was reached.

We next ran PRIMUS[100] on the whole dataset (potential relatives and non-relatives, considering different reference sets for inferring the population allele frequencies) to confirm the "manually" inferred pedigree structure and identify additional potential cryptic relationships. By doing so, we confirmed all initially inferred pedigrees. We also confirmed the distant but significant relationship between members for two nuclear families: one composed by individuals CL145, CL145, CL93, and CL92; and the other by individuals CL97, CL87, CL83, CL84, and CL102. The relationship between these nuclear families is unclear, but it excludes individual CL151 and seems to be more distant than that of third degree. We indicate this more cryptic relationship by dashed lines connecting both pedigrees (Fig 3B). We note that inbreeding in CL97 is suggested by the high value of k_1 but 0 for k_2 in relation to his likely nephews CL83 and CL84. i.e. there are more alleles with IBD=1 than would be expected for a second degree relative, but less than would be expect for a parent offspring relationship. If CL97 was inbred we would expect this to occur because alleles transmitted to the nephews would already have IBD within CL97 (i.e. Jacquard identity modes S3 or S5[101]).

We also detected biological relationship between individual SZ6 and individuals SZ15 and SZ19. The degree to which these individuals are related is unclear, but this signal is not seen between SZ15 or SZ19 and any other individuals in that kindred (*Kindred SZ1*), not even SZ8 and SZ14, to which SZ6 is most related (almost to the degree of siblings but k_2 is too low). We confirmed the relationship and general k values

between SZ6 and the other individuals using both pairwise PCA and a modified version of `lcMLkin` that took into account admixture based on the model from Moltke and Albrechtsen[102] and incorporating ancestry estimates from the `ADMIXTURE` analysis above (note, we could not apply this method to all pairs because it is computationally intensive). No standard biological relationship could fit the estimated kinship coefficients, which may could be a consequence of SZ6 being of low coverage (0.048x) or some degree of inbreeding in this individual's history. Therefore we connected SZ6, SZ15 and SZ19 to *Kindred SZ1* via dashed lines to indicate our uncertainty (Fig 3B).

This approach allowed us to identify four kindred in Szólád and three in Collegno (Fig 1B-C). We established the most likely pedigree for each one of the three largest kindreds (Fig 3). For the remaining four small kindreds, possible pedigree structures were many and because of the small number of individuals, we were not able to cross-validate exact relationships and choose a single best structure. The following relationships are likely: SZ41/SZ42=first cousins, CL110/CL121=first cousins, SZ18/SZ23=half siblings. The remaining five relationships are unclear.

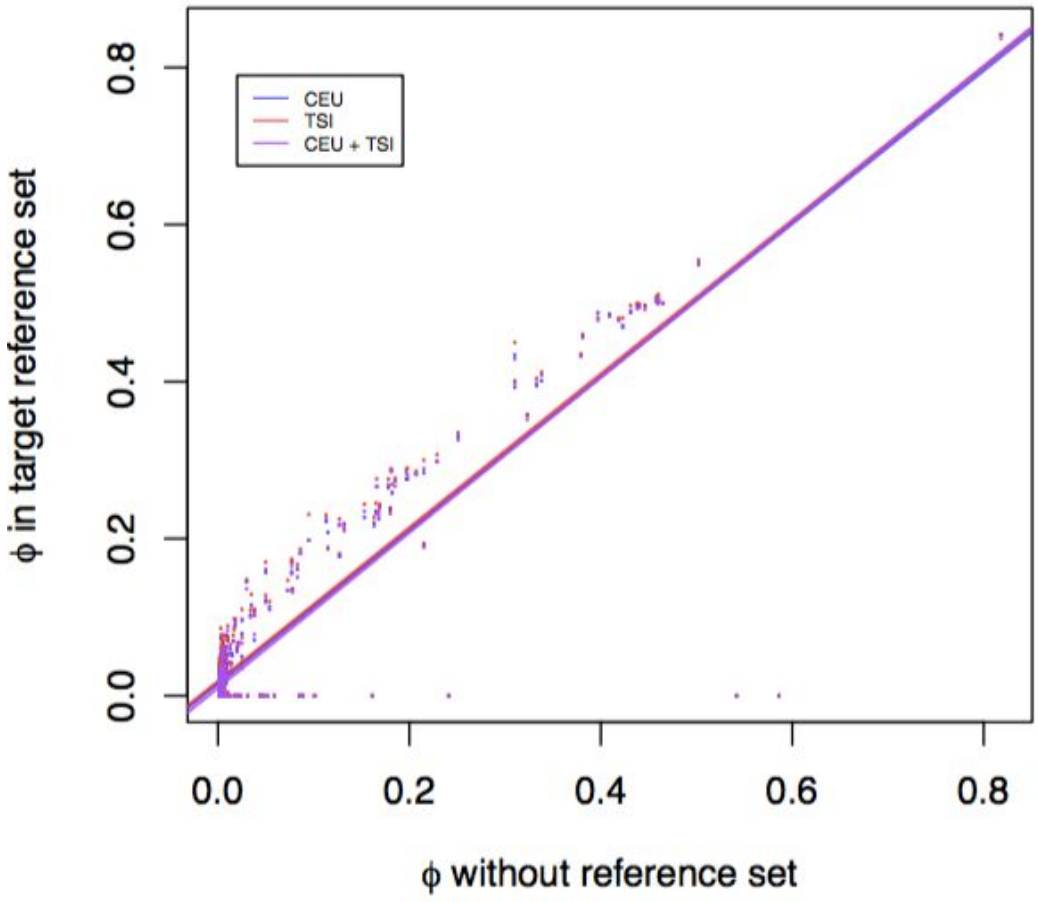

Figure S12.1 Distribution of kinship coefficient ϕ inferred using different population reference sets (CEU, TSI or both merged) against values inferred using no reference set (i.e. estimating allele frequencies from the target ancient samples).

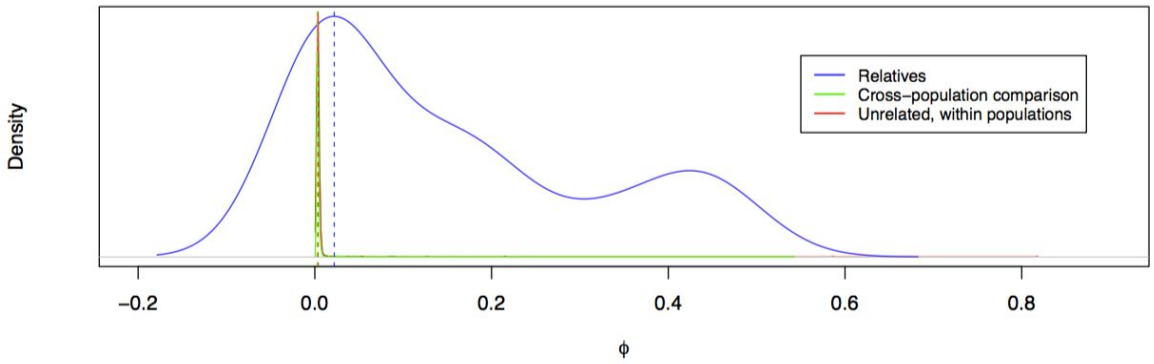

Figure S12.2. Distribution of kinship coefficient ϕ for pairs of individuals from different cemeteries (green curve), for potentially unrelated individuals from the same cemetery (red curve), and for potentially related individuals (blue curve).

Table S12.1. Kinship coefficients and *k*s for putatively related individuals.

[See Excel spreadsheet]

S13. SPATIAL ANCESTRY ANALYSIS

Krishna R. Veeramah

Spatial Ancestry Analysis (SPA)[103] is a model-based framework that, amongst other things, allows the inference of the relative geographic location of an individual's ancestors for an arbitrary number of generations in the past (though typically this will be applied to infer this location for an individual's two parents. This can allow the identification of individuals with mixed ancestry. It does this by fitting genotype data to a spatial model of allele gradients (determined by a logistic function) previously inferred using a reference set of unadmixed individuals.

This logistic function is parameterized for each SNP *j* like so:

$$f_j(x) = \frac{1}{\exp^{(-a_j^T x - b_j)} + 1}$$

where *a* and *b* are function coefficients and *x* the geographic location being considered.

When inferring the parental locations of an admixed individuals we must consider two such locations, *x* and *y* and thus two functions, $p_j = f_j(x)$ and $m_j = f_j(y)$. The original probability distribution for this function when considering diploid genotype calls is as so:

$$\begin{aligned} P(g_j = 2|x,y) &= p_j m_j \\ P(g_j = 1|x,y) &= p_j(1-m_j) + m_j(1-p_j) \\ P(g_j = 0|x,y) &= (1-p_j)(1-m_j) \end{aligned}$$

where g_j is the observed number of minor alleles. Inference can then be made by maximizing the likelihood function across all SNPs.

$$L(g; x, y) = \sum_j \ln P(g_j | x, y)$$

However, in some cases full diploid genotypes are not possible due to low coverage (for example due to the use of ancient DNA as in this study). In such case only one allele of a true diploid genotype will be represented in the observed genotype. In this case we must adjust the probability distribution (note, that $P(g_j = 2 \mid x,y)$ is no longer possible):

$$\begin{aligned} P(g_j = 1|x, y) &= \frac{p_j(1-m_j)}{2} + \frac{m_j(1-p_j)}{2} + p_j m_j = \frac{p_j + m_j}{2} \\ P(g_j = 0|x, y) &= \frac{p_j(1-m_j)}{2} + \frac{m_j(1-p_j)}{2} + (1-p_j)(1-m_j) = \frac{2 - p_j - m_j}{2} \end{aligned}$$

In addition, if the ancestry of one of the parents of a child of mixed ancestry is known (i.e. x), it should be possible to identify the the ancestry of the other parent by searching for the maximum likelihood of y over a fairly simple space (for example a two dimensional space involving latitude-like and longitude-like coordinates. Assuming the European genetic variation today is approximately structured similarly to the fifth to sixth centuries, we aimed to exploit this to identify the approximate geographic ancestry of missing parents in our various pedigrees from Szólád and Collegno.

We first used the original diploid-based `SPA` software to estimate the a and b function coefficient for each SNP and 2-dimensional x coordinate for each individual in the POPRES imputed dataset assuming a single parental original (i.e. both parents from the same location). We then estimated the appropriate x for each Medieval sample

assuming a single parental origin using the haploid version of the likelihood function for all callable SNPs for that sample. This analysis was implemented in Python using the a nonlinear conjugate gradient algorithm (`fmin_cg` in `scipy.optimize`) with 5 random start points. The resulting inference strongly resembled the PCA analysis (Figure S13.1).

We then took every set of Medieval individuals for which there was an inferred parent-offspring relationship but for which data from one parent was missing. We then estimated the likely relative geographical location of the missing parent, y, conditional on the offspring haploid data and a known x. We used the same optimization strategy above, except we used 10 random start points, as well as start points that matched the final estimated position for the known parent of offspring from above. When there were more than one offspring per parent, we maximized the summed likelihoods across offspring (this will tend to weight offspring with more SNP data). When there was no known parent, we used avuncular individuals as surrogates for the missing parent.

There were eight sets of parent/avuncular-offspring relationships analysed using this approach, three from *Kindred_SZ1* (including one pair with the same offspring but using different avuncular surrogates, four from Fam_CL1 and one from *Kindred_CL2*. Three sets (one from *Kindred_SZ1* and two from *Kindred_CL1*) show very little to no difference between the geographical placement of the known and unknown parent (Figure S13.2-4), while the other five show small (at the scale of the European continent) but noticeable differences that suggest admixture between parents of different ancestry within Europe (Figure S13.5-9). For four of these cases, our inferences are supported by

having more than one offspring. Using both SZ14 and SZ22 as surrogates, individuals SZ8 and SZ14 appear to be the result of mating between an individual from central/northern Europe and an unknown parent that resembles individuals from modern France. This is supported by the notieceably increased TSI ancestry in the ADMIXTURE analysis for these offspring. Offspring CL83 to CL84 appear to have an unknown parent with more Scandinavian-type ancestry than the other sampled parent, CL87. CL87 themselves appears to be the result of mating between CL102 and an unknown parent from Northwestern Europe, which would explain why CL102 has increased/reduced TSI/CEU+GBR ancestry compared to CL87. Finally, CL53 and CL47 are inferred to have an unknown parent with greater eastern European ancestry than the sampled parent, CL49.

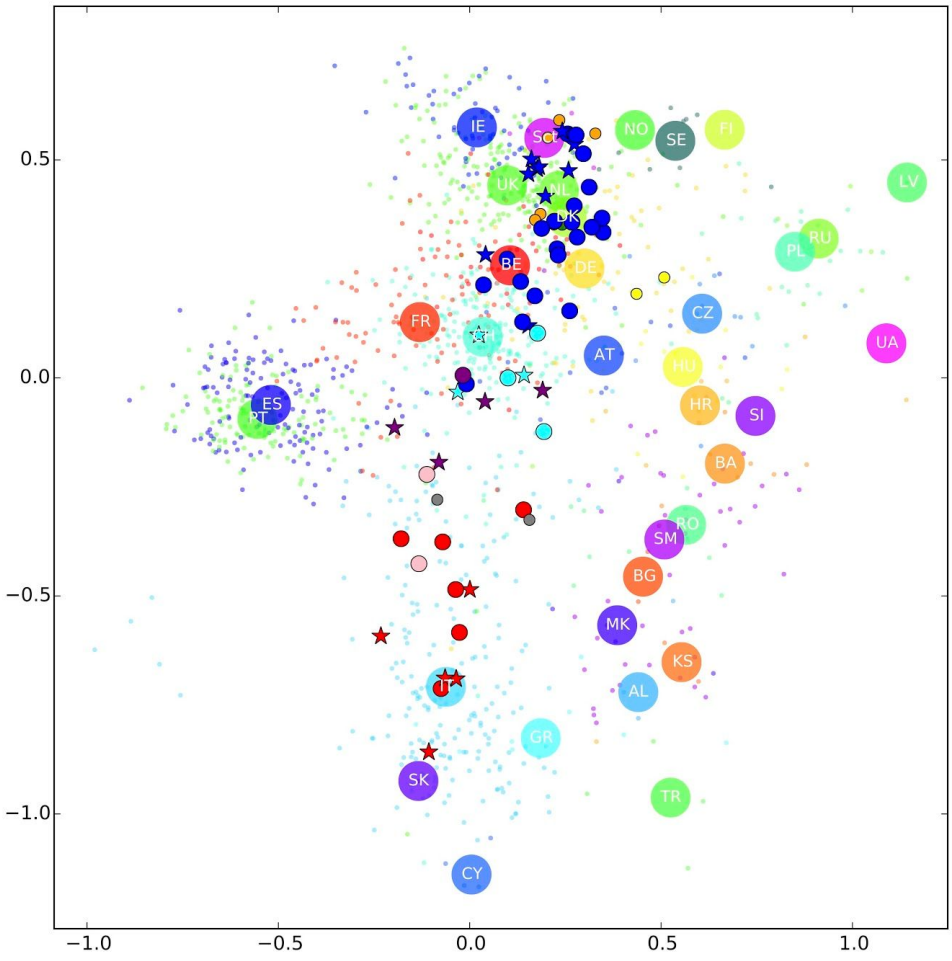

Figure S13.1. SPA analysis allowing 2-dimensional coordinates for diploid POPRES individuals and haploid Medieval samples assuming a single parental origin.

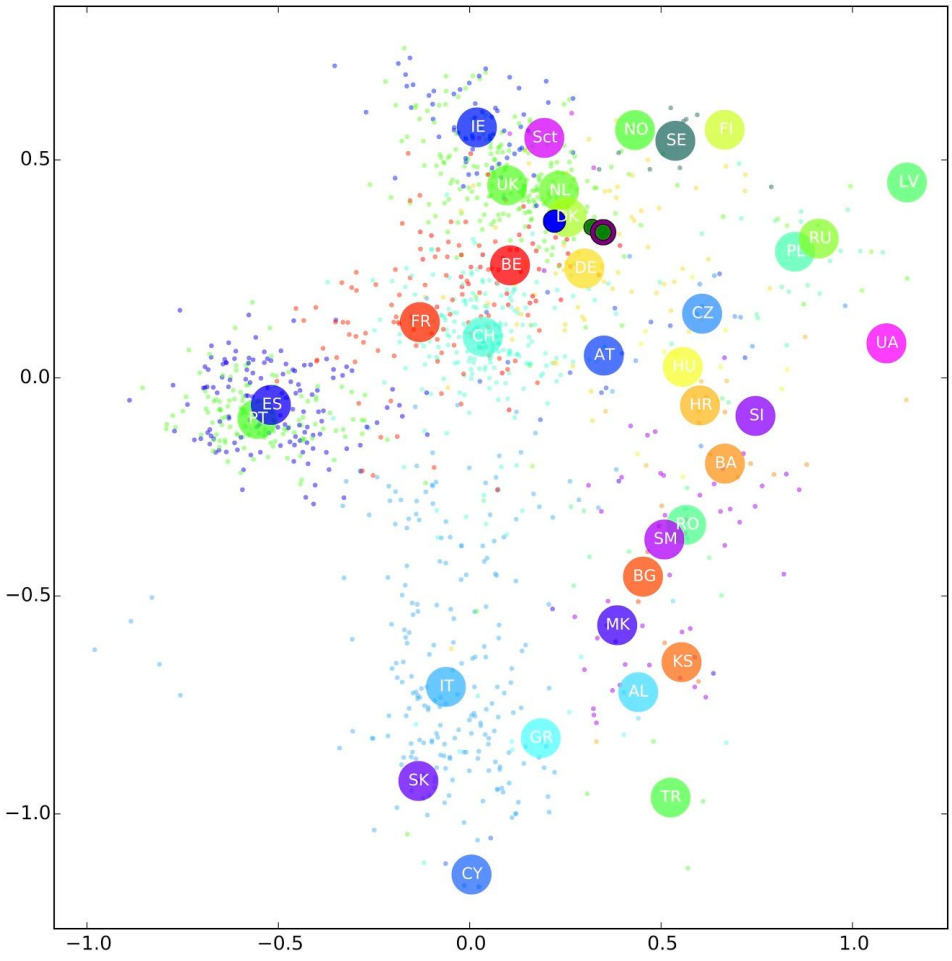

Figure S13.2. SPA-based analysis of unknown parent for parent/avuncular (SZ24) and offspring (SZ13, SZ22). Known parent = blue filled circle, unknown parent = purple filled circle, offspring = green filled circles.

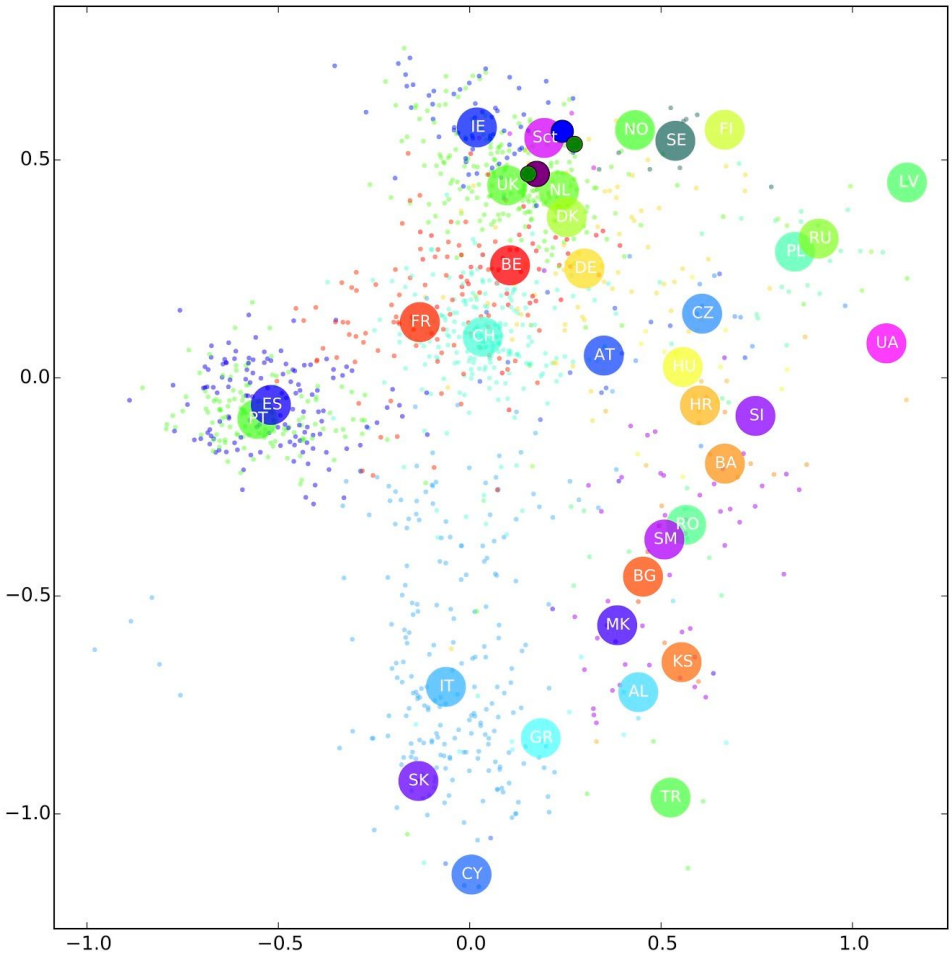

Figure S13.3. SPA-based analysis of unknown parent for parent/avuncular (CL151) and offspring (CL145, CL146). Known parent = blue filled circle, unknown parent = purple filled circle, offspring = green filled circles.

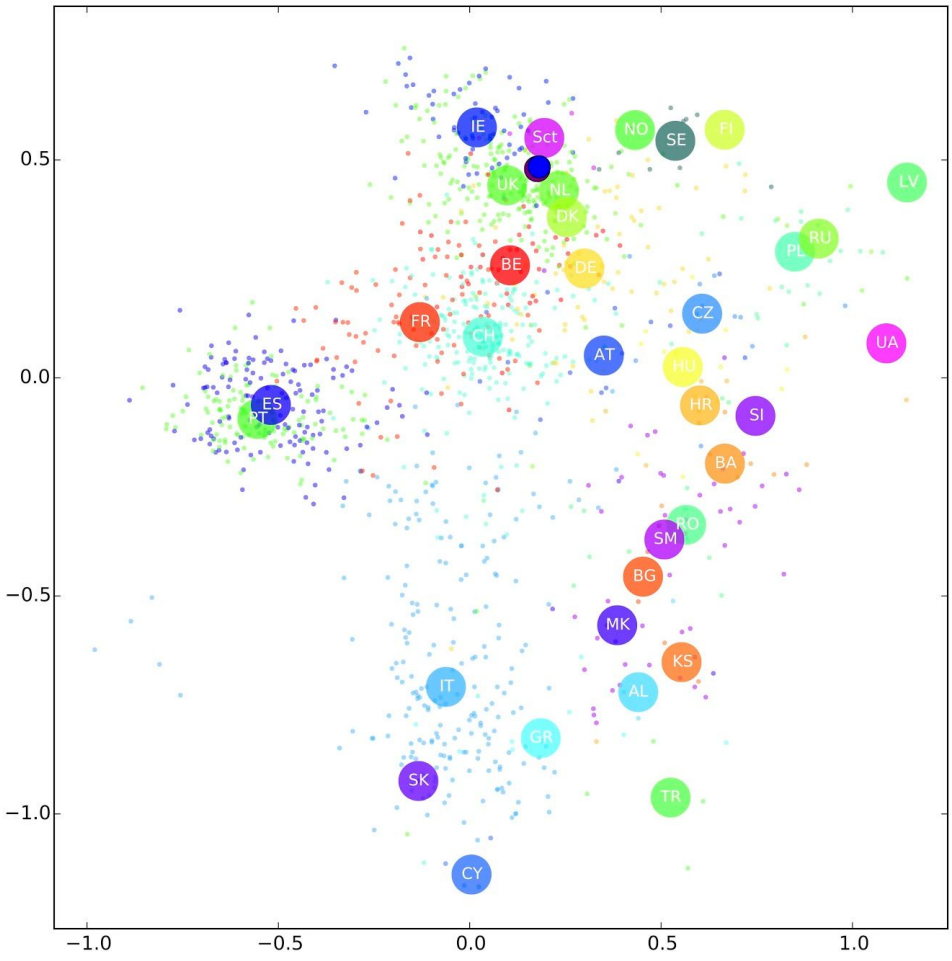

Figure S13.4. SPA-based analysis of unknown parent for parent/avuncular (CL93) and offspring (CL92). Known parent = blue filled circle, unknown parent = purple filled circle, offspring = green filled circles.

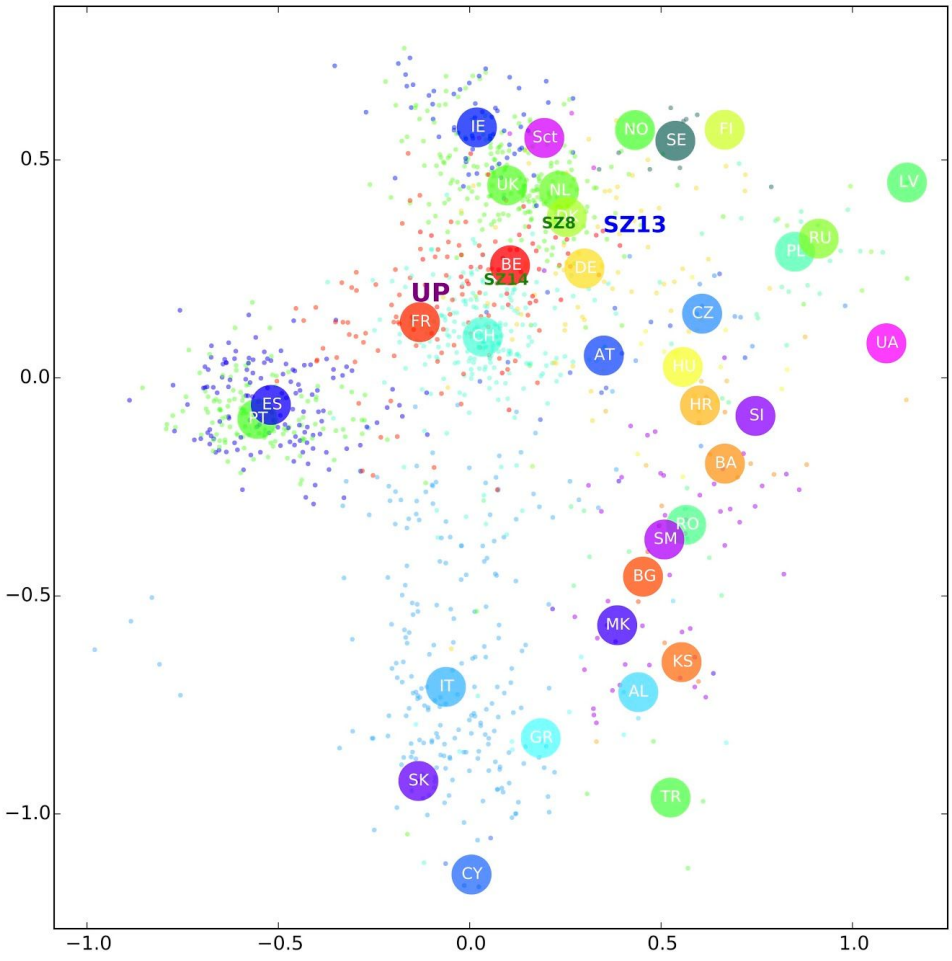

Figure S13.5. SPA-based analysis of unknown parent for parent/avuncular (SZ13) and offspring (SZ8, SZ14). Known parent = blue, unknown parent = purple UP, offspring = green.

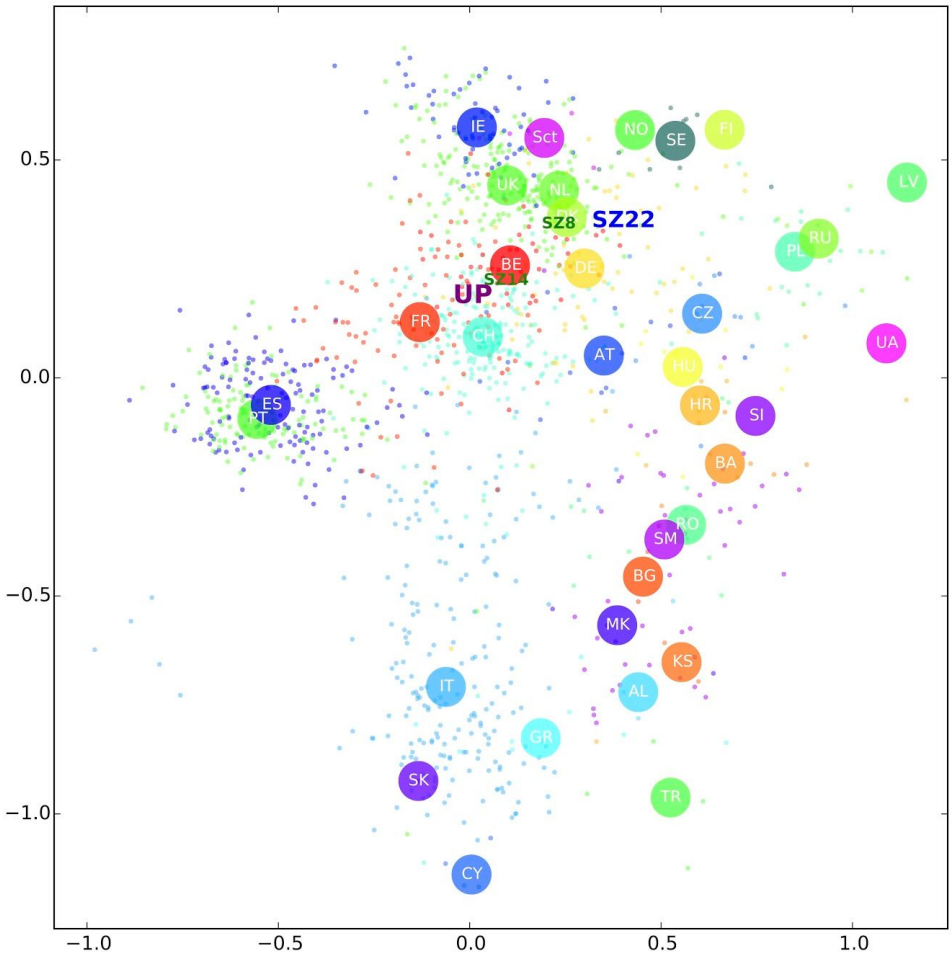

Figure S13.6. SPA-based analysis of unknown parent for parent/avuncular (SZ22) and offspring (SZ8, SZ14). Known parent = blue, unknown parent = purple UP, offspring = green.

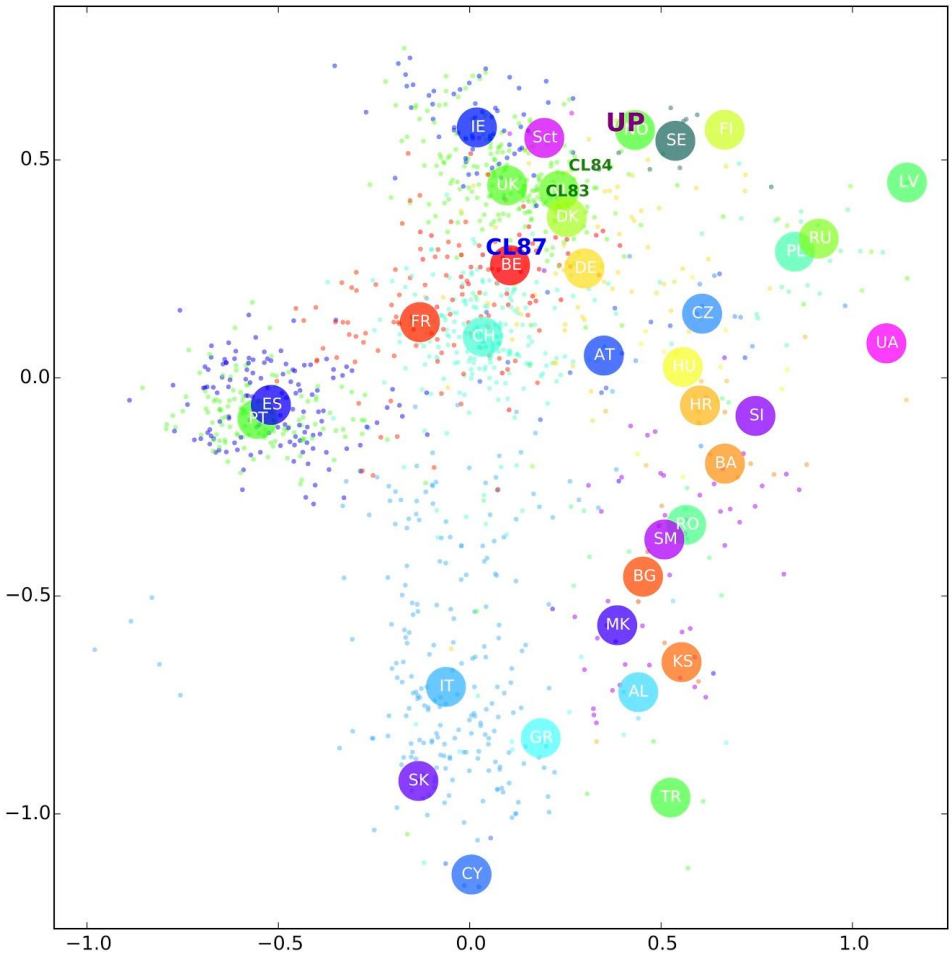

Figure S13.7. SPA-based analysis of unknown parent for parent/avuncular (CL87) and offspring (CL83, CL84). Known parent = blue, unknown parent = purple UP, offspring = green.

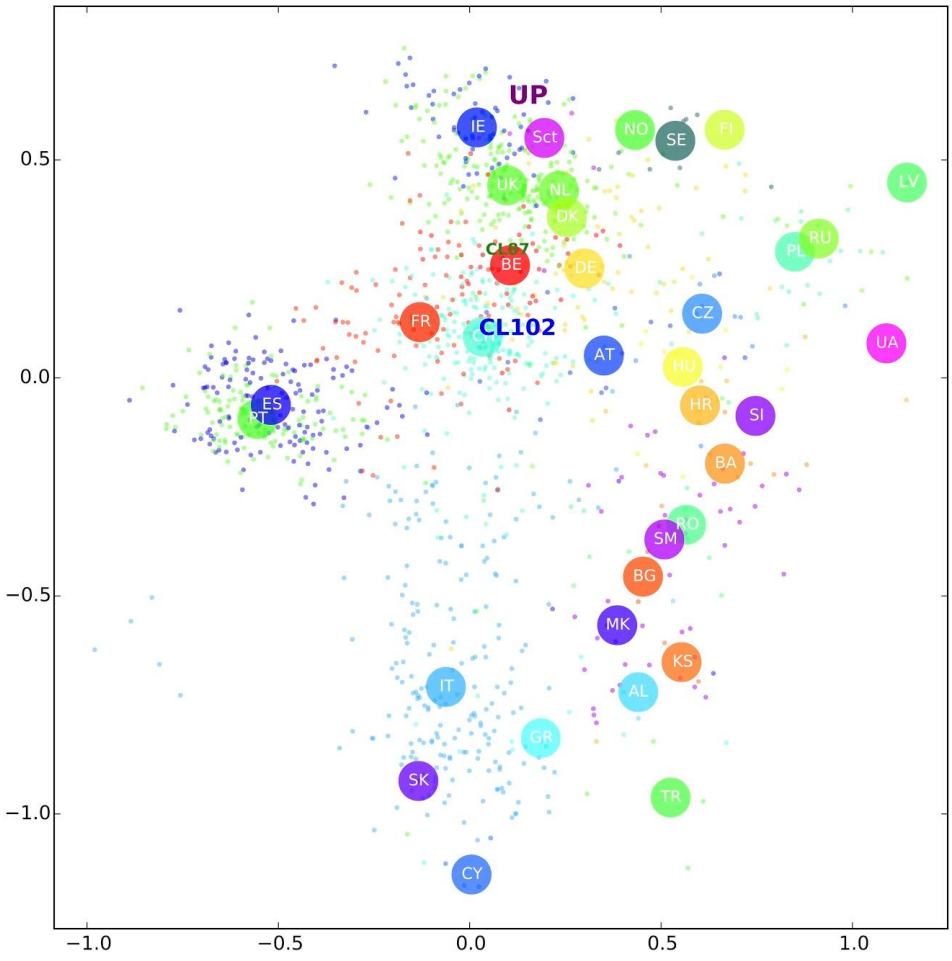

Figure S13.8. SPA-based analysis of unknown parent for parent/avuncular (CL102) and offspring (CL87). Known parent = blue, unknown parent = purple UP, offspring = green.

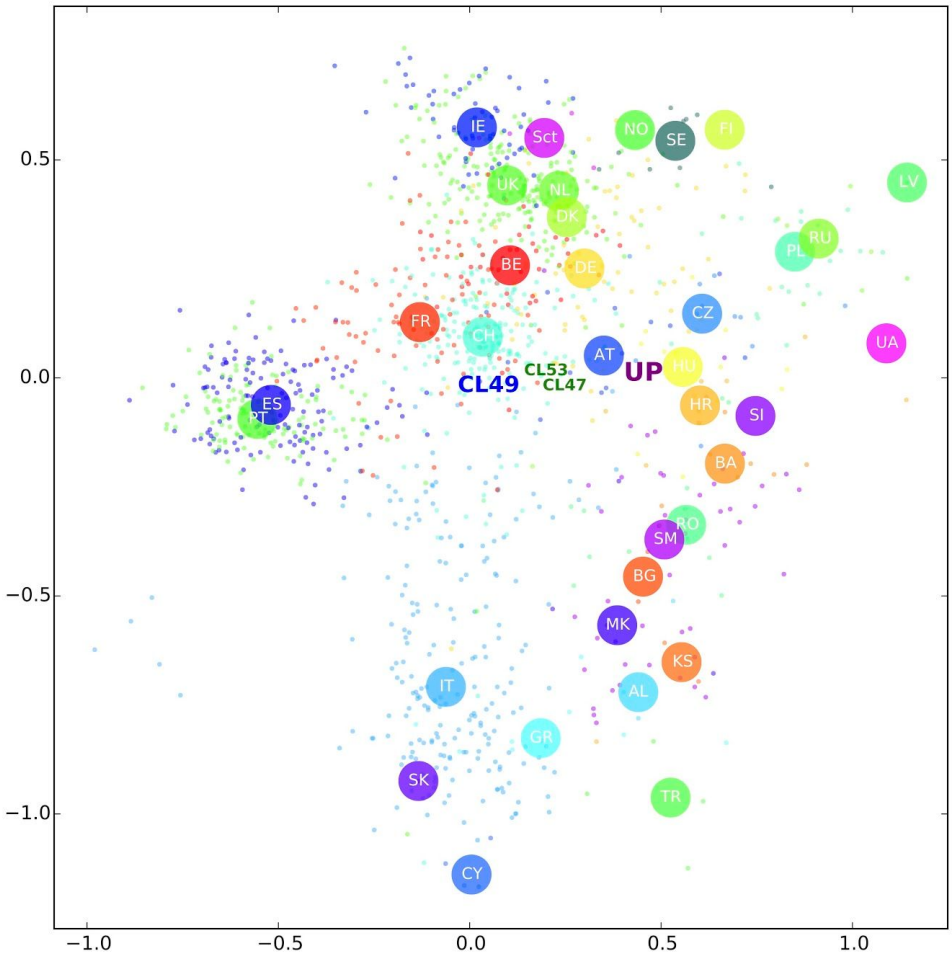

Figure S13.9. SPA-based analysis of unknown parent for parent/avuncular (CL49) and offspring (CL53, CL47). Known parent = blue, unknown parent = purple UP, offspring = green.

S14. COMPARING GENETIC ANCESTRY, GRAVE GOODS AND MORTUARY PRACTICES

Carlos Eduardo G. Amorim, István Koncz, Daniel Winger, Caterina Giostra

A visual inspection of Fig 1 (main text) reveals that the distribution of grave goods (yellow dots) as well as the grave types (green dots) are not uniform across graves of individuals of different genetic ancestries. To statistically test for an association between genetic ancestry and archeology, we implemented a series of Fisher exact tests on contingency tables as described below. We first (a) classified individuals into genetic ancestry groups, then (b) tested the association between these and grave furnishing and typology, and finally (c) tested whether particular artifacts were more often seen in graves with individuals of a given ancestry.

a. Defining groups based on genetic ancestry

We first classified individuals into three categorical variables *N, S,* and *I,* according to their genetic ancestry estimates (Fig 2B-C main text and Supplementary Text S8). We classified an individual as *N* if the proportion of genetic ancestry from Northern/Central European populations from the 1000 Genomes Project[71], namely CEU, GBR or FIN, had reached a given threshold *T.* In doing so, we considered the sum of the ancestry proportion estimates corresponding to these three populations. Conversely, we classified an individual as *S* if the estimated proportion of genetic ancestry from Southern European (TSI) or Iberian (IBS) populations from the same dataset had reached the same threshold *T*, again considering the sum of ancestries for these populations. If the estimates for a

given individual did not reach the threshold *T*, we defined it as *I* and further excluded it from the statistical tests (but see subsection "d" below). *T* was initially set to 70%, but other more extreme values were also considered (e.g. 60% and 90%). The use of different thresholds only changes the sample size minimally (Table S14.1) and did not have a considerable impact on the statistical significance (Table S14.2).

In these analyses, we did not consider individuals *CL57* and *CL94* because their graves presented signals of disturbance and there are reasons to believe the grave goods found in their tombs during excavation of the site are not representative of the actual grave furnishing at the moment of the burial of these individuals. Sample *CL36* was excluded because it does not belong to the first period of occupation of Collegno as the remaining samples and sample *CL31* was excluded due high contamination (~27%).

b. Is grave furnishing/typology associated with genetic ancestry?

A burial is a performance that has an important role in creating the connections between persons (living or deceased). Mortuary practices can shape memories the community has about the deceased, but ultimately they communicate how the living individuals chose to represent the one being buried. In some cases, they may tell us much more about how living individuals want to display their status and power, than anything about the deceased. For a more thoroughly discussion on these issues see [104–108]. In this regard, although it is difficult to connect legal or social status to archeological findings in general, the uneven distribution of specific artifacts may reflect social and cultural differences among individuals and kindred. For instance, in Szólád, weapons are

commonly seen in graves with male adults but also amongst those with adolescents at the time of death: individuals SZ7, SZ14, and SZ15, for instance, are thought to be 12-17 yo. at the time of death[28] and were buried with spears, shield and/or swords. This does not necessarily mean these individuals were warriors, but that weapons in this case may have been socially symbolic, potentially indicating the assigned status of those buried with them. Clearly not all male adults in these communities (warrior or not) were buried with weapons, so there was a possible conscious choice to bury a person with such artifacts, which in turn could tell us about different social roles amongst individuals or about different cultures and funerary customs. As another example, knives, combs, purses (with objects for personal use) and belt buckles (the type used for clothing, not for holding weapons) are very common to different cultures and regions during the migration period, and cannot be associated to any sort of social condition. In contrast to that, we see that certain traditions of pottery and jewelry, as well some behaviors such as the use of food offerings, are restricted to certain groups and/or periods, and thus are thought to reflect the presence of a certain group defined in terms of material culture.

The analyses in this section attempts to examine whether shared a common genetic ancestry (whether indirectly known by the individuals themselves or not) was a relevant aspect in shaping customs and mortuary practices in these societies. We are <u>not</u> assuming the individuals buried with a certain material culture marker or genetic ancestry were or were not "Longobards," but we are inquiring whether biological relationship (i.e. shared genetic ancestry) was perceived as a structural element in this society, assuming if

that is the case, then mortuary practices should be distinct for individuals of different genetic ancestries.

In both cemeteries we found graves that were devoid of grave goods and some that presented at least one of such artifacts (Fig 1B-C, main text). As a common characteristic of both cemeteries, all *N* individuals were buried with grave goods (e.g. jewelry, pottery, food offerings, knives, combs, weapons etc.). This is always true regardless of the different values of *T*. Graves with *S* individuals were more variable (Table S14.2), but with the exception of a couple of cases (*SZ19* and *SZ31*, see discussion below) grave goods are everyday objects used by everyone, some of which are common to many different cultures in the Migration Period (e.g. purse with personal objects, comb, belt buckle and other clothes elements, knife). We do not see weapons buried with *S* individuals.

To test for an association between the presence of grave goods and genetic ancestry, we focused on those artifacts that are more restricted to certain cultures and periods, particularly weaponry and related accessories, stamped pottery, food offerings, and jewelry, the reason being that these can be considered "cultural markers" of a culture or a group. In Szólád we specifically looked at the following grave goods: jewelry (e.g. amulet, bracelet, rings, brooches etc.), strike-a-light, pottery, weapons (e.g. spatha, spear, shields etc.), beads (from necklaces or pendants), food offerings (animal bones, eggshells, etc.), and spindle whorls. In Collegno, the following artifacts were considered: beads, stamped pottery, weapons, and strike-a-lights. In both cases, the presence of grave goods is significantly associated with genetic ancestry (p-value < 0.05, according to a Fisher

exact test applied on contingency tables), regardless of the value of *T* chosen (Table S14.2), showing that certain grave goods are mostly found in graves with individuals of *N* genetic ancestry.

We also implemented the same test considering the different grave typologies. Grave types were either (i) simple pits or (ii) graves with wooden constructions. The latter were never documented in Mediterranean regions and cultures, and are somewhat similar across cemeteries. In Szólád, they presented ledges in the sidewalls supported by wooden beams covering the coffins (see Fig S2.5 and S2.6). These were significantly more often seen among *N* graves (p-value < 0.0001; Table S14.3). In Collegno, the second type of grave was constituted by a wooden chamber that was not seen in the simpler grave type. The association between grave type and genetic ancestry is also significant in Collegno (p-value < 0.05; Table S14.3).

In summary, we see that in both cemeteries individuals are accorded different mortuary practices depending on their genetic ancestry. Obviously these individuals were not aware of their genetic ancestry in ways we understand it, but indirectly there could be the recognition between persons of similar origins (e.g. from Northern/Central versus Southern Europe), i.e. a certain acknowledgement of belonging to a group that potentially share common customs and, due to a common origin, also share genetic ancestry.

Despite the statistically significant association between archeology and genetic ancestry, there are some exceptions to the general trend of "*N* → richer graves / *S* → simple graves". These exceptions are described in more detail below:

- *SZ19*: female *S* (100%) individual buried in the half-ring structure surrounding *N* male individuals (see Fig S2.2). This individual is the only female buried with a bracelet (see Fig S2.10). This type of artifact is uncommon in cemeteries commonly termed "Longobard," but was common in Mediterranean cultures, associated with a late antique tradition. Moreover, this grave is also of the simple pit type and shallow, and contains a reduced amount of offerings of grave goods when compared to other graves in the same half-ring structure in this cemetery. We note that this woman was distantly related to individual SZ6, member of the large *Kindred SZ1*.
- *SZ31*: female *S* (99%) individual buried in a ledge-wall-type of grave amongst *N* women, in the half-ring structure surrounding the *N* male warriors. Her daughter is buried nearby. Along with SZ19, she is the only *S* individual that has a relative buried in Szólád. Together, this could potentially indicate that the barrier between groups was somewhat permeable, at least to some females.
- *SZ38*: *N* (89%) female individual buried in a simple pit (in contrast to other *N* women in that cemetery that have a ledge-wall-type of grave). Despite being a simple grave, some artifacts were buried with this individual, namely a ring, a pair of S-brooches and beads.
- *CL151*: *N* (100%) woman of advanced age. As opposed to other adult women in Collegno, only a belt buckle was found in her grave and her grave is a simple pit (i.e. does not contain a wooden chamber). The dating of her burial is imprecise, but the lack of a wooden chamber could be a consequence of temporal changes in grave

architecture that is seen in Collegno (see below) or particular family customs, while the lack of grave goods could be due to her advanced age.

- *CL97*: *N* (100%) individual with simple grave (no wood chamber). This individual is likely from the early stage of occupation of Collegno, a time period where the wooden chambers were used in the region (as seen in other graves). The reason for such a discrepancy is unclear. However, this grave, as others with *N* individuals, was furnished with several weapons.

c. What artifacts are more often seen in graves with *N* individuals?

We further performed the test for each type of grave good independently ($T = 70\%$; Table S14.4), as opposed to considering their general absence/presence as above. In these tests, we ignored artifacts that were present with only one individual (being that *N* or *S*), and focused on the eight types of artifacts in Szólád and the three types of artifacts in Collegno that were seen in at least two graves. If an artifact was not seen buried with members of one sex, we excluded all individuals from that sex from the analyses. We also excluded male individuals that were younger than 12 yo. when we analyzed weapons.

Three grave goods are significantly more often buried with *N* individuals: "Beads" (female) and "Food offerings" (both female and male) in Szólád, and "Weapons" (male) in both Collegno and Szólád. Additionally, we observe that stamped pottery and the articulated 5-pieces belts used to hold weapons (often decorated with animalistic patterns) are only seen with *N* individuals. We note that a chronological factor

may also be relevant in this case since the more articulated kind of belt only appears in the Longobard-associated cemeteries around the year 600 CE, hence the low frequency of these amongst first phase graves in Collegno.

d. Notes on *Kindred CL2*

Kindred CL2 is located in the eastern part of Collegno. Genetic evidence supports the relationship between CL47, CL49, CL53, and CL57 (Fig 3). The position of grave CL48 between CL47 and CL49, in a single row, suggests these individuals could potentially be related (biologically, due to first-second degree relationship, or socially, for instance, as members of the same household) to the female buried in graved CL48. In fact, as noted in Supplementary Text S3, this grave contains artifacts not common to the region, with likely transalpine origins, similarly to CL47. Moreover, the fact CL48 and CL47 both present a form of hereditary scaphocephaly further strengthens the possibility of this relationship being also biological.

Members of this kindred did not reach the threshold *T* for being considered *N* or *S* in the previous analyses, but we consider it is worth mentioning their graves contain artifacts that seem to be, at least in part, from a different tradition in comparison to other graves in Collegno (Supplementary Text S3), such as jewelry and accessories seen in the transalpine area. We also see that members of this kin group are the only ones seen with golden crosses in this early stage of occupation of Collegno.

In resemblance to graves with *N* individuals, graves CL47, CL48 an CL49 have wooden chambers, and adult males CL49 and CL53 were buried with weapons. Because

of the way we implemented this analysis, i.e. considering the classification of individuals in two categories *N* and *S*, we were not able to include members of this kin group in the tests, but we see that certain artifacts and traditions are unique to members of a single kindred, giving further evidence for the idea that biological relatedness might have had been an important structural element in these societies.

Table S14.1 Individuals considered for the different ancestry groups.

Ancestry group	Individuals (T = 70%)	Excluded if T = 90%	Included if T = 60%
N	*SZ7, SZ22, SZ13, SZ12, SZ4, SZ9, SZ41, SZ30, SZ11, SZ16, SZ2, SZ24, SZ15, SZ42, SZ8, SZ38, SZ14, SZ6, SZ3, SZ25, SZ23, CL93, CL145, CL146, CL84, CL92, CL151, CL83, CL97, CL87,* and *CL63*	*SZ38, SZ14, SZ6, SZ3, SZ25, SZ23,* and *CL63*	*SZ5,* and *CL102*
S	*SZ37, SZ28, SZ36, SZ31, SZ43, SZ40, SZ32, SZ19, CL23, CL110, CL121, CL30, CL38,* and *CL25*	*SZ37* and *SZ28*	-

Table S14.2. Contingency tables describing the distribution of artifacts in graves of individuals of different genetic ancestries: Northern (N) and Southern (S) European genetic ancestry.

	T (%)	*N* with grave goods	*N* no grave goods	*S* with grave goods	*S* no grave goods	p-value
Szólád	**60**	22	0	2	6	0.0000
	70	21	0	2	6	0.0001
	90	15	0	2	5	0.0008
Collegno	**60**	9	2	0	6	0.0070
	70	8	2	0	6	0.0070
	90	7	2	0	6	0.0070

Table S14.3. Contingency tables for the different grave types containing individuals of different genetic ancestries: Northern (N) and Southern (S) European genetic ancestry.

	***N* simple pit**	***N* wooden elements**	***S* simple pit**	***S* wooden elements**	**p-value**
Szólád	1	20	7	1	<0.0001
Collegno	4	6	6	0	0.0338

Table S14.4. Contingency tables for Fisher exact test for the association between the presence and absence of grave goods and genetic ancestry. Individuals are classified according to their genetic ancestry as *N* (northern European) or *S* (southern European or Iberian). Each contingency table was stretched in one line. The first column describes the artifact that is being tested. In parenthesis a character describes if an artifact is restricted to females (F), males (M) or none (B). The following four columns describe how many individuals were seen with and without the corresponding grave good, given the genetic ancestry (*N* or *S* accordingly). The column "Cemetery" describes the site where specimens were sampled and the last column the p-value for a Fisher Exact test. Significant p-values are shared in dark grey.

Artifact	N with	N without	S with	S without	Population	P-value
Amulet (F)	2	4	0	5	Szólád	0.4545
S-Brooch (F)	4	2	1	4	Szólád	0.2424
Beads (F)	6	0	1	4	Szólád	0.0152
Ring (F)	1	5	1	4	Szólád	1.0000
Spindle whorl (F)	2	4	0	5	Szólád	0.4545
Strike-a-light (M)	3	12	0	3	Szólád	1.0000
Weaponry (M)	10	0	0	2	Szólád	0.0152
Pottery (B)	7	14	1	7	Szólád	0.3805
Food offering (B)	17	4	0	8	Szólád	0.0001
Weaponry (M)	5	1	0	5	Collegno	0.0152
Belt for weapons (M)	3	3	0	5	Collegno	0.1818
Strike-a-light (M)	2	5	0	5	Collegno	0.4697

S15. ISOTOPE ANALYSES IN COLLEGNO AND COMPARISON TO SZÓLÁD

Susanne Hakenbeck

S15.1. Background

Isotope analysis was carried out on individuals from Collegno to identify first-generation migrants and to determine whether such migrants might have brought with them dietary habits that were different from those of the local population of northern Italy. The degree to which migrants changed their dietary habits to those of the population among which they settled provides important clues about relationships between newcomers and the existing population[109].

Strontium and oxygen isotope values are used to determine whether an individual grew up where he or she was buried. $^{87}Sr/^{86}Sr$ values in organisms reflect the values of the underlying geology, with older geological formations generally having higher $^{87}Sr/^{86}Sr$ ratios than younger ones. Bioavailable strontium enters the foodchain through water. Strontium isotope ratios are measured in enamel apatite which forms during childhood and juvenility. Isotopic values of tooth enamel are thus a reflection of the place of residence in childhood. Contrasted with local bioavailable $^{87}Sr/^{86}Sr$ values, they can be used to determine a change in residence since childhood[110] .

Oxygen isotope ratios ($\delta^{18}O$) also vary geographically, primarily due to differences in temperature, becoming more depleted from the equator to the poles and with increasing altitude[111]. Across Eurasia values are also depleted from west to east, along with the prevailing winds. Via an offset, organisms reflect the isotopic value of drinking water, which in turn usually reflects rainwater. Attempts have been made to

develop a conversion algorithm for the offset from drinking water to body tissue for different species, but these have not been fully satisfactory [112,113]. Furthermore, in many published studies intra-population variation of oxygen isotope ratios is greater than large-scale geographical variations of precipitation (e.g. from Scandinavia to the Mediterranean)[114]. This may be due to water sources other than rainwater and changes in isotopic ratios due to cooking, brewing or stewing[115] . Our study therefore uses the unconverted values from enamel carbonate and restricts itself conservatively to intra-population comparisons. It is important to note that only individuals who grew up in a location with different geological strontium or water oxygen ratios can be identified as non-local. Strontium and oxygen isotope analysis can therefore only indicate a non-local upbringing, but it cannot definitely indicate a local upbringing.

Carbon and nitrogen isotope ratios in bone collagen, reported as $\delta^{13}C$ and $\delta^{15}N$, reflect the relative contribution of terrestrial, marine and freshwater resources to diet. Carbon isotope ratios enable us to distinguish dietary contributions from C3 and C4 plants, since these plants have isotopic ratios that do not overlap[116,117]. Isotopic values are enriched by approximately 1 to 2% from diet to body tissue[118]. Most plants, in particular most domesticated plants, utilise the C3 pathway, while the C4 pathway is used by plants in hot and dry climates, mostly grasses and sedges. They key cultivars in pre-colonial Europe are millet and sago, while maize plays an important role in the Americas. In Europe millet is considered one of the minor crops and has been used preferentially in unstable climatic or economic conditions[119].

Nitrogen isotope values allow us to determine the relative amount of animal protein (meat or milk, including breast milk) consumed by an organism. $\delta^{15}N$ is enriched by about 3% with each trophic level[120,121], though the enrichment can be as high as 6% in some instances[122]. Both freshwater and marine organisms are enriched in $\delta^{15}N$, though freshwater fish in particular are strongly affected by their ecological context[123].

S15.2. Environmental context and samples

The site of Collegno is located on the floodplain of the river Po and beside a small tributary, the river Dora. The floodplain is made up of Pleistocene gravels. To the west are the Alpine foothills; this area is made up of Pleistocene glacial deposits and an oophiolite complex of serpentinite and green schist. To the east there is an outcrop of Miocene clays and marls. To determine 'local' bioavailable strontium values, samples of water, vegetation and soil were collected both at the site of the cemetery of Collegno and at locations considered to be about a day's walk from the site that are geologically different from the plain (Figure S15.1), following the procedure outlined in Maurer et al.[124]. Water was collected from the rivers Po and Dora and from a small lake to the west of Collegno. Soil samples were taken with an auger to below the topsoil, reaching depths of 0.25 to 0.70 m. Fields under cultivation were avoided to mitigate the impact of fertiliser use. Similarly, tree leaves were collected only from areas far from cultivated fields.

Fauna can provide a local ecological baseline for human diet. We chose six from different species from an excavation in Piazza Castello in Turin, dating from the first to

third/fourth centuries AD, since no contemporary fauna was available. Bone samples from fauna were variable, though cortical bone was preferred. Human bone samples (0.5-1.5 g) were taken from ribs where available, otherwise from long bones. For tooth samples, the second premolar was preferred since its crown begins to form from two years of age and is completed by seven years[125] and it therefore retains information about childhood residence.

S15.3. Analytical methods

Human teeth and bones were collected from burials at Collegno (Supplementary Text 3) targeting the first period. Environmental samples for strontium analysis were pre-treated following the methods described in Maurer et al.[124]. Water samples were filtered through 0.2um nylon filters into 60ml acid cleaned HDPE bottles and acidified with distilled ultra-pure nitric acid to maintain a pH = 2. Soil leachates were obtained by shaking 2 g of soil in 20 ml deionised ultrapure water for 24 h in acid-cleaned polypropylene tubes, followed by 1 h in an ultrasonic bath. The solution was centrifuged for 15 minutes at 2000 rpm and filtered through 0.2um nylon filters. Water and soil leachates were evaporated to dryness. Leaves were rinsed with deionised ultrapure water and dried in an oven at 50°C overnight. Approximately 1 g of dried leaves was then ground and ashed in acid-washed silica crucibles at 550C for 12 h. All samples were then transferred into acid-cleaned Teflon vials. For strontium isotope analysis of tooth enamel, the enamel surface of the tooth was abraded to a depth of >100 microns using a tungsten carbide dental burr and the removed material discarded. Tooth enamel powder was then

collected, and the samples were transferred to a clean (class 100, laminar flow) working area for further preparation. In a clean laboratory, the samples were first washed in high purity acetone to remove any grease that might have come from handling the enamel. Then the sample was cleaned ultrasonically in high purity water, rinsed, dried and then weighed into pre-cleaned Teflon vials. The samples were mixed with ^{84}Sr spike solution and dissolved in Teflon distilled 8M HNO3.

Strontium isotope samples were analysed at the Isotope Geochemistry Laboratory of the Department of Earth Sciences, University of Cambridge. Strontium was separated using Dowex 50 x 8 (200-400 mesh) cation exchange resin and the strontium isotopic ratios were measured on single Ta filaments on the VG Sector 54 TIMs using triple collector dynamic algorithm, normalised to $^{86}Sr/^{88}Sr$ 0.1194 with an exponential fractionation correction[126]. The 46 analyses of NBS 987 during the two year period up to and including these analyses gave a mean value of 0.710257+/-0.000006 (1 sigma).

For oxygen isotope analysis of enamel apatite, tooth enamel powder was obtained using a using a dental drill with a diamond drill attachment. The exterior of the enamel was mechanically abraded to remove any dirt, and the drill bit was cleaned before each sample was taken. The bioapatite extraction method is described in Balasse et al.[127]. Enamel was treated with sodium hypochlorite 2–3% (24 h) to remove organic matter and then with 0.1 M acetic acid (4 h, 0.1 ml/mg) to remove exogenous carbonate. The samples were lyophilised to remove any remaining liquid. The samples were then transferred into vials sealed with a screw cap holding a septa and PCTFE washer to make a vacuum seal, and the samples reacted with 100% orthophosphoric acid at 90°C using a

Micromass Multicarb Sample Preparation System. The carbon dioxide produced was dried and transferred cryogenically into a VG SIRA mass spectrometer for isotopic analysis. Results are reported with reference to the international standard VPDB calibrated through the NBS19 standard[128,129]. The precision is better than ±0.08‰ for $^{13}C/^{12}C$ and better than ±0.10‰ for $^{18}O/^{16}O$.

Collagen was extracted from human and faunal bones following the standard laboratory protocol of the Department of Archaeology, University of Cambridge, based on the method detailed by Privat et al.[130]. The surfaces of the bone pieces were cleaned by sand-blasting. The pieces were demineralized in 0.5 M aq. HCl at 4°C until all mineral was dissolved (7-14 days). Samples were rinsed with distilled water and then gelatinized in acidic solution (pH 3) at 75–78°C for 48 h. The liquid fraction containing the gelatinized protein was frozen and lyophilised. Approximately 0.8 mg portions of this final 'collagen' product were used for each analysis. Samples were analysed in triplicate at the Godwin Laboratory, University of Cambridge, using an automated elemental analyser (Costech) coupled in continuous flow mode to an isotope ratio-monitoring mass spectrometer (Finnegan MAT253). Results are reported using the delta scale in units of 'per mil' (‰) relative to internationally accepted standards, VPDB for carbon and AIR for nitrogen. Measurement errors are less than ±0.2‰ for $\delta^{13}C$ and $\delta^{15}N$, as determined by replicate analyses of international and laboratory standards.

S15.4. Results

The full results of human and fauna samples together with relevant osteological and genomic data can be found in Tables S15.1-3. All collagen samples produced collagen of good quality. The atomic C/N ratios were between 3.09 and 3.22, well within the range of 2.9-3.6 considered to be indicative of good collagen preservation[131]. Every collagen sample yielded carbon in excess of >13% and nitrogen in excess of 4.8%; many samples were in the range of modern human collagen (40-50% carbon and 15-18% nitrogen), as defined by Ambrose[132].

Evidence for migrants at Collegno.

Bioavailable strontium isotope values local to the cemetery and hypothetical settlement at Collegno were determined by soil and vegetation values near the site, with the values of Po and Dora as likely endpoints (Fig 4). Environmental values from the Alpine foothills and the marl outcrop further away are elevated compared to these, in line with the greater antiquity of the underlying geology. The four sub-adults at Collegno fall within the local strontium isotope range, indicating that they grew up nearby. A number of adults, however, lie well outside the local range. Of these, one female individual (CL147) and two males (CL23 and CL94) have isotopic values that do not occur near Collegno, while several others are very close to the local environmental end values (female individuals CL48 and CL102 and males CL49, CL93 and CL9). These likely did not grow up locally,

but moved to Collegno from another location. This interpretation is supported by the oxygen isotope data (Figure S15.2). Here CL94 and CL147 are also outliers and at opposite ends of the data range. The woman from grave CL25 has an oxygen isotope value that is similarly enriched to that of the female individual CL147. However, her strontium value is local. This woman might be a migrant, but the evidence is not conclusive.

When considering the genomic ancestry groups together with the isotopic evidence, we find that the four individuals with >70% TSI ancestry are likely local to Collegno (with uncertainty surrounding CL25). The two men with > 50% 'Iberian + southern' ancestry clearly did not grow up locally, while two of the adults with 50-70% 'northern' admixture (CL102 and 49) are probably not local. The strontium isotope values of the individuals with a contribution of >50% 'northern' ancestry have a greater range than those of the individuals with a greater contribution of 'southern' ancestry, suggesting generally higher levels of mobility. The rest are genetically undetermined, but of these, several did not grow up locally. Excluding the subadults, about 28% of the sampled population can be considered not to have grown up near Collegno.

Considering kinship relationships at Collegno (Fig. 3C, Figure S15.3), the woman in grave CL102 who is of the first known generation of *Kindred CL2* has a low $^{87}Sr/^{86}Sr$ value, making it likely that she did not grow up locally. Her daughter, in grave CL87, also has a low strontium isotope value, though not quite as low as her mother's, also making her a potential migrant. She may have grown up elsewhere, or perhaps she moved with her mother while her permanent teeth were still forming. Similarly, the man in grave

CL93 may not have grown up in Collegno, but his son in grave CL92 apparently never moved. In *Kindred CL2* the man in grave CL49, of the first known generation, also had a likely non-local $^{87}Sr/^{86}Sr$ value, making him a migrant to Collegno. His son, daughter and nephew however (CL53, CL47 and CL57) had local strontium isotope values, suggesting that they spent their entire lives close to Collegno. This means that the woman in grave CL102 and the man in grave CL49 were first-generation migrants to Collegno, while all individuals who were in the third generation in either kin group were likely born locally.

A comparison of ancestry groups with the evidence of mobility at Szólád, as previously published in Alt et al.[28], shows much greater heterogeneity than at Collegno. Like at Collegno, most children display local isotopic values. However, at Szólád there is a distinct cluster of children with >70% 'northern' ancestry who clearly all grew up together (identified as Range II in [56]), whereas the two children with >70% 'southern' ancestry (SZ36 and 40) grew up in a different location from them (in Range I). The adults are highly variable. Individuals with >70% 'northern' ancestry have a greater range of strontium isotope values than those with >70% 'southern' ancestry. The latter group may have been local to the Balaton environs, based on bioavailable reference data from the region, but their strontium isotope values do not overlap with the tight cluster of children in 'range II'.

At Szólád an evaluation of mobility across generations is more difficult, since not enough isotope data are available for the complex pedigree of *Kindred SZ1*. However, a comparison of individuals from the second and the third generation shows that all adults were highly mobile (SZ13, SZ22 and ZZ14) and only the children can be linked to

Szólád. This suggests a kin group moving together and only settling in Szólád when the children SZ6 and SZ8 were born (but presumably before the birth of SZ14).

Dietary variation

To determine the diet of the population of Collegno the isotopic values of humans were considered in the context of the local fauna. The faunal results are within the expected ranges for terrestrial mammals in a temperate ecosystem[133] (Tables S15.4-5). The herbivores fed primarily on C3 plants, while isotopic values of the omnivores (dog, chicken) are very similar to those of humans, indicating considerable input of human-provided fodder or remains of human diet. The pig, also an omnivore, has a $\delta^{13}C$ value more like the herbivores, suggesting that it foraged in the wild for some of its food. In line with commonly observed offsets between humans and fauna in the same ecosystem, there is an increase of about 3‰ in $\delta^{15}N$ and 3 to 4 ‰ in $\delta^{13}C_{coll}$ values from the two herbivores to the average human diet[121,134,135]. This may indicate that roughly around 60 % of the protein was derived from animal proteins [121]. There is no indication that fish played a significant role in diet. The two-year old child in grave CL83 had an elevated $\delta^{15}N$ value, likely because she was still breastfed at or close to her death. The $\delta^{13}C_{coll}$ values of humans suggests a diet of mostly C3 plants with an approximate contribution of 20 to 30 % of C4 plants[135].

Considering the diet of individuals at Collegno and Szólád in the context of their migration status and ancestry, we can see that the non-local individuals are not marked

out by a distinctly different diet (Figure S15.4-5). At Collegno both $\delta^{13}C_{coll}$ and $\delta^{15}N$ values are distributed across the entire data range, while at Szólád the diet of non-local individuals firmly lies in a central cluster. We note however that iopic information from their childhood diets, prior to their migration, would be obscured by continued bone remodelling in adulthood[136]. Conversely, the three individuals who were dietary outliers at Szólád (graves SZ5, SZ23 and SZ44) were probably local, according to their strontium isotope values.

At both Collegno and Szólád individuals with >70% 'southern' ancestry had lower levels of $\delta^{15}N$ than other ancestry groups, if we exclude infants whose values are elevated due their consumption of breastmilk (Figure S15.6-7). This suggests that members of this ancestry group had less access to animal protein than others at these sites.

S15.5. Discussion

As was already suggested[28], the population at Szólád was heterogeneous and composed of different kin groups that experienced several shifts in residence prior to settling and dying at Szólád. The most mobile individuals were those with >70% 'northern' ancestry, though there are exceptions (e.g. the female in grave SZ28). Conversely, all individuals with >70% 'southern' ancestry had relatively homogenous $^{87}Sr/^{86}Sr$ values, suggesting somewhat of a shared background, that was nevertheless in a different place from what has been interpreted to be local for Szólád[28]. In Collegno, on the other hand, there is evidence for the migration and settlement of specific kin groups. We can identify several

first-generation migrants to Collegno (individuals in graves CL49, 102 and perhaps 93). The following two generations are then firmly settled at Collegno. Here, as at Szólád, individuals with >70% 'northern' ancestry display greater levels of mobility than those with >70% 'southern' ancestry, suggesting that the 'southern' group was largely local. Two individuals with >50% Iberian and some 'southern' ancestry (in graves CL23 and CL94) are also clearly not local to Collegno, though they are not related to the other kindred. At both sites women experienced somewhat higher levels of mobility than men. This is in keeping with patterns that have been identified elsewhere and quite likely relates to exogamous social structures that seem to have been prevalent in many regions throughout the early medieval period[137–139].

At both sites, the individuals with greater degrees of 'southern' admixture had less access to animal protein, suggesting that they may have been less privileged compared to members of other ancestry groups. Social distinction through preferential access to animal protein has been observed in early medieval Bavaria[140,141], as well as more generally among elites in prehistory and the medieval periods[142]. At Szólád and Collegno the 'southern' individuals, who were also more local, may have been in a socially inferior position to the more mobile individuals with different ancestry. This suggests that the migration of the latter groups did not diminish their social standing. Instead, they were able to maintain a position of privilege. This is also evident in the high levels of burial wealth deposited in some of their graves, as well as an abundance of weaponry. The older female buried in grave CL48, for example, was buried with a rich

assemblage, made up of a pair of fire-gilded brooches and a gold foil cross[37]. She had the most enriched $\delta^{15}N$ value of all individuals at Collegno and had not grown up locally.

Finally, the migration of these groups does not appear to have brought about large scale dietary changes in their host environment (Figure S15.8, Tables S15.2-3). Unfortunately there are so far no data available from other late antique or early medieval cemeteries in northern Italy that would allow us to track potential dietary shifts over time. In Pannonia, a comparison of the data from Szólád with two fifth-century cemeteries in the Balaton region, Hács-Béndekpussta and Keszthely-Fenékpuszta, shows that local diet remained relatively consistent in the fifth and sixth centuries, though with the caveat that extremely high levels of mobility have also been identified at Hács-Béndekpussta and Keszthely-Fenékpuszta[143–145]. The populations at all three sites consumed a considerable amount of C4 plants, most likely millet, with a slight drop-off in the sixth century. For contrast, at Altenerding and Straubing, two large cemeteries in Bavaria that span the fifth to seventh centuries, the populations consumed almost exclusively C3 plants[109,146,147]. The $\delta^{13}C$ values there are therefore much more depleted than at the sites in Pannonia. Individuals at Szólád had slightly more access to animal protein than those at Hács-Béndekpussta and Keszthely-Fenékpuszta, but the pattern is skewed by the large number of children elevated $\delta^{15}N$ due to breastfeeding who were sampled in Szólád but not at the other sites.

Diet in Collegno is relatively similar to that of the Pannonian sites, taking into consideration the slightly different ecological context of northern Italy. The isotopic values of both $\delta^{13}C_{coll}$ and $\delta^{15}N$ at Collegno are more tightly clustered than at other sites,

suggesting that diet was relatively homogeneous for the population there. Castiglioni and Rottoli identified a small amount of millet at Collegno, but there was considerable evidence for it at other sites in the Piedmont[119]. In the absence of comparative data from other sites from northern Italy it is difficult to ascertain whether we see evidence of new dietary habits being introduced at Collegno by the migrants.

S15.6. Conclusion

At both Szólád and Collegno there is a pattern of migration by elite kindred who have high percentages of 'northern' ancestry. At Szólád several of these individuals experienced more than one change in residence before settling together with a group of individuals with high percentages of 'southern' ancestry who were also not local to Szólád. At Collegno it has been possible to identify first-generation migrants with 'northern' ancestry, who were followed by two or three generations of stable settlement. They settled among individuals with high percentages of 'southern' ancestry. At both sites, the individuals with higher levels of 'southern' ancestry appear to have been a less privileged local class, as indicated by their reduced access to animal protein and fewer grave goods. The migration and settlement of the more privileged outsiders appears not to have brought about a dietary shift, suggesting that the new elites may not have concerned themselves with subsistence agriculture directly, having instead the ability to access local resources through their privileged status.

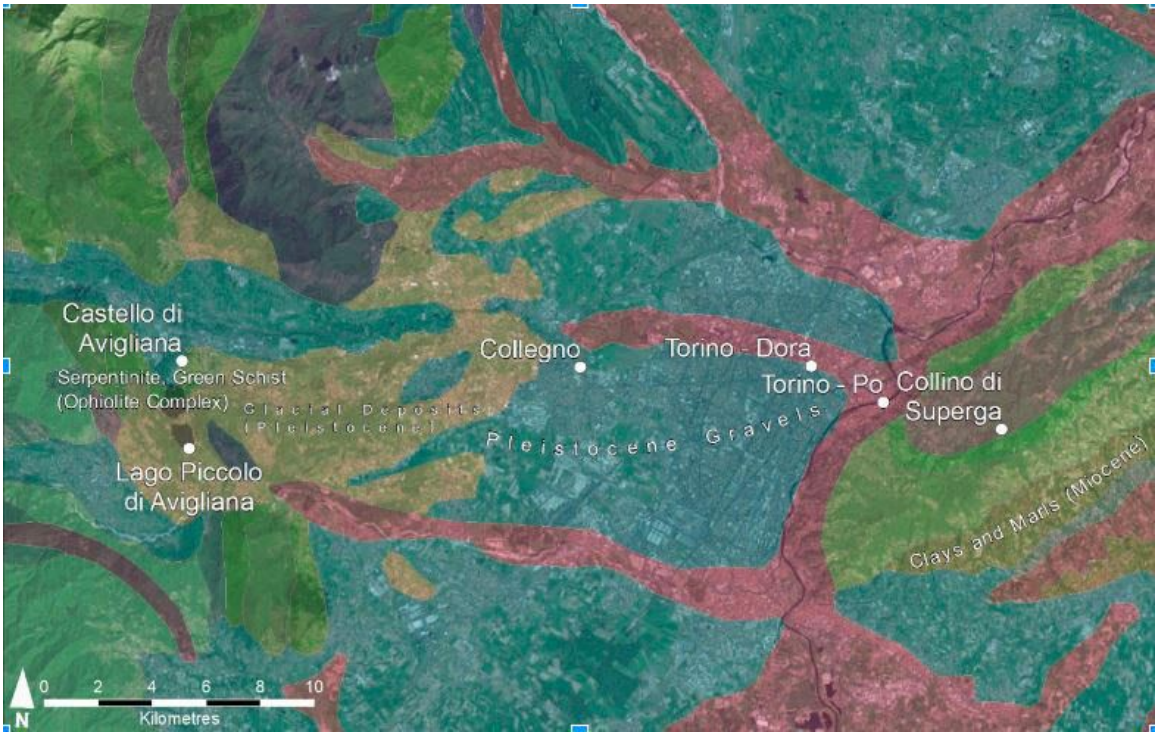

Figure S15.1. Map of the geological environment of Collegno with sampling locations (Drawn by D. Redhouse). Geological data from the Geoportale Nazionale (http://www.pcn.minambiente.it/) under a Creative Commons Attribution --- Share Alike 3.0 Italy Licence. Imagery from ArcGIS 10.2. Source: Esri, DigitalGlobe, GeoEye, Earthstar Geographics, CNES/Airbus DS, USDA, USGS, AEX, Getmapping, Aerogrid, IGN, IGP, swisstopo, and the GIS User Community.

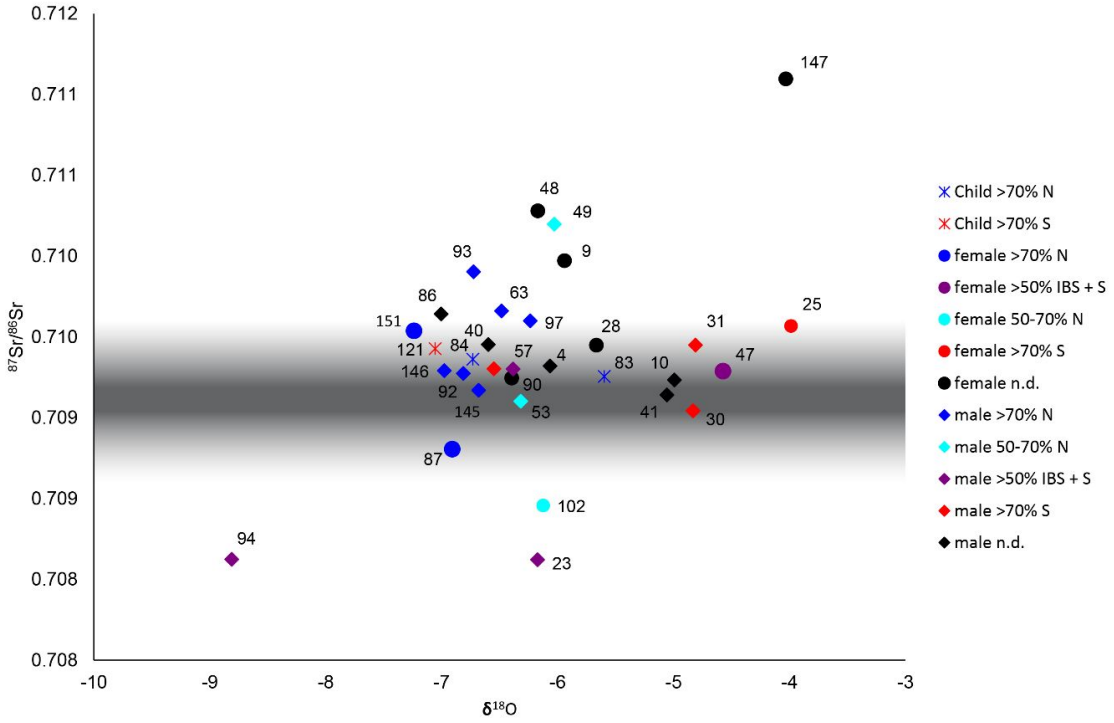

Figure S15.2. Evidence for migrants at Collegno revealed by $^{87}Sr/^{86}Sr$ and $\delta^{18}O$ values of human tooth enamel. The grey band denotes the local bioavailable strontium range. Key: blue: >70% N; cyan: 50-70% N; red: >70% S; purple: >50% IBS+S; black: no ancestry data.

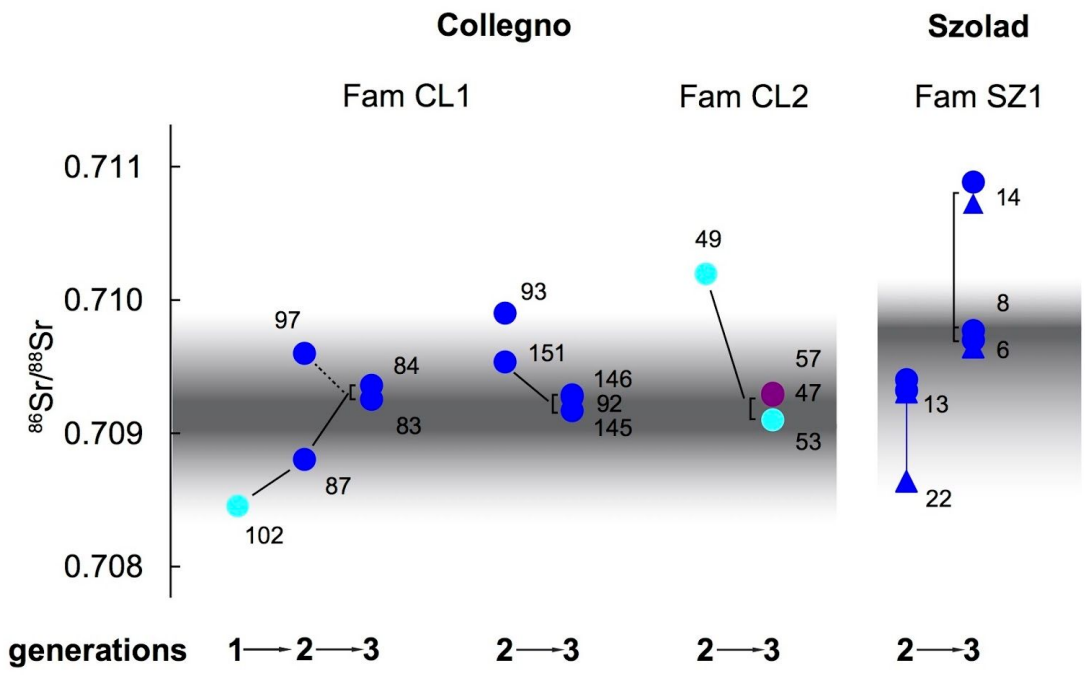

Figure S15.3. First generation migrants at Collegno and Szólád, as suggested by $^{87}Sr/^{86}Sr$ values of individuals from known kinship groups. The grey band denotes the local bioavailable strontium range. Generational relationships are indicated with lines.

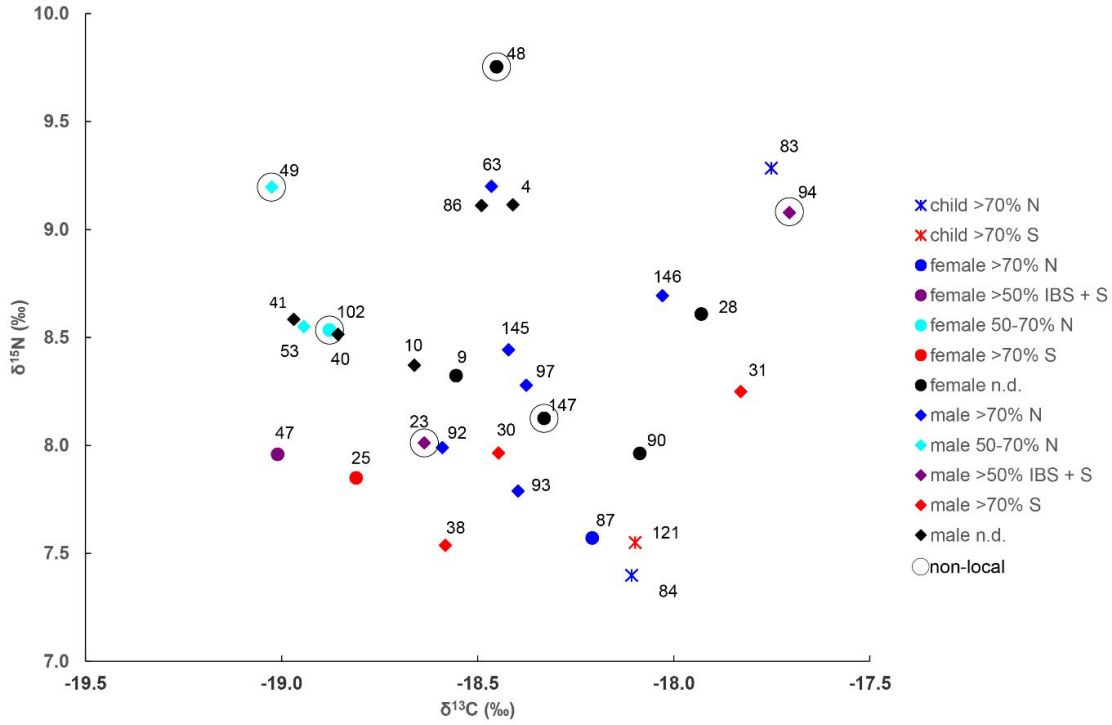

Figure S15.4. Dietary evidence at Collegno, as indicated by $\delta^{13}C_{coll}$ and $\delta^{15}N$ values of bone collagen. Ancestry groups and migration status are highlighted.

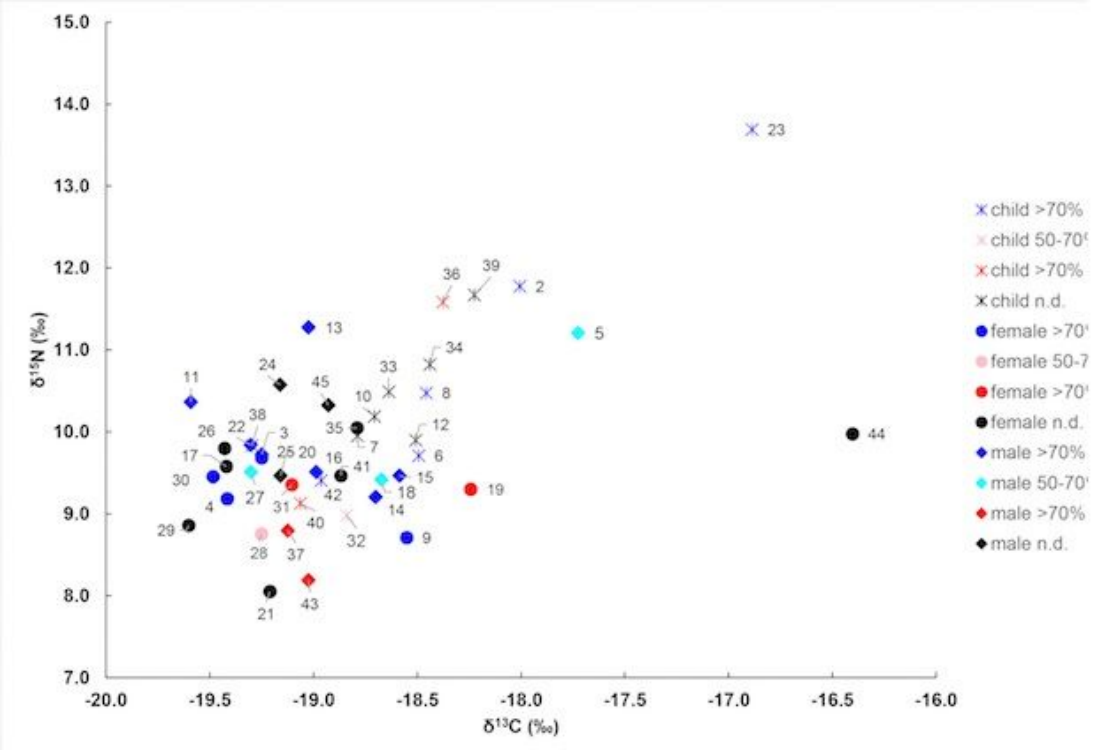

Figure S15.5. Dietary evidence at Szólád, as indicated by $\delta^{13}C_{coll}$ and $\delta^{15}N$ values of bone collagen. Ancestry groups and migration status are highlighted.

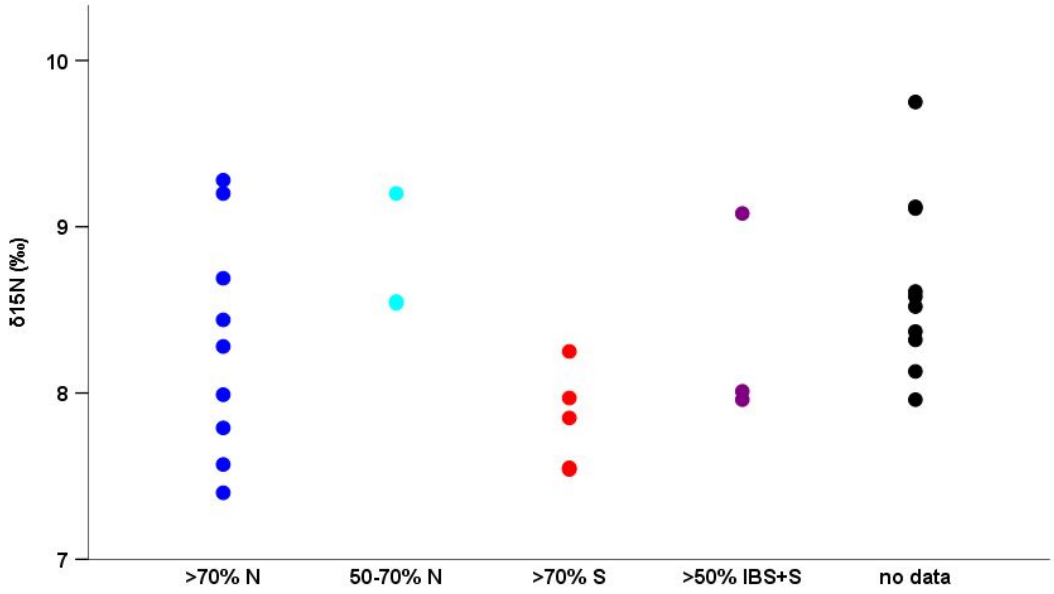

Figure S15.6. Variation in $\delta^{15}N$ values of adults of different ancestry groups at Collegno. Key: blue: >70% N; cyan: 50-70% N; red: >70% S; purple: >50% IBS+S; black: no ancestry data.

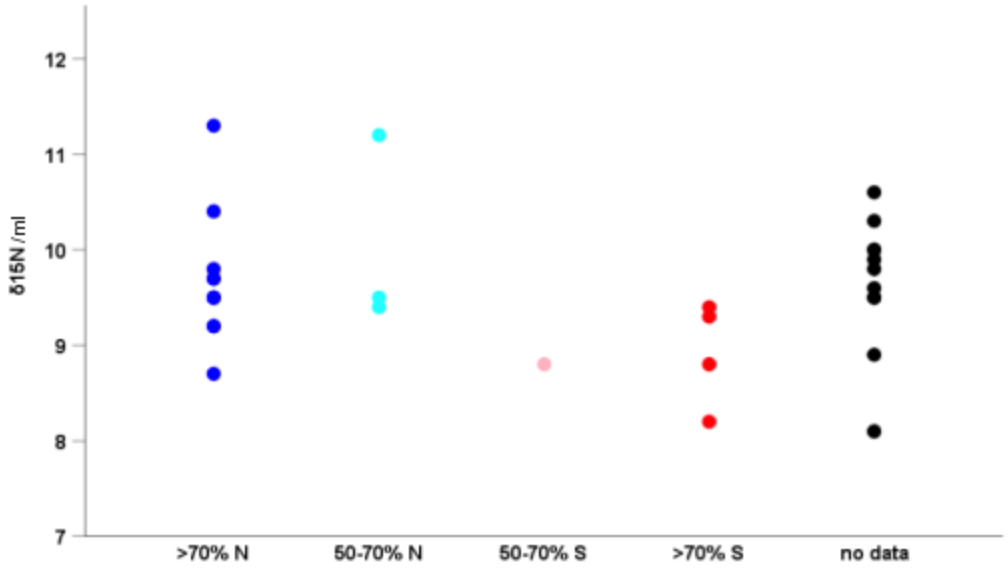

Figure S15.7. Variation in $\delta^{15}N$ values of adults of different ancestry groups at Szólád. Key: blue: >70% N; cyan: 50-70% N; pink: 50-70% S; red: >70% S; black: no ancestry data.

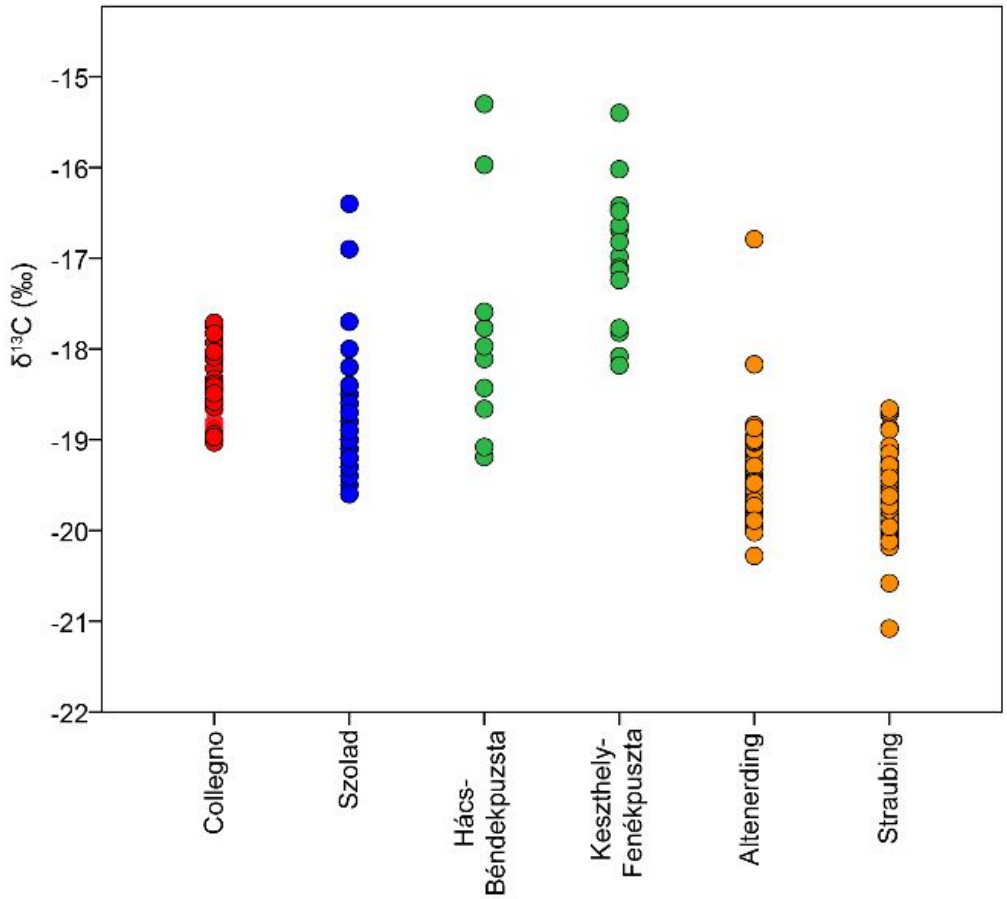
δ13C (‰)
-15
-16
-17
-18
-19
-20
-21
-22
Collegno
Szolad
Hács-Béndekpuzsta
Keszthely-Fenékpuszta
Altenerding
Straubing

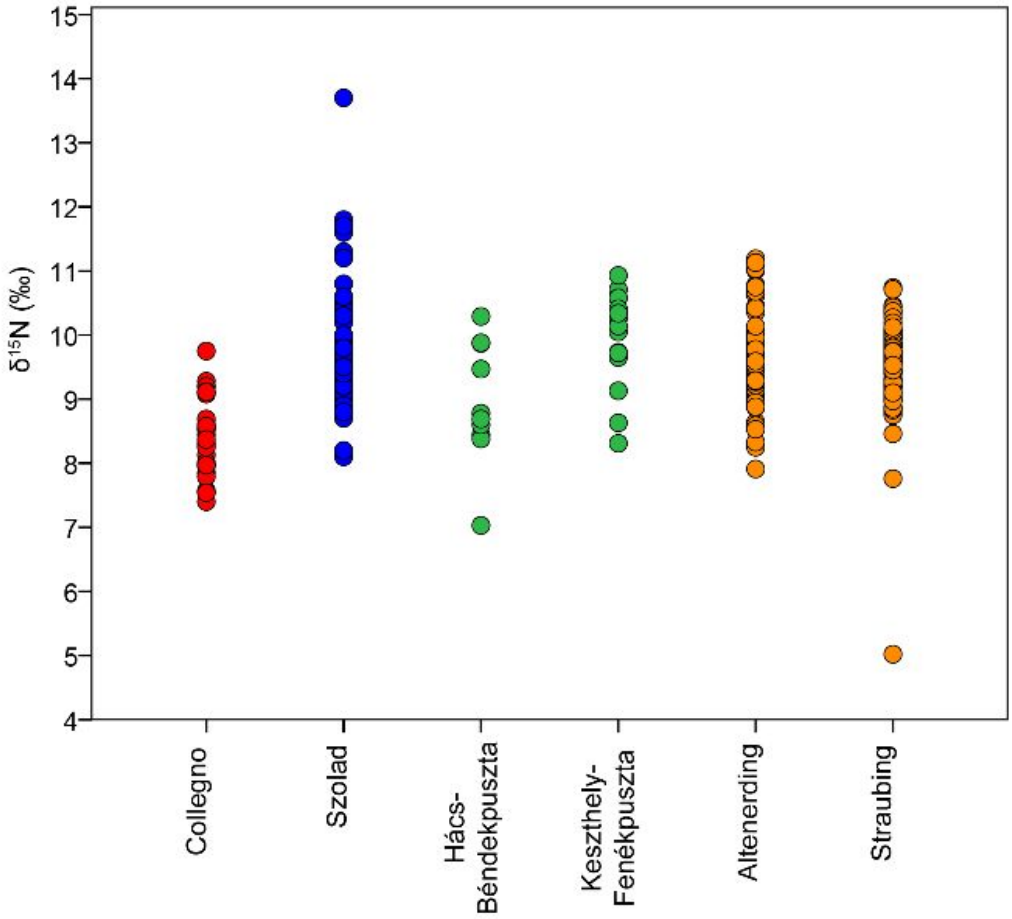

Figure S15.8. Range and distribution of $\delta^{13}C$ and $\delta^{15}N$ values from bone collagen at Collegno (red), Szólád (blue) and comparative sites in Pannonia (green) and Bavaria (orange) (Data from Hakenbeck et al.[138] and Hakenbeck et al.[145])

Table S15.1. Isotope values from human samples in Collegno.

Table S15.2. Isotope values from fauna for comparison to Collegno.

Table S15.3. Isotope values from fauna for comparison to Collegno.

[See Excel spreadsheet]

Table S15.4. Summary statistics of $\delta^{13}C_{collagen}$ (‰) values from bone collagen from Collegno, Szólád and comparative sites in Pannonia and Bavaria.

$\delta^{13}C_{collagen}$ (‰)	Mean	1 standard deviation	Min	Max	Range
Collegno	-18.4	0.4	-19.0	-17.7	1.3
Szólád	-18.8	0.6	-19.6	-16.4	3.2
Hács-Béndekpuzsta	-17.8	1.3	-19.2	-15.3	3.9
Keszthely-Fenékpuszta	-17.0	0.8	-18.2	-15.4	2.8
Altenerding	-19.4	0.5	-20.3	-16.8	3.5
Straubing	-19.7	0.4	-20.1	-18.7	1.4

Table S15.5. Summary statistics of $\delta^{15}N$ (‰) values from bone collagen from Collegno, Szólád and comparative sites in Pannonia and Bavaria.

$\delta^{15}N$ (‰)	Mean	1 standard deviation	Min	Max	Range
Collegno	8.4	0.6	7.4	9.8	2.4
Szólád	9.9	1.0	8.1	13.7	5.6
Hács-Bénde kpuzsta	9.0	1.0	7.0	10.3	3.3
Keszthely-Fenékpuszta	10.0	0.7	8.3	11.0	2.7
Altenerding	9.6	0.7	7.9	11.2	3.3
Straubing	9.6	0.7	5.0	10.7	5.7

REFERENCES

1. Jarnut, J. *Geschichte Der Langobarden*. (Kohlhammer, 1982).
2. Pohl, W. *Kingdoms of the Empire: The Integration of Barbarians in Late Antiquity*. (BRILL, 1997).
3. Bergamo, N. *I Longobardi: dalle origini mitiche alla caduta del regno in Italia*. (Libreria Editrice Goriziana, 2012).
4. Ausenda, G., Delogu, P. & Wickham, P. *The Langobards before the Frankish Conquest: An Ethnographic Perspective*. (Boydell Press, 2009).
5. Gasparri, S. *Italia longobarda: Il regno, i Franchi, il papato*. (Gius.Laterza & Figli Spa, 2016).
6. Hen, Y. & Innes, M. *The Uses of the Past in the Early Middle Ages*. (Cambridge University Press, 2000).
7. Diaconus, P. Historia Langobardorum,. in *Monumenta Germaniae Historica, Scriptores Rerum Langobardorum* (ed. Waitz, G.) 12–187 (1878).
8. Goffart, W. A. *The Narrators of Barbarian History (A.D. 550-800): Jordanes, Gregory of Tours, Bede, and Paul the Deacon*. (Publications in Medieval Studies, 1988).
9. Skinner, P. Gender, memory and Jewish identity: reading a family history from medieval southern Italy. *Early Medieval Europe* **13,** 277–296 (2005).
10. Pohl, W. *Werkstätte der Erinnerung: Montecassino und die Gestaltung der langobardischen Vergangenheit*. (Oldenbourg Verlag, 2001).
11. Ausenda, G. & Barnish, S. A Comparative Discussion Of Langobardic Feud And Blood-Money Compensation With Parallels From Contemporary Anthropology And From Medieval History. in *The Langobards before the Frankish Conquest: An Ethnographic Perspective* (eds. Ausenda, G., Delogu, P. & Wickham, C.) 309–339 (Boydell Press, 2009).

12. Murray, A. C. *Germanic Kinship Structure: Studies in Law and Society in Antiquity and in the Early Middle Ages*. (PIMS, 1983).
13. Wickham, C. *Early Medieval Italy: Central Power and Local Society, 400-1000*. (1981).
14. Christie, N. Pannonia: Foundations of Langobardic Power and Identity. in *The Langobards before the Frankish Conquest: An Ethnographic Perspective* (eds. Ausenda, G., Delogu, P. & Wickham, C.) 6–29 (Boydell Press, 2009).
15. Costambeys, M. Kinship, Gender and Property in Lombard Italy. in *The Langobards before the Frankish Conquest: An Ethnographic Perspective* (eds. Ausenda, G., Delogu, P. & Wickham, C.) 69–94 (Boydell Press, 2009).
16. Green, D. Linguistic and Literary Traces of the Langobards. in *The Langobards before the Frankish Conquest: An Ethnographic Perspective* (eds. Ausenda, G., Delogu, P. & Wickham, C.) 174–194 (Boydell Press, 2009).
17. von Freeden, U., Vida, T. & Skriba, P. Ausgrabung des langobardenzeitlichen Gräberfeldes von Szólád, Komitat Somogy, Ungarn: Vorbericht und Überblick über langobardenzeitliche Besiedlung am Plattensee. *Germania: Anzeiger der Römisch-Germanischen Komission des Deutschen Archäologischen Institute* **85,** 359–384 (2007).
18. Honti, S. *et al.* A tervezett M7-es autópálya Somogy megyei szakaszának megelőző régészeti feltárása (2002-2003) Előzetes jelentés III.--Preliminary Report III. The preceding archaeological excavations (2002-2003) of the M7 highway in Somogy County. *Somogyi Múzeumok Közleményei* **16,** (2004).
19. von Freeden, U. Ausgewählte Befunde aus dem langobardenzeitlichen Gräberfeld von Szólád, Komitat Somogy, Ungarn. in *Kulturwandel in Mitteleuropa Langobarden – Awaren – Slawen* (eds. Bemmann, J. & Schmauder, J.) 399–413 (2008).
20. Sudhoff, I. *Kreisgräben, Grabhügel und verwandte Sonderformen von Grabanlagen im*

Merowingerreich. (Rheinische Friedrich-Wilhelms-Universität, Bonn, 1999).

21. Passard, F. & Urlacher, J. P. Architectures funéraires des la nécropole des Saint-Vi. in *Burgondes, Alamans, Francs, Romains dans l'Est de la France, le Sud-Ouest de l'Allemagne et la Suisse, 5e-7e siècle après J.-C* (2003).
22. Neugebauer, J. W. Rettungsgrabungen im Unteren Traisental in den Jahren 2000 und 2001. *Fundberichte aus Österreich* **40,** 191–300 (2001).
23. Webster, C. J. & Brunning, R. A. A Seventh-Century ad Cemetery at Stoneage Barton Farm, Bishop's Lydeard, Somerset and Square-Ditched Burials in Post-Roman Britain. *Archaeological Journal* **161,** 54–81 (2004).
24. Winger, D. & Bartelt, D. Auf der Suche nach dem Haus des „Fürsten" – Siedlung und Prunkgrab der Merowingerzeit von Hemmingen-Hiddestorf, Region Hannover. in *Niedersächsisches Institut für historische Küstenforschung (Hrsg.), Aktuelle Forschungen an Gräberfeldern des 1. Jahrtausends n.Chr. Siedlungs- und Küstenforschung im südlichen Nordseegebiet 39 (Rahden/Westfalen 2016) 122-127.* (ed. Niedersächsisches Institut Für) 122–127 (2016).
25. Mengarelli, R. La necropoli barbarica di Castel Trosino. in *Monumenti Antichi* (ed. Accademia dei Lincei, R.) **12,** (1902).
26. Horváth, E. A langobard ékkő-és üvegberakás technológiai sajátosságainak vizsgálata a várpalotai és jutasi fibulákon. *Veszprém Megyei Múzeumok Közleményei* **24,** 49–66 (2006).
27. Pánczél-Bajnok, K., Pánczél, P., Szakmány, G. & Vida, T. 5-6. századi, Pannónia területéről származó kerámiák archaeometriai elemzése. *Archeometriai Műhely* **XI,** 1–12 (2014).
28. Alt, K. W. *et al.* Lombards on the Move – An Integrative Study of the Migration Period Cemetery at Szólád, Hungary. *PLoS One* **9,** e110793 (2014).
29. Geary, P. J. Rethinking Barbarian Invasions through Genomic History. *Hungarian*

Archaeology 1–8 (2014).

30. Stuiver, M. & Polach, H. A. Discussion Reporting of 14C Data. *Radiocarbon* **19,** 355–363 (1977).
31. Reimer, P. J. *et al.* IntCal13 and Marine13 Radiocarbon Age Calibration Curves 0–50,000 Years cal BP. *Radiocarbon* **55,** 1869–1887 (2013).
32. Peirani Baricco, L. L'insediamento e le necropoli dal VI all'VIII secolo. in *Presenze longobarde. Collegno nell'alto medioevo* (ed. Pejrani Baricco, L.) 17–52 (2004).
33. Pejrani Baricco, L. Longobardi da guerrieri a contadini. Le ultime ricerche in Piemonte. in *Archeologia e società nell'Italia altomedievale (V-IX secolo)* (eds. Brogiolo, G. P. & Chavarria Arnau, A.) 363–383 (2007).
34. Pejrani Baricco, L. Il Piemonte tra Ostrogoti e Longobardi. in *I Longobardi. Dalla caduta dell'impero all'alba dell'Italia* (eds. Brogiolo, G. P. & Chavarria Arnau, A.) 255–267 (2007).
35. Ferembach, D., Schwidetzky, I. & Stloukal, M. Recommandations pour déterminer l'âge et le sexe sur le squelette. *Bull. Mem. Soc. Anthropol. Paris* **6,** 7–45 (1979).
36. Bedini, E. & Bertoldi, F. Aspetto fisico, stile di vita e stato di salute del gruppo umano. in *Presenze longobarde. Collegno nell'alto medioevo* (ed. Pejrani Baricco, L.) 217–235 (2004).
37. Giostra, C. Gli oggetti di corredo; Catalogo. in *Presenze longobarde. Collegno nell'alto medioevo* (ed. Pejrani Baricco, L.) 53–152 (2004).
38. Giostra, C. La necropoli di Collegno (scheda 4.27). Tomba femminile 47. Tomba femminile 48. Tomba maschile 49. Tomba maschile 53. Tomba maschile 17. in *I Longobardi. Dalla caduta dell'Impero all'alba dell'Italia, catalogo della mostra* (eds. Brogiolo, G. P. & Chavarria Arnau, A.) 268–273 (2007).
39. Giostra, C. Goths and Lombards in Italy: the potential of archaeology with respect to

ethnocultural identification. *Post-Classical Archaeologies* **1,** 7–36 (2011).

40. Martin, R. & Saller, K. *Lehrbuch der Anthropologie in systematischer Darstellung*. (Fischer, 1956-1959).
41. Bartoli, F. & Bedini, E. Le abitudini alimentari. in *Presenze longobarde. Collegno nell'alto medioevo* (ed. Pejrani Baricco, L.) 241–247 (2004).
42. Castiglioni, E., Cottini, M., Rettore, E. & Rottoli, M. Il legno, i tessuti, i cuoi e gli altri materiali organici dalla necropoli longobarda e dall'abitato. in *Presenze longobarde. Collegno nell'alto medioevo* (ed. Pejrani Baricco, L.) 177–206 (2004).
43. Giostra, C. La struttura sociale nelle necropoli longobarde italiane: una lettura archeologica. in *Archeologia dei Longobardi: dati e metodi per nuovi percorsi di analisi* (ed. Giostra, C.) 83–112 (2017).
44. Pinhasi, R. *et al.* Optimal Ancient DNA Yields from the Inner Ear Part of the Human Petrous Bone. *PLoS One* **10,** e0129102 (2015).
45. Dabney, J. *et al.* Complete mitochondrial genome sequence of a Middle Pleistocene cave bear reconstructed from ultrashort DNA fragments. *Proc. Natl. Acad. Sci. U. S. A.* **110,** 15758–15763 (2013).
46. Meyer, M. & Kircher, M. Illumina Sequencing Library Preparation for Highly Multiplexed Target Capture and Sequencing. *Cold Spring Harb. Protoc.* **2010,** db.prot5448–pdb.prot5448 (2010).
47. Kircher, M., Sawyer, S. & Meyer, M. Double indexing overcomes inaccuracies in multiplex sequencing on the Illumina platform. *Nucleic Acids Res.* **40,** e3 (2012).
48. Peltzer, A. *et al.* EAGER: efficient ancient genome reconstruction. *Genome Biol.* **17,** 60 (2016).
49. Li, H. & Durbin, R. Fast and accurate short read alignment with Burrows-Wheeler

transform. *Bioinformatics* **25,** 1754–1760 (2009).

50. Kircher, M. Analysis of high-throughput ancient DNA sequencing data. *Methods Mol. Biol.* **840,** 197–228 (2012).
51. Lassmann, T., Hayashizaki, Y. & Daub, C. O. TagDust--a program to eliminate artifacts from next generation sequencing data. *Bioinformatics* **25,** 2839–2840 (2009).
52. Jónsson, H., Ginolhac, A., Schubert, M., Johnson, P. L. F. & Orlando, L. mapDamage2.0: fast approximate Bayesian estimates of ancient DNA damage parameters. *Bioinformatics* **29,** 1682–1684 (2013).
53. Rohland, N., Harney, E., Mallick, S., Nordenfelt, S. & Reich, D. Partial uracil-DNA-glycosylase treatment for screening of ancient DNA. *Philos. Trans. R. Soc. Lond. B Biol. Sci.* **370,** 20130624–20130624 (2014).
54. Mittnik, A., Wang, C.-C., Svoboda, J. & Krause, J. A Molecular Approach to the Sexing of the Triple Burial at the Upper Paleolithic Site of Dolní Věstonice. *PLoS One* **11,** e0163019 (2016).
55. Fu, Q. *et al.* DNA analysis of an early modern human from Tianyuan Cave, China. *Proc. Natl. Acad. Sci. U. S. A.* **110,** 2223–2227 (2013).
56. Haak, W. *et al.* Massive migration from the steppe was a source for Indo-European languages in Europe. *Nature* **522,** 207–211 (2015).
57. DePristo, M. A. *et al.* A framework for variation discovery and genotyping using next-generation DNA sequencing data. *Nat. Genet.* **43,** 491–498 (2011).
58. Fu, Q. *et al.* The genetic history of Ice Age Europe. *Nature* **534,** 200–205 (2016).
59. Korneliussen, T. S., Albrechtsen, A. & Nielsen, R. ANGSD: Analysis of Next Generation Sequencing Data. *BMC Bioinformatics* **15,** 356 (2014).
60. Renaud, G., Slon, V., Duggan, A. T. & Kelso, J. Schmutzi: estimation of contamination and

endogenous mitochondrial consensus calling for ancient DNA. *Genome Biol.* **16,** 224 (2015).

61. Vianello, D. *et al.* HAPLOFIND: a new method for high-throughput mtDNA haplogroup assignment. *Hum. Mutat.* **34,** 1189–1194 (2013).
62. Schiffels, S. *et al.* Iron Age and Anglo-Saxon genomes from East England reveal British migration history. *Nat. Commun.* **7,** 10408 (2016).
63. Veeramah, K. R. *et al.* Population genomic analysis of elongated skulls reveals extensive female-biased immigration in Early Medieval Bavaria. *Proc. Natl. Acad. Sci. U. S. A.* (in press).
64. Hofmanová, Z. *et al.* Early farmers from across Europe directly descended from Neolithic Aegeans. *Proc. Natl. Acad. Sci. U. S. A.* **113,** 6886–6891 (2016).
65. Botigué, L. R. *et al.* Ancient European dog genomes reveal continuity since the Early Neolithic. *Nat. Commun.* **8,** 16082 (2017).
66. Purcell, S. *et al.* PLINK: A Tool Set for Whole-Genome Association and Population-Based Linkage Analyses. *Am. J. Hum. Genet.* **81,** 559–575 (2007).
67. Nelson, M. R. *et al.* The Population Reference Sample, POPRES: a resource for population, disease, and pharmacological genetics research. *Am. J. Hum. Genet.* **83,** 347–358 (2008).
68. Novembre, J. *et al.* Genes mirror geography within Europe. *Nature* **456,** 98–101 (2008).
69. Das, S. *et al.* Next-generation genotype imputation service and methods. *Nat. Genet.* **48,** 1284–1287 (2016).
70. Loh, P.-R. *et al.* Reference-based phasing using the Haplotype Reference Consortium panel. *Nat. Genet.* **48,** 1443–1448 (2016).
71. 1000 Genomes Project Consortium *et al.* A global reference for human genetic variation. *Nature* **526,** 68–74 (2015).
72. Hellenthal, G. *et al.* A genetic atlas of human admixture history. *Science* **343,** 747–751

(2014).

73. Mallick, S. *et al.* The Simons Genome Diversity Project: 300 genomes from 142 diverse populations. *Nature* **538,** 201–206 (2016).

74. Danecek, P. *et al.* The variant call format and VCFtools. *Bioinformatics* **27,** 2156–2158 (2011).

75. Mathieson, I. *et al.* Genome-wide patterns of selection in 230 ancient Eurasians. *Nature* **528,** 499–503 (2015).

76. Patterson, N., Price, A. L. & Reich, D. Population structure and eigenanalysis. *PLoS Genet.* **2,** e190 (2006).

77. Veeramah, K. R. & Hammer, M. F. The impact of whole-genome sequencing on the reconstruction of human population history. *Nat. Rev. Genet.* **15,** 149–162 (2014).

78. Lazaridis, I. *et al.* Ancient human genomes suggest three ancestral populations for present-day Europeans. *Nature* **513,** 409–413 (2014).

79. Allentoft, M. E. *et al.* Population genomics of Bronze Age Eurasia. *Nature* **522,** 167–172 (2015).

80. Alexander, D. H., Novembre, J. & Lange, K. Fast model-based estimation of ancestry in unrelated individuals. *Genome Res.* **19,** 1655–1664 (2009).

81. Francalacci, P. *et al.* Low-pass DNA sequencing of 1200 Sardinians reconstructs European Y-chromosome phylogeny. *Science* **341,** 565–569 (2013).

82. Hallast, P. *et al.* The Y-chromosome tree bursts into leaf: 13,000 high-confidence SNPs covering the majority of known clades. *Mol. Biol. Evol.* **32,** 661–673 (2015).

83. Karmin, M. *et al.* A recent bottleneck of Y chromosome diversity coincides with a global change in culture. *Genome Res.* **25,** 459–466 (2015).

84. Francalacci, P. *et al.* Detection of phylogenetically informative polymorphisms in the entire

euchromatic portion of human Y chromosome from a Sardinian sample. *BMC Res. Notes* **8,** 174 (2015).

85. International Society of Genetic Genealogy (ISOGG). Available at: https://isogg.org/tree/index.html.
86. Y Chromosome Consortium. A nomenclature system for the tree of human Y-chromosomal binary haplogroups. *Genome Res.* **12,** 339–348 (2002).
87. Felsenstein, J. *PHYLIP (Phylogeny Inference Package)*. (2005).
88. Rambaut, A. *Fig.Tree. Tree Figure Drawing Tool*. (2012).
89. Francalacci, P. & Sanna, D. History and geography of human Y-chromosome in Europe: a SNP perspective. *J. Anthropol. Sci.* **86,** 59–89 (2008).
90. Semino, O. *et al.* The genetic legacy of Paleolithic Homo sapiens sapiens in extant Europeans: a Y chromosome perspective. *Science* **290,** 1155–1159 (2000).
91. Rootsi, S. *et al.* Phylogeography of Y-chromosome haplogroup I reveals distinct domains of prehistoric gene flow in europe. *Am. J. Hum. Genet.* **75,** 128–137 (2004).
92. Nasidze, I. *et al.* Mitochondrial DNA and Y-chromosome variation in the caucasus. *Ann. Hum. Genet.* **68,** 205–221 (2004).
93. Keller, A. *et al.* New insights into the Tyrolean Iceman's origin and phenotype as inferred by whole-genome sequencing. *Nat. Commun.* **3,** 698 (2012).
94. Mendez, F. L. *et al.* Increased resolution of Y chromosome haplogroup T defines relationships among populations of the Near East, Europe, and Africa. *Hum. Biol.* **83,** 39–53 (2011).
95. Genome of the Netherlands Consortium. Whole-genome sequence variation, population structure and demographic history of the Dutch population. *Nat. Genet.* **46,** 818–825 (2014).
96. Besenbacher, S. *et al.* Novel variation and de novo mutation rates in population-wide de

novo assembled Danish trios. *Nat. Commun.* **6,** 5969 (2015).

97. Lipatov, M., Sanjeev, K., Patro, R. & Veeramah, K. Maximum Likelihood Estimation of Biological Relatedness from Low Coverage Sequencing Data. (2015). doi:10.1101/023374
98. Weir, B. S., Anderson, A. D. & Hepler, A. B. Genetic relatedness analysis: modern data and new challenges. *Nat. Rev. Genet.* **7,** 771–780 (2006).
99. Anderson, A. D. & Weir, B. S. A maximum-likelihood method for the estimation of pairwise relatedness in structured populations. *Genetics* **176,** 421–440 (2007).
100. Staples, J. *et al.* PRIMUS: rapid reconstruction of pedigrees from genome-wide estimates of identity by descent. *Am. J. Hum. Genet.* **95,** 553–564 (2014).
101. Jacquard, A. *The Genetic Structure of Populations*. (Springer-Verlag, 1974).
102. Moltke, I. & Albrechtsen, A. RelateAdmix: a software tool for estimating relatedness between admixed individuals. *Bioinformatics* **30,** 1027–1028 (2014).
103. Yang, W.-Y., Novembre, J., Eskin, E. & Halperin, E. A model-based approach for analysis of spatial structure in genetic data. *Nat. Genet.* **44,** 725–731 (2012).
104. van Gennep, A. *Les rites de passage: étude systématique des rites de la porte et du seuil, de l'hospitalité, de l'adoption, de la grossesse et de l'accouchement, de la naissance, de l'enfance, de la puberté, de l'initiation, de l'ordination, du couronnement des fiançailles et du mariage, des funérailles, des saisons, etc*. (1981).
105. Insoll, T. *The Archaeology of Identities: A Reader*. (Routledge, 2007).
106. Rummel, P. *Habitus barbarus*. (2007).
107. Brather, S. *Ethnische Interpretationen in der frühgeschichtlichen Archäologie: Geschichte, Grundlagen und Alternativen*. (Walter de Gruyter, 2004).
108. Halsall, G. *Cemeteries and Society in Merovingian Gaul: Selected Studies in History and Archaeology, 1992-2009*. (BRILL, 2010).

109. Hakenbeck, S., McManus, E., Geisler, H., Grupe, G. & O'Connell, T. Diet and mobility in Early Medieval Bavaria: a study of carbon and nitrogen stable isotopes. *Am. J. Phys. Anthropol.* **143,** 235–249 (2010).

110. Alexander Bentley, R. Strontium Isotopes from the Earth to the Archaeological Skeleton: A Review. *J Archaeol Method Theory* **13,** 135–187 (2006).

111. IAEA/WMO. Global Network of Isotopes in Precipitation. The GNIP Database. (2006).

112. Daux, V. *et al.* Oxygen isotope fractionation between human phosphate and water revisited. *J. Hum. Evol.* **55,** 1138–1147 (2008).

113. Pollard, A. M., Pellegrini, M. & Lee-Thorp, J. A. Technical note: some observations on the conversion of dental enamel δ18O(p) values to δ18O(w) to determine human mobility. *Am. J. Phys. Anthropol.* **145,** 499–504 (2011).

114. Lightfoot, E. & O'Connell, T. C. On the Use of Biomineral Oxygen Isotope Data to Identify Human Migrants in the Archaeological Record: Intra-Sample Variation, Statistical Methods and Geographical Considerations. *PLoS One* **11,** e0153850 (2016).

115. Brettell, R., Montgomery, J. & Evans, J. Brewing and stewing: the effect of culturally mediated behaviour on the oxygen isotope composition of ingested fluids and the implications for human provenance studies. *J. Anal. At. Spectrom.* **27,** 778–785 (2012).

116. O'Leary, M. H. Carbon Isotopes in Photosynthesis. *Bioscience* **38,** 328–336 (1988).

117. Edgar Hare, P., Fogel, M. L., Stafford, T. W., Mitchell, A. D. & Hoering, T. C. The isotopic composition of carbon and nitrogen in individual amino acids isolated from modern and fossil proteins. *J. Archaeol. Sci.* **18,** 277–292 (1991).

118. Ambrose, S. H. Stable carbon and nitrogen isotope analysis of human and animal diet in Africa. *J. Hum. Evol.* **15,** 707–731 (1986).

119. Castiglioni, E. & Rottoli, M. Broomcorn millet, foxtail millet and sorghum in north Italian

Early Medieval sites. *Eur. J. Postclassical Archaeol* **3,** 131–144 (2013).

120. Bocherens, H. & Drucker, D. Trophic level isotopic enrichment of carbon and nitrogen in bone collagen: case studies from recent and ancient terrestrial ecosystems. *Int. J. Osteoarchaeol.* **13,** 46–53 (2003).

121. Hedges, R. E. M. & Reynard, L. M. Nitrogen isotopes and the trophic level of humans in archaeology. *J. Archaeol. Sci.* **34,** 1240–1251 (2007).

122. O'Connell, T. C., Kneale, C. J., Tasevska, N. & Kuhnle, G. G. C. The diet-body offset in human nitrogen isotopic values: a controlled dietary study. *Am. J. Phys. Anthropol.* **149,** 426–434 (2012).

123. Dufour, E., Bocherens, H. & Mariotti, A. Palaeodietary Implications of Isotopic Variability in Eurasian Lacustrine Fish. *J. Archaeol. Sci.* **26,** 617–627 (1999).

124. Maurer, A.-F. *et al.* Bioavailable 87Sr/86Sr in different environmental samples--effects of anthropogenic contamination and implications for isoscapes in past migration studies. *Sci. Total Environ.* **433,** 216–229 (2012).

125. Woelfel, J. B. & Scheid, R. C. *Dental anatomy: its relevance to dentistry*. (Lippincott Williams & Wilkins, 2012).

126. Bickle, M. J. *et al.* Fluxes of Sr into the headwaters of the Ganges. *Geochim. Cosmochim. Acta* **67,** 2567–2584 (2003).

127. Balasse, M., Ambrose, S. H., Smith, A. B. & Price, T. D. The Seasonal Mobility Model for Prehistoric Herders in the South-western Cape of South Africa Assessed by Isotopic Analysis of Sheep Tooth Enamel. *J. Archaeol. Sci.* **29,** 917–932 (2002).

128. Coplen, T. B. New IUPAC guidelines for the reporting of stable hydrogen, carbon, and oxygen isotope-ratio data. *J. Res. Natl. Inst. Stand. Technol.* **100,** 285 (1995).

129. Hoefs, J. *Stable Isotope Geochemistry*. (2009).

130. Privat, K. L., O'connell, T. C. & Richards, M. P. Stable Isotope Analysis of Human and Faunal Remains from the Anglo-Saxon Cemetery at Berinsfield, Oxfordshire: Dietary and Social Implications. *J. Archaeol. Sci.* **29,** 779–790 (2002).

131. DeNiro, M. J. Postmortem preservation and alteration of in vivo bone collagen isotope ratios in relation to palaeodietary reconstruction. *Nature* **317,** 806 (1985).

132. Ambrose, S. H. Preparation and characterization of bone and tooth collagen for isotopic analysis. *J. Archaeol. Sci.* **17,** 431–451 (1990).

133. Schoeninger, M. J. & DeNiro, M. J. Nitrogen and carbon isotopic composition of bone collagen from marine and terrestrial animals. *Geochim. Cosmochim. Acta* **48,** 625–639 (1984).

134. van der Merwe, N. J. & Vogel, J. C. 13C content of human collagen as a measure of prehistoric diet in woodland North America. *Nature* **276,** 815–816 (1978).

135. Lee-Thorp, J. A. On isotopes and old bones. *Archaeometry* **50,** 925–950 (2008).

136. Hedges, R. E. M., Clement, J. G., Thomas, C. D. L. & O'connell, T. C. Collagen turnover in the adult femoral mid-shaft: modeled from anthropogenic radiocarbon tracer measurements. *Am. J. Phys. Anthropol.* **133,** 808–816 (2007).

137. de Jong, M. An Unresolved Riddle: Early Medieval Incest Legislation. in *Franks and Alamanni in the Merovingian Period: An Ethnographic Perspective* (ed. Wood, I.) (Boydell & Brewer Ltd, 2003).

138. Hakenbeck, S. E. Roman or barbarian? Shifting identities in early medieval cemeteries in Bavaria. *Post-Classical Archaeologies* **1,** 37–66 (2011).

139. Hakenbeck, S. 'Hunnic' modified skulls: physical appearance, identity and the transformative nature of migrations. in *Mortuary practices and social identities in the Middle Ages* (eds. Williams, H. & Sayer, D.) 64–80 (Exeter University Press, 2009).

140. Czermak, A., Ledderose, A., Strott, N., Meier, T. & Grupe, G. Social Structures and Social Relations—An Archaeological and Anthropological Examination of three Early Medieval Separate Burial Sites in Bavaria. *Anthropol. Anz.* 297–310 (2006).

141. Czermak, A. M. Soziale Stratifizierung im frühen Mittelalter. (Ludwig-Maximilians-Universität München, 2011).

142. Knipper, C. *et al.* A distinct section of the Early Bronze Age society? Stable isotope investigations of burials in settlement pits and multiple inhumations of the Únětice culture in central Germany. *Am. J. Phys. Anthropol.* **159,** 496–516 (2016).

143. Kiss, A. Das germanische Gräberfeld von Hács-Béndekpuzsta (Westungarn) aus dem 5.-6. Jahrhundert. *Acta Antiquae Academiae Scientiarum Hungaricae* **36,** 275–342 (1995).

144. Straub, P. Angaben zum hunnenzeitlichen ostgermanischen Fundhorizont in Südtransdanubien—Ausgehend von der Nekropole in Keszthely-Fenékpuszta. *Keszthely-Fenékpuszta in Kontext spätantiker Kontinuitätsforschung zwischen Noricum und Moesia. Castellum Pannonicum Pelsonense. Rahden/Westf. : Marie Leidorf* 325–345 (2011).

145. Hakenbeck, S. E., Evans, J., Chapman, H. & Fóthi, E. Practising pastoralism in an agricultural environment: An isotopic analysis of the impact of the Hunnic incursions on Pannonian populations. *PLoS One* **12,** e0173079 (2017).

146. Sage, W. Das Reihengräberfeld von Altenerding in Oberbayern I.--Germanische Denkmäler der Völkerwanderungszeit, Serie A, 14, Gebr. (1984).

147. Geisler, H., Ganslmeier, R. & Christlein, R. *Das frühbairische Gräberfeld Straubing-Bajuwarenstrasse I: Katalog der archäologischen Befunde und Funde*. (Leidorf, 1998).